

***THE UNITED STATES PATENT AND TRADEMARK OFFICE
BEFORE THE BOARD OF PATENT APPEALS AND INTERFERENCES***

Applicant: Elliott et al.
Title: KINASES AND PHOSPHATASES
Appl. No.: 10/554,917
International Filing Date: 3/24/2004
371(c) Date: 04/27/07
Examiner: Swope, Sheridan
Art Unit: 1652
Confirmation Number: 9780

BRIEF ON APPEAL

Mail Stop Appeal Brief - Patents
P.O. Box 1450
Alexandria, VA 22313-1450

Under the provisions of 37 C.F.R. § 41.37, this Appeal Brief is being filed together with a credit card payment form in the amount of \$540.00 covering the 37 C.F.R. § 41.20(b)(2) appeal fee. If this fee is deemed to be insufficient, authorization is hereby given to charge any deficiency (or credit any balance) to the undersigned deposit account 19-0741.

TABLE OF CONTENTS

I.	REAL PARTY IN INTEREST	1
II.	RELATED APPEALS AND INTERFERENCES	2
III.	STATUS OF CLAIMS	3
IV.	STATUS OF AMENDMENTS	4
V.	SUMMARY OF CLAIMED SUBJECT MATTER.....	5
VI.	GROUND OF REJECTION TO BE REVIEWED ON APPEAL	6
VII.	ARGUMENT	7
A.	Appellants' specification teaches that SEQ ID NO: 13 is a novel variant of the β-adrenergic receptor kinase 2 and also illustrates a specific, substantial and credible utility	8
1.	Appellants' specification teaches that SEQ ID NO: 13 is 94% identical at the amino acid level to <i>Homo sapiens</i> beta-adrenergic receptor kinase 2	8
2.	Appellants' specification teaches that the probability of randomly obtaining a polypeptide corresponding to SEQ ID NO: 13 is nil	10

3.	Appellants' specification teaches that almost all of the signature sequences, domains or motifs are 100% identical between SEQ ID NO: 13 and the β -adrenergic receptor kinase 2 sequence	12
B.	The skilled artisan would reasonably believe that the assay methods used to establish a specific, substantial and credible utility for SEQ ID NO: 56 are valid.....	13
C.	The references cited in the January 13, 2010 reply are relevant.....	16
D.	The skilled artisan would find the stated utility significant, substantial and credible without additional statistical analysis	18
E.	Summary regarding the utility rejection under 35 U.S.C. § 101	19
F.	The claimed invention meets the enablement requirement under 35 U.S.C. § 112, first paragraph	20
VIII.	CONCLUSION	21
IX.	CLAIMS APPENDIX.....	22
X.	EVIDENCE APPENDIX.....	34
XI.	RELATED PROCEEDINGS APPENDIX	36

TABLE OF AUTHORITIES

Guidelines:

M.P.E.P. § 2107.01.II	21
------------------------------------	-----------

I. REAL PARTY IN INTEREST

The real party in interest is INCYTE CORPORATION.

II. RELATED APPEALS AND INTERFERENCES

The Appellants are unaware of any related appeals or interferences.

III. STATUS OF CLAIMS

Claims 1-4, 6-7, 11, 14-20, 23, 26-32, 34, 36, 44-55, and 142-144 are currently pending.

Claims 1, 2, 11, 14-20, 23, 26-32, 34, 36 and 44-55 currently are withdrawn.

Claims 3, 4, 6, 7 and 142-144 are pending and under examination.

The rejection of claims 3, 4, 6, 7 and 142-144 is appealed.

IV. STATUS OF AMENDMENTS

No amendment has been filed subsequent to the issuance of the final office Action dated October 16, 2009.

V. SUMMARY OF CLAIMED SUBJECT MATTER

Independent claim 3 is to be argued in the brief. The relevant citation to the specification is shown in the parentheses below.

Independent claim 3 reads as follows:

3. An isolated polynucleotide encoding a polypeptide {**page 23, line 30**}, wherein the polypeptide consists of the amino acid sequence of SEQ ID NO: 13 {**page 23, lines 31-32**}.

VI. GROUNDS OF REJECTION TO BE REVIEWED ON APPEAL

(1) Whether claims 3, 4, 6, 7, 142-144 are unpatentable under 35 U.S.C. § 101 as allegedly lacking a specific, substantial and credible utility.

(2) Whether claims 3, 4, 6, 7, 142-144 are unpatentable under 35 U.S.C. § 112, first paragraph, due to the alleged lack of utility.

VII. ARGUMENT

The specification provides numerous asserted utilities for the claimed polynucleotides and encoded polypeptides. One of these utilities, “as a tissue marker for brain” is explicitly asserted at page 102, line 18.

With respect to this utility, the final Office Action dated October 16, 2009 asserted that “the skilled artisan would not conclude that SEQ ID NO: 56 is a marker for brain tissue based on the specification disclosing that SEQ ID NO: 56 has a mere two-fold higher expression in brain than in the reference sample.” Office Action dated October 16, 2009 at page 3, emphasis added. No further support for the rejection is provided in this Office Action.

In the Advisory Action dated January 26, 2010, the rejection was maintained on the same grounds, namely that a “[t]wo-fold higher expression of SEQ ID NO: ...[56] in brain than in the reference sample does not provide evidence that SEQ ID NO: ... [56] is a specific marker for brain.” Advisory Action dated January 26, 2010 at page 2, emphasis added. In support, the Advisory Action puts forth three assertions. First, the Advisory action asserts that “[t]he reference sample, comprising heart, kidney, ling, placenta, small intestine, spleen, stomach, testis and uterus, comprises some tissue having a level of SEQ ID NO: ... [56] that is higher ... [than] the reference samples which is an average of all included tissues,” and that “[m]ore likely than not, compared to brain, one or more tissues within the reference sample have the same or higher levels of SEQ ID NO: ... [56].” *Id.*

Second, the Advisory Action asserts that “[n]one of Yue et al., Lee et al or Vasseur et al discusses using polynucleotides that are tissue-specific markers,” and that “[e]ach of said references discusses using a polynucleotide as a probe to detect differences in expression of the complementary polynucleotide in, for example, different tissues (Yue) or due to parameters such as ageing and caloric restriction (Lee), or transformation with ras (Vasseur).” *Id.*

Third, the Advisory Action asserts that “[t]he skilled artisan would have been aware of statistical methods that can be used to analyze variability and determine whether a difference is significant; for example the Student’s t-test,” and that “for a substance to be considered a tissue-specific marker, the expression of the substance in the tissue must be essentially exclusive, *i.e.*, not expressed in other tissues.” *Id.*

Appellants respectfully traverse these grounds for rejection.

A. Appellants’ specification teaches that SEQ ID NO: 13 is a novel variant of the β -adrenergic receptor kinase 2 and also illustrates a specific, substantial and credible utility

1. Appellants’ specification teaches that SEQ ID NO: 13 is 94% identical at the amino acid level to *Homo sapiens* beta-adrenergic receptor kinase 2

Table 1 of the specification at page 113 show that the polypeptide of SEQ ID NO: 13 is encoded by the polynucleotide of SEQ ID NO: 56. Specifically, Table 1 is described at page 43 of the specification as follows: “Table 1 summarizes the nomenclature for the full length polynucleotide and polypeptide embodiments of the invention. Each polynucleotide and its corresponding polypeptide are correlated to single Incyte project identification number (Incyte

Project ID).” Specification at page 43, lines 25-27. Thus, the amino acid of SEQ ID NO: 13 is encoded by the polynucleotide sequence of SEQ ID NO: 56.

Table 2 of the specification at page 121 provides homology data regarding the polypeptide of SEQ ID NO: 13. SEQ ID NO: 13 is 94% identical at the amino acid level to *Homo sapiens* beta-adrenergic receptor kinase 2 identified in Table 2 as g312395, and as shown in the sequence alignment below. Differences between the amino acid sequences are bold, underlined.

Alignment of SEQ ID NO: 13 and g312395

Score = 1338 bits (3462), Expect = 0.0, Method: Compositional matrix adjust.
Identities = 647/688 (94%), Positives = 649/688 (94%), Gaps = 38/688 (5%)

Query	1	MADLEAVLADVSYLMAMEKSKATPAARASKRIVLPEPSIRSVMQKYLAERNEITLDKIFN	60
		MADLEAVLADVSYLMAMEKSKATPAARASKRIVLPEPSIRSVMQKYLAERNEITDKIFN	
Sbjct	1	MADLEAVLADVSYLMAMEKSKATPAARASKRIVLPEPSIRSVMQKYLAERNEITFDKIFN	60
Query	61	QKIGFLLFKDFCLNEINEAVPQVKFYEEIKEYEKLDNEEDRLCRSRQIYDAYIMKELLSC	120
		QKIGFLLFKDFCLNEINEAVPQVKFYEEIKEYEKLDNEEDRLCRSRQIYDAYIMKELLSC	
Sbjct	61	QKIGFLLFKDFCLNEINEAVPQVKFYEEIKEYEKLDNEEDRLCRSRQIYDAYIMKELLSC	120
Query	121	SHPFSKQAVEHVQSHLSKKQVTSTLFQPYIEEICESLRGDIQKFMESDKFTRFCQWKNV	180
		SHPFSKQAVEHVQSHLSKKQVTSTLFQPYIEEICESLRGDIQKFMESDKFTRFCQWKNV	
Sbjct	121	SHPFSKQAVEHVQSHLSKKQVTSTLFQPYIEEICESLRGDIQKFMESDKFTRFCQWKNV	180
Query	181	ELNIHLTMNEFSVHRIIGRGGFGEVYGCRKADTGKMYAMKCLDKKRIKMKQGETLALNER	240
		ELNIHLTMNEFSVHRIIGRGGFGEVYGCRKADTGKMYAMKCLDKKRIKMKQGETLALNER	
Sbjct	181	ELNIHLTMNEFSVHRIIGRGGFGEVYGCRKADTGKMYAMKCLDKKRIKMKQGETLALNER	240
Query	241	IMLSLVSTGDCPFIVCMTYAFHTPDKLCFILDLMNGGDLHYHLSQHGVFSEKEMRFYATE	300
		IMLSLVSTGDCPFIVCMTYAFHTPDKLCFILDLMNGGDLHYHLSQHGVFSEKEMRFYATE	
Sbjct	241	IMLSLVSTGDCPFIVCMTYAFHTPDKLCFILDLMNGGDLHYHLSQHGVFSEKEMRFYATE	300
Query	301	IILGLEMHNRVVFYRDLKPANILLDEHGHARISDLGLACDFSKKKPHASVGTHGYMAPE	360
		IILGLEH+HNRVVFYRDLKPANILLDEHGHARISDLGLACDFSKKKPHASVGTHGYMAPE	
Sbjct	301	IILGLEHVHNRVVFYRDLKPANILLDEHGHARISDLGLACDFSKKKPHASVGTHGYMAPE	360
Query	361	VLQKGTAYDSSADWFSLGCMFLKLLRGHSPFRQHKTKDKHEIDRMTLTVNVELPDTFSPE	420
		VLQKGTAYDSSADWFSLGCMFLKLLRGHSPFRQHKTKDKHEIDRMTLTVNVELPDTFSPE	
Sbjct	361	VLQKGTAYDSSADWFSLGCMFLKLLRGHSPFRQHKTKDKHEIDRMTLTVNVELPDTFSPE	420
Query	421	LKSLLEGLLQRDVSKRLGCHGGGSQEVKEHSFFKGVQHVYLQKYPPPLIPPRGEVNAA	480

Sbjct	421	LKSLLEGLLQRDVSKRLGCHGGGSQEVKEHSFFKGVDWQHVVYLQKYPPPLIPPRGEVNAA	480
Query	481	DAFDIGSFDEEDTKGIKLLDCDQELYKNFPLVISERWQQEVTETVYEAVNADTDKIEARK	540
Sbjct	481	DAFDIGSFDEEDTKGIKLLDCDQELYKNFPLVISERWQQEVTETVYEAVNADTDKIEARK	540
Query	541	RAKNKQLGHEEDYALGKDCIMHGYMLKLGNPFLTQWQRRYFYLFPNRLEWRGEGESR---	597
Sbjct	541	RAKNKQLGHEEDYALGKDCIMHGYMLKLGNPFLTQWQRRYFYLFPNRLEWRGEGESRQNL	600
Query	598	-----SDPEFVQWKKEKNETFKEARLLRR	622
Sbjct	601	LTMEQILSVEETQIKDKKCILFRIKGGKQFVLQCESDPEFVQWKKEKNETFKEAQLLLRR	660
Query	623	APKFLNKPRSGTVELPKPSLCHRNSNGL	650
Sbjct	661	APKFLNKPRSGTVELPKPSLCHRNSNGL	688

2. Appellants' specification teaches that the probability of randomly obtaining a polypeptide corresponding to SEQ ID NO: 13 is nil

Table 2 of the Specification at page 121 shows that the BLAST probability score is 0.0, "which indicates the probability of obtaining the observed polypeptide sequence alignment by chance." Specification at page 44, lines 19-21. Table 2 also references Parruti et al., "Molecular cloning, functional expression and mRNA analysis of human beta adrenergic receptor kinase 2," *Biochem. Biophys. Res. Commun.*, 190:475-481 (1993) ("Parruti," EXHIBIT A), which is incorporated into the specification by reference (*see* Table 2 at page 121; Specification at page 44, lines 9-10). Parruti describes the sequence of human beta-adrenergic receptor kinase 2 polypeptide, the cDNA sequence of which was submitted the to the GenBank/EMBL data Bank with accession number X69117. An alignment of the polypeptide associated with accession number X69117 and g312395 illustrates that these two sequences are 100% identical at the amino acid level.

Alignment of X69117 (QUERY) G312395 (SBJCT)

Score = 1437 bits (3721), Expect = 0.0, Method: Compositional matrix adjust.
Identities = 688/688 (100%), Positives = 688/688 (100%), Gaps = 0/688 (0%)

Query	1	MADLEAVLADVSYLMAMEKSKATPAARASKRIVLPEPSIRSVMQKYLAERNEITFDKIFN	60
Sbjct	1	MADLEAVLADVSYLMAMEKSKATPAARASKRIVLPEPSIRSVMQKYLAERNEITFDKIFN	60
Query	61	QKIGFLLFKDFCLNEINEAVPQVKFYEEIKEYEKLDNEEDRLCSRQIYDAYIMKELLSC	120
Sbjct	61	QKIGFLLFKDFCLNEINEAVPQVKFYEEIKEYEKLDNEEDRLCSRQIYDAYIMKELLSC	120
Query	121	SHPFSKQAVEHVQSHLSKKQVTSTLFQPYIEEICESLRGDIQKFMESDKFTRFCQWKNV	180
Sbjct	121	SHPFSKQAVEHVQSHLSKKQVTSTLFQPYIEEICESLRGDIQKFMESDKFTRFCQWKNV	180
Query	181	ELNIHLTMNEFSVHRIIGRGGFGEVYGCRKADTGKMYAMKCLDKKRIKMKQGETLALNER	240
Sbjct	181	ELNIHLTMNEFSVHRIIGRGGFGEVYGCRKADTGKMYAMKCLDKKRIKMKQGETLALNER	240
Query	241	IMLSLVSTGDCPFIVCMTYAFHTPDKLCFILDLMNGGDLHYHLSQHGVFSEKEMRFYATE	300
Sbjct	241	IMLSLVSTGDCPFIVCMTYAFHTPDKLCFILDLMNGGDLHYHLSQHGVFSEKEMRFYATE	300
Query	301	IILGLEHVHNRFFVYRDLKPANILLDEHGHARISDLGLACDFSKKKPHASVGTHGYMAPE	360
Sbjct	301	IILGLEHVHNRFFVYRDLKPANILLDEHGHARISDLGLACDFSKKKPHASVGTHGYMAPE	360
Query	361	VLQKGTAYDSSADWFSLGCMFLKLLRGHSPFRQHKTCDKHEIDRMTLTVNVELPDTFSPE	420
Sbjct	361	VLQKGTAYDSSADWFSLGCMFLKLLRGHSPFRQHKTCDKHEIDRMTLTVNVELPDTFSPE	420
Query	421	LKSLLLEGLLQRDVS KRLGCHGGGSQEVKEHSFFKGVDWQHVVYLQKYPPLIPPRGEVNAA	480
Sbjct	421	LKSLLLEGLLQRDVS KRLGCHGGGSQEVKEHSFFKGVDWQHVVYLQKYPPLIPPRGEVNAA	480
Query	481	DAFDIGSFDEEDTKGIKLLDCDQELYKNFPLVISERWQQEVTETVYEAVNADTDKIEARK	540
Sbjct	481	DAFDIGSFDEEDTKGIKLLDCDQELYKNFPLVISERWQQEVTETVYEAVNADTDKIEARK	540
Query	541	RAKNKQLGHEEDYALGKDCIMHGYMLKLGNPFLTQWQRRYFYLFPNRLEWRGEGESRQNL	600
Sbjct	541	RAKNKQLGHEEDYALGKDCIMHGYMLKLGNPFLTQWQRRYFYLFPNRLEWRGEGESRQNL	600
Query	601	LTMEQILSVEETQIKDKKCILFR IKGGKQFVLQCESDPEFVQWKKELNETFKEAQRLLRR	660
Sbjct	601	LTMEQILSVEETQIKDKKCILFR IKGGKQFVLQCESDPEFVQWKKELNETFKEAQRLLRR	660
Query	661	APKFLNKPRSGTVELPKPSLCHRNSNGL	688
Sbjct	661	APKFLNKPRSGTVELPKPSLCHRNSNGL	688

Accordingly, SEQ ID NO: 13 is 94% identical at the amino acid level to the human β -adrenergic receptor kinase 2.

3. Appellants' specification teaches that almost all of the signature sequences, domains or motifs are 100% identical between SEQ ID NO: 13 and the β -adrenergic receptor kinase 2 sequence

Table 3 at page 146 of the Specification describes signature sequences, domains and motifs present in SEQ ID NO: 13. Numerous signature sequences, domains and motifs are presented for SEQ ID NO: 13, all of which are present in the β -adrenergic receptor kinase 2 sequence. Moreover, almost all of the signature sequences, domains or motifs are 100% identical between SEQ ID NO: 13 and the β -adrenergic receptor kinase 2 sequence. Exceptions include domains which span the mismatched amino acids (*e.g.*, the Regulator of G protein signaling domain, T54-C175, which includes a single amino acid mismatch at position 55 of SEQ ID NO: 13; β -adrenergic receptor kinase β -ARK G-protein coupled transferase serine/threonine protein ATP-binding multi-gene PD151831 T612-L650, which includes a single amino acid mismatch at position 617 of SEQ ID NO: 13). It is noted that the serine/threonine protein kinase catalytic domain F191-F453 is 100% identical between SEQ ID NO: 13 and the β -adrenergic receptor kinase 2 sequence. Accordingly, SEQ ID NO: 13 is a novel variant of the β -adrenergic receptor kinase 2.

B. The skilled artisan would reasonably believe that the assay methods used to establish a specific, substantial and credible utility for SEQ ID NO: 56 are valid

The Advisory Action alleges that the “reference sample comprising heart, kidney, lung, placenta, small intestine, spleen, stomach, testis and uterus, comprises some tissue having a level of SEQ ID NO: 56 that is higher than the reference sample, which is an average of all tissues included.” Advisory Action at page 2, emphasis added. The Advisory Action continues, asserting that “[m]ore likely than not, compared to brain, one or more tissues within the reference sample have the same or higher levels of SEQ ID NO: 5[6],” and that “[t]herefore the skilled artisan would not concluded that SEQ ID NO: 5[6] can be used [a]s a marker to identify brain tissue.” (Id). Appellants respectfully disagree with this assessment of the assay.

The specification at pages 95-98 describes the microarray assays that were performed to determine the relative expression levels of the novel polypeptides disclosed in the present application in different tissues. Briefly, the microarray assays were performed as follows.

The novel sequences disclosed in the present specification (“SEQs”) were affixed to a specific location on a solid support (see specification at page 96, line 35, continuing to page 97, lines 1-14) to generate the microarrays to be tested. A common reference sample was prepared which included RNA isolated from a variety of tissues: brain, heart, kidney, lung, placenta, small intestine, spleen, stomach, testis and uterus (Specification at page 102, lines 4-8). The common reference sample was then exposed to the microarray SEQs (Specification at page 102, lines 3-12) under stringent hybridization conditions (Specification at page 97, lines 16-24).

When the common reference sample was exposed to the microarray, each SEQ on the microarray provided a “signal” proportional to the amount of RNA which hybridized to that SEQ. Specification at page 98, line 18 and lines 22-24. For purposes of this discussion, the signal generated by hybridization of the common reference sample to a SEQ will be termed the “CR signal.” The skilled artisan would understand that in general, those SEQs which are expressed in more tissues will have a higher CR signal than those SEQs which are expressed in fewer tissues, and those SEQs which have higher levels of expression in any given tissue or tissues will have a higher CR signal than SEQs which have lower expression levels in the same tissue or tissues.

The next step of the assay was to expose the microarray to RNA derived from specific tissues. The tissue specific RNA was “obtained from at least three different donors,” and “RNA from each donor was separately isolated and individually hybridized to the microarray.” Specification at page 102, lines 8-10. Again, each SEQ on the microarray provided a “signal” which was proportional to the amount of RNA in the specific tissue which hybridized to that SEQ. Specification at page 98, line 18 and lines 22-23. The “signal” generated by the tissue-specific samples was then compared to the CR value. Signal-to-background and array element spot size were also evaluated (specification at page 98, lines 25-27). SEQs “that exhibit at least about a two-fold change in expression, a signal-to-background ratio of at least about 2.5, and an element spot size of at least about 40%, are considered to be differentially expressed.” *Id.*

Thus, if the signal generated by tissue X is lower than the CR signal (and background and spot size are within acceptable parameters), it is unlikely that that particular SEQ is expressed in

tissue X, or is expressed at very extremely low levels. If the signal generated by tissue X is at least about two-fold higher than the CR signal (and background and spot size are within acceptable parameters), then that sequence is considered to be differentially expressed.

Specification at page 98, lines 25-27. In the case of SEQ ID NO: 56, the tissue-specific signal was increased *by at least two-fold* in brain as compared to the reference sample. Specification at page 102, lines 17-18. No other tissue-specific expression is described in the specification for SEQ ID NO: 56, thus no other specific tissue provided a signal that was higher than the CR signal and met the background and spot size parameters.

The Advisory Action asserts that the “reference sample comprises some tissue having a level of SEQ ID NO: 56 that is higher than the reference sample,” and that “[m]ore likely than not, compared to brain, one or more tissues within the reference sample have the same or higher levels of SEQ ID NO: ...[56].” However, the tissue-specific testing rules this possibility out. For example, if one or more tissues, say heart and lung, within the reference sample have the same or higher levels of SEQ ID NO: 56 as expressed in brain, it follows that the signal produced in the heart and lung tissue-specific expression test would be at least as high as it was for brain tissue. The results of the microarray analysis indicate that this is not the case. Of the tissue types tested, *only brain* showed a difference in expression level as compared to the common reference sample, and that difference was “at least two-fold.” Specification at page 102, lines 17-18. This “at least two-fold difference,” in conjunction with an appropriate signal-to-background level and spot size, was deemed sufficient to be considered “differential

expression.” Specification at page 98, lines 25-27. Accordingly, Appellants respectfully contend that this reason for rejection is without merit and should be withdrawn.

C. The references cited in the January 13, 2010 reply are relevant

In the Reply dated January 13, 2010 to the final Office Action dated October 16, 2009, Appellants provided references to demonstrate that a two-fold difference in expression in microarray analysis is considered significant by those of skill in the art. The references teach that one of skill in the art could reasonably believe that an at least two-fold difference in expression is credible.

For example, numerous microarray studies have deemed fold-difference values of between 1.4 and 2 fold as significant. *See e.g.*, (1) Yue et al., *Nucleic Acid Research*, 29(8) e41 (2001), reporting a **1.4 fold** change in expression as significant, *see* abstract (EXHIBIT B); (2) Lee et al., *Science*, 285:1390-93, page 1392 (1999), reporting **1.8 fold** induction and **1.6 fold** reduction in gene expression as significant (EXHIBIT C); and (3) Vasseur et al., *Molecular Cancer*, 2(19) (2003), stating at page 2 that “differential expression values of greater than **1.7** are likely to be significant, based on internal quality control data,” however, that a “more stringent ratio” of “at least 2.0 fold” was used (EXHIBIT D). Indeed, reviews on the topic conclude that “there is no magical absolute cut-off for a meaningful fold value” and that essentially, the parameters of each analysis must be considered in determining a meaningful cut-off value for that particular analysis. *See e.g.*, Tsien et al., “On reporting fold differences,” *Pacific Symposium on Biocomputing*, 6:496-507, at 504 (2001) (EXHIBIT E). Note that each of these reference was

submitted with the reply dated January 13, 2010, and entered into the record on January 14, 2010.

This is confirmed in the Advisory action dated January 26, 2010.

With respect to the present application, the inventors concluded that for this microarray analysis, an “at least about 2-fold change in expression” relative to the common reference sample, in conjunction with “a signal-to-background ratio of at least about 2.5, and an element spot size of at least about 40%”, was sufficient to conclude that a particular sequence was differentially expressed.

With respect to the teachings of these references, the Examiner asserted that “[n]one of Yue et al., Lee et al or Vasseur et al discusses using polynucleotides that are tissue-specific markers,” and that “[e]ach of said references discusses using a polynucleotide as a probe to detect differences in expression of the complementary polynucleotide in, for example, different tissues (Yue) or due to parameters such as ageing and caloric restriction (Lee), or transformation with ras (Vasseur).” Advisory Action dated January 26, 2010 at page 2, emphasis added. The Examiner concludes that “[i]n such assays, a 2-fold change may or may not be significant, depending on the variability in the compared samples.” Advisory Action dated January 26, 2010 at page 2. Appellants respectfully disagree with the Examiner’s assertion that the cited references are not relevant to the present microarray analysis and results.

The microarray assay described in the present specification does precisely what the Examiner alleges it does not: that is, it uses “a polynucleotide as a probe to detect difference in expression of the complementary polynucleotide in, for example, different tissues.” Advisory Action dated January 26, 2010 at page 2. As described in the specification, RNA is isolated from

different, specific tissue samples. The RNA is then exposed to the polynucleotides (*e.g.*, SEQ ID NO: 56) affixed on the microarray solid support. If the RNA complement of SEQ ID NO: 56 is present in the sample, it will hybridize to the polynucleotide of SEQ ID NO: 56 and generate signal proportional to the amount of RNA hybridized. If the RNA complement of SEQ ID NO: 56 is not expressed in the specific tissue, no hybridization will occur and no signal will be generated. Accordingly, like the microarray analysis in Yue, SEQ ID NO: 56 is “used as a probe to detect differences in expression of the complementary polynucleotide in ... different tissues.”

Accordingly, Appellants respectfully contend that this argument is without merit and should be withdrawn.

D. The skilled artisan would find the stated utility significant, substantial and credible without additional statistical analysis

With respect to the “greater than two-fold difference” shown in the microarray analysis for SEQ ID NO: 56 in brain, the Examiner asserts that “[t]he skilled artisan would have been aware of statistical methods that can be used to analyze variability and determine whether a difference is significant, for example, the Student’s t-test.” Appellants do not dispute the assertion that the skilled artisan would have been aware of statistical methods to analyze variability and determine whether a difference was significant or not. However, as described in section II above, the skilled artisan also knew that numerous microarray studies deemed fold-difference values of between 1.4 and 2 fold as significant. Accordingly, the implication that some statistical analysis must be present to support the asserted utility is without merit, especially in light of the values that were routinely relied upon in the microarray arena.

The Advisory Action also asserts that “for a substance to be considered a tissue-specific marker, the expression of the substance in the tissue must be essentially exclusive, *i.e.*, not expressed in other tissues.” Advisory Action dated January 26, 2010 at page 2. Appellants respectfully contend that this has no bearing on the present situation. The expression of SEQ ID NO: 56 is increased by at least two-fold in brain as compared to the reference sample. No other tissue tested showed such differential expression. Accordingly, the skilled artisan would reasonably believe that if an unknown tissue was tested and showed “at least a two-fold difference in expression of SEQ ID NO: 56 as compared to the reference sample,” that tissue would likely be brain tissue. If an unknown tissue was tested and it showed a less than two-fold difference in expression of SEQ ID NO: 56 as compared to the reference sample, that tissues would most likely not be brain tissue. The skilled artisan would understand that relative levels of expression can also used as markers and that “essentially exclusive” expression not always a requirement or limitation.

E. Summary regarding the utility rejection under 35 U.S.C. § 101

Appellants respectfully contend that requirements for utility have more than been met.

As noted in the reply dated January 13, 2010,

The claimed invention must only be capable of performing some beneficial function...An invention does not lack utility merely because the particular embodiment disclosed in the patent lacks perfection or performs crudely...A commercially successful product is not required...Nor is it essential that the invention accomplish all its intended functions...or operate under all conditions ...partial success being sufficient to demonstrate patentable utility...In short, the defense of non-utility cannot be

sustained *without proof of total incapacity. If an invention is only partially successful in achieving a useful result, a rejection of the claimed invention as a whole based on a lack of utility is not appropriate.*

M.P.E.P. § 2107.01.II (citations omitted, emphasis added). Thus, while a higher “fold difference” and statistical analysis may be required in some circumstances - *e.g.*, FDA approval - such conditions are not required to meet the utility requirement under 35 U.S.C. § 101. In the present case, the expression level of SEQ ID NO: 56 is “at least two-fold higher” in brain tissue as compared to the control sample, and the art supports the “at least two-fold” difference in expression to be significant, *i.e.*, credible.

Accordingly, for at least the reasons stated above, the claimed invention has a specific, substantial and credible utility, and reconsideration and withdrawal of the rejection under 35 U.S.C. § 101 is respectfully requested.

F. The claimed invention meets the enablement requirement under 35 U.S.C. § 112, first paragraph

The Office asserts that “since the claimed invention is not supported by either a specific and substantial asserted utility or a well-established utility...one skilled in the art clearly would not know how to use the claimed invention.” Office Action dated October 16, 2009 at page 3. Appellants respectfully traverse this ground for rejection.

As noted above in sections A-E above, the claimed polynucleotides and encoded polypeptides have a specific, substantial and credible utility. As such, reconsideration and withdrawal of the rejection under 35 U.S.C. § 112, first paragraph, is respectfully requested.

VIII. CONCLUSION

For at least the reasons discussed above, Appellants respectfully submit that claims 3, 4, 6, 7, and 142-144 meet the requirements of 35 U.S.C. sections 101 and 112. Accordingly, Appellants respectfully request that the rejections be reversed in whole, and that the claims be allowed to issue.

Respectfully submitted,

Date: March 26, 2010

By /Michele M. Simkin/

FOLEY & LARDNER LLP
Customer Number: 22428
Telephone: (202) 672-5538
Facsimile: (202) 672-5399

Michele M. Simkin
Attorney for Appellant
Registration No. 34,717

IX. CLAIMS APPENDIX

1. (Withdrawn) An isolated polypeptide selected from the group consisting of:
 - a) a polypeptide comprising an amino acid sequence selected from the group consisting of SEQ ID NO:1-43,
 - b) a polypeptide comprising a naturally occurring amino acid sequence at least 90% identical to an amino acid sequence selected from the group consisting of SEQ ID NO:1, SEQ ID NO:22-23, SEQ ID NO:28, SEQ ID NO:30-32, SEQ ID NO:36-41 and SEQ ID NO:43,
 - c) a polypeptide comprising a naturally occurring amino acid sequence at least 91% identical to the amino acid sequence of SEQ ID NO:5,
 - d) a polypeptide comprising a naturally occurring amino acid sequence at least 93% identical to the amino acid sequence of SEQ ID NO:27,
 - e) a polypeptide comprising a naturally occurring amino acid sequence at least 94% identical to an amino acid sequence selected from the group consisting of SEQ ID NO:35 and SEQ ID NO:29,

- f) a polypeptide comprising a naturally occurring amino acid sequence at least 95% identical to an amino acid sequence selected from the group consisting of SEQ ID NO:4, SEQ ID NO:11, and SEQ ID NO:20,
- g) a polypeptide comprising a naturally occurring amino acid sequence at least 96% identical to the amino acid sequence of SEQ ID NO:9 and SEQ ID NO:18,
- h) a polypeptide comprising a naturally occurring amino acid sequence at least 97% identical to the amino acid sequence selected from the group consisting of SEQ ID NO:26, SEQ ID NO:33, and SEQ ID NO:34,
- i) a polypeptide comprising a naturally occurring amino acid sequence at least 98% identical to an amino acid sequence selected from the group consisting of SEQ ID NO:6 7,
- j) a polypeptide comprising a naturally occurring amino acid sequence at least 99% identical to the amino acid sequence of SEQ ID NO:16,
- k) a polypeptide consisting essentially of a naturally occurring amino acid sequence at least 90% identical to an amino acid sequence selected from the group consisting of SEQ ID NO:2-3, SEQ ID NO:8, SEQ ID NO:10, SEQ ID NO:12-15, SEQ ID NO:17, SEQ ID NO:19, SEQ ID NO:21, and SEQ ID NO:42,

- l) a biologically active fragment of a polypeptide having an amino acid sequence selected from the group consisting of SEQ ID NO:1-43, and
 - m) an immunogenic fragment of a polypeptide having an amino acid sequence selected from the group consisting of SEQ ID NO:1-43.
2. (Withdrawn) An isolated polypeptide of claim 1 comprising an amino acid sequence selected from the group consisting of SEQ ID NO:1-43.
3. (Previously Presented) An isolated polynucleotide encoding a polypeptide, wherein the polypeptide consists of the amino acid sequence of SEQ ID NO: 13.
4. (Previously Presented) The isolated polynucleotide of claim 3 wherein the polynucleotide sequence consists of SEQ ID NO: 56.
5. (Canceled).
6. (Previously Presented) A recombinant polynucleotide comprising a promoter sequence operably linked to the polynucleotide of claim 3.
7. (Previously Presented) A cell transformed with the recombinant polynucleotide of claim 6.
- 8.-10. (Canceled).
11. (Withdrawn) An isolated antibody which specifically binds to a polypeptide of claim 1.

12.-13. (Canceled).

14. (Withdrawn) A method of detecting a target polynucleotide in a sample, said target polynucleotide comprising the polynucleotide of claim 3, the method comprising:

- a) hybridizing the sample with a probe comprising at least 20 contiguous nucleotides comprising a sequence complementary to said target polynucleotide in the sample, and which probe specifically hybridizes to said target polynucleotide, under conditions whereby a hybridization complex is formed between said probe and said target polynucleotide or fragments thereof, and
- b) detecting the presence or absence of said hybridization complex, and, optionally, if present, the amount thereof.

15. (Withdrawn) A method of claim 14, wherein the probe comprises at least 60 contiguous nucleotides.

16. (Withdrawn) A method of detecting a target polynucleotide in a sample, said target polynucleotide comprising the polynucleotide of claim 3, the method comprising:

- a) amplifying said target polynucleotide or fragment thereof using polymerase chain reaction amplification, and
- b) detecting the presence or absence of said amplified target polynucleotide or fragment thereof, and, optionally, if present, the amount thereof.

17. (Withdrawn) A composition comprising a polypeptide of claim 1 and a pharmaceutically acceptable excipient.
18. (Withdrawn) A composition of claim 17, wherein the polypeptide comprises an amino acid sequence selected from the group consisting of SEQ ID NO:1-43.
19. (Withdrawn) A method for treating a disease or condition associated with decreased expression of functional KPP, comprising administering to a patient in need of such treatment the composition of claim 17.
20. (Withdrawn) A method of screening a compound for effectiveness as an agonist of a polypeptide of claim 1, the method comprising:
- a) contacting a sample comprising a polypeptide of claim 1 with a compound, and
 - b) detecting agonist activity in the sample.
- 21.-22. (Canceled).
23. (Withdrawn) A method of screening a compound for effectiveness as an antagonist of a polypeptide of claim 1, the method comprising:
- a) contacting a sample comprising a polypeptide of claim 1 with a compound, and
 - b) detecting antagonist activity in the sample.

24.-25. (Canceled).

26. (Withdrawn) A method of screening for a compound that specifically binds to the polypeptide of claim 1, the method comprising:

- a) combining the polypeptide of claim 1 with at least one test compound under suitable conditions, and
- b) detecting binding of the polypeptide of claim 1 to the test compound, thereby identifying a compound that specifically binds to the polypeptide of claim 1.

27. (Withdrawn) A method of screening for a compound that modulates the activity of the polypeptide of claim 1, the method comprising:

- a) combining the polypeptide of claim 1 with at least one test compound under conditions permissive for the activity of the polypeptide of claim 1,
- b) assessing the activity of the polypeptide of claim 1 in the presence of the test compound, and
- c) comparing the activity of the polypeptide of claim 1 in the presence of the test compound with the activity of the polypeptide of claim 1 in the absence of the test compound, wherein a change in the activity of the polypeptide of claim 1 in the presence of the test compound is indicative of a compound that modulates the activity of the polypeptide of claim 1.

28. (Withdrawn) A method of screening a compound for effectiveness in altering expression of a target polynucleotide, wherein said target polynucleotide comprises the polynucleotide sequence of claim 3, the method comprising:

- a) contacting a sample comprising the target polynucleotide with a compound, under conditions suitable for the expression of the target polynucleotide,
- b) detecting altered expression of the target polynucleotide, and
- c) comparing the expression of the target polynucleotide in the presence of varying amounts of the compound and in the absence of the compound.

29. (Withdrawn) A method of screening for potential toxicity of a test compound, the method comprising:

- a) treating a biological sample containing nucleic acids with the test compound,
- b) hybridizing the nucleic acids of the treated biological sample with a probe comprising at least 20 contiguous nucleotides of the polynucleotide of claim 3 under conditions whereby a specific hybridization complex is formed between said probe and a target polynucleotide in the biological sample, said target polynucleotide comprising the polynucleotide of claim 3,
- c) quantifying the amount of hybridization complex, and

- d) comparing the amount of hybridization complex in the treated biological sample with the amount of hybridization complex in an untreated biological sample, wherein a difference in the amount of hybridization complex in the treated biological sample indicates potential toxicity of the test compound.

30. (Withdrawn) A method for a diagnostic test for a condition or disease associated with the expression of KPP in a biological sample, the method comprising:

- a) combining the biological sample with an antibody of claim 11, under conditions suitable for the antibody to bind the polypeptide and form an antibody:polypeptide complex, and
- b) detecting the complex, wherein the presence of the complex correlates with the presence of the polypeptide in the biological sample.

31. (Withdrawn) The antibody of claim 11, wherein the antibody is:

- a) a chimeric antibody,
- b) a single chain antibody,
- c) a Fab fragment,
- d) a F(ab')₂ fragment, or
- e) a humanized antibody.

32. (Withdrawn) A composition comprising an antibody of claim 11 and an acceptable excipient.

33. (Canceled).

34. (Withdrawn) A composition of claim 32, further comprising a label.

35. (Canceled).

36. (Withdrawn) A method of preparing a polyclonal antibody with the specificity of the antibody of claim 11, the method comprising:

- a) immunizing an animal with a polypeptide consisting of an amino acid sequence selected from the group consisting of SEQ ID NO:1-43, or an immunogenic fragment thereof, under conditions to elicit an antibody response,
- b) isolating antibodies from the animal, and
- c) screening the isolated antibodies with the polypeptide, thereby identifying a polyclonal antibody which specifically binds to a polypeptide comprising an amino acid sequence selected from the group consisting of SEQ ID NO:1-43.

37.-43. (Canceled).

44. (Withdrawn) A method of detecting a polypeptide comprising an amino acid sequence selected from the group consisting of SEQ ID NO:1-43 in a sample, the method comprising:

- a) incubating the antibody of claim 11 with the sample under conditions to allow specific binding of the antibody and the polypeptide, and
 - b) detecting specific binding, wherein specific binding indicates the presence of a polypeptide comprising an amino acid sequence selected from the group consisting of SEQ ID NO:1-43 in the sample.
45. (Withdrawn) A method of purifying a polypeptide comprising an amino acid sequence selected from the group consisting of SEQ ID NO:1-43 from a sample, the method comprising:
- a) incubating the antibody of claim 11 with the sample under conditions to allow specific binding of the antibody and the polypeptide, and
 - b) separating the antibody from the sample and obtaining the purified polypeptide comprising an amino acid sequence selected from the group consisting of SEQ ID NO:1-43.
46. (Withdrawn) A microarray wherein at least one element of the microarray is a polynucleotide of claim 13.
47. (Withdrawn) A method of generating an expression profile of a sample which contains polynucleotides, the method comprising:
- a) labeling the polynucleotides of the sample,

- b) contacting the elements of the microarray of claim 46 with the labeled polynucleotides of the sample under conditions suitable for the formation of a hybridization complex, and
- c) quantifying the expression of the polynucleotides in the sample.

48. (Withdrawn) An array comprising different nucleotide molecules affixed in distinct physical locations on a solid substrate, wherein at least one of said nucleotide molecules comprises a first oligonucleotide or polynucleotide sequence specifically hybridizable with at least 30 contiguous nucleotides of a target polynucleotide, and wherein said target polynucleotide is a polynucleotide of claim 12.

49. (Withdrawn) An array of claim 48, wherein said first oligonucleotide or polynucleotide sequence is completely complementary to at least 30 contiguous nucleotides of said target polynucleotide.

50. (Withdrawn) An array of claim 48, wherein said first oligonucleotide or polynucleotide sequence is completely complementary to at least 60 contiguous nucleotides of said target polynucleotide.

51. (Withdrawn) An array of claim 48, wherein said first oligonucleotide or polynucleotide sequence is completely complementary to said target polynucleotide.

52. (Withdrawn) An array of claim 48, which is a microarray.

53. (Withdrawn) An array of claim 48, further comprising said target polynucleotide hybridized to a nucleotide molecule comprising said first oligonucleotide or polynucleotide sequence.
54. (Withdrawn) An array of claim 48, wherein a linker joins at least one of said nucleotide molecules to said solid substrate.
55. (Withdrawn) An array of claim 48, wherein each distinct physical location on the substrate contains multiple nucleotide molecules, and the multiple nucleotide molecules at any single distinct physical location have the same sequence, and each distinct physical location on the substrate contains nucleotide molecules having a sequence which differs from the sequence of nucleotide molecules at another distinct physical location on the substrate.
- 56.-141.(Canceled).
142. (Previously Presented) An isolated polynucleotide complementary to the polynucleotide of claim 3.
143. (Previously Presented) An isolated polynucleotide complementary to the polynucleotide of claim 4.
144. (Previously Presented) An RNA equivalent of the polynucleotide of claim 3.

X. EVIDENCE APPENDIX

Exhibit A:

Parutti *et al.*, *Molecular Cloning, Functional Expression and mRNA Analysis of Human Beta-Adrenergic Receptor Kinase 2*, Biochemical and Biophysical Research Communications, Vol. 190(2): 475-481 (1993).

The Parutti *et al.* reference was incorporated into the specification by reference (*see* Table 2 at page 121; Specification at page 44, lines 9-10). With respect to incorporation by reference, “[t]he information incorporated is as much a part of the application as filed as if the text was repeated in the application, and should be treated as part of the text of the application as filed.” (MPEP § 2163.07(b)). Accordingly, Parutti *et al.*, is inherently part of the record.

Exhibit B:

Yue *et al.*, *An Evaluation of the Performance of cDNA Microarrays for Detecting Changes in Global mRNA Expression*, Nucleic Acids Research, Vol. 29(8): e41 (2001).

The Yue *et al.* reference was submitted with the reply dated January 13, 2010, and entered into the record on January 14, 2010. This is confirmed in the Advisory action dated January 26, 2010.

Exhibit C:

Lee *et al.*, *Gene Expression Profile of Aging and its Retardation by Caloric Restriction*, Science, Vol. 285(5432):1390-93 (1999).

The Lee et al. reference was submitted with the reply dated January 13, 2010, and entered into the record on January 14, 2010. This is confirmed in the Advisory action dated January 26, 2010.

Exhibit D:

Vasseur *et al.*, *Gene Expression Profiling by DNA Microarray Analysis in Mouse Embryonic Fibroblast transformed by ras^{v12} Mutated Protein and the EIA Oncogene*, Molecular Cancer, Vol. 2(19), (2003).

The Vasseur et al. reference was submitted with the reply dated January 13, 2010, and entered into the record on January 14, 2010. This is confirmed in the Advisory action dated January 26, 2010.

Exhibit E:

Tsien *et al.*, *On Reporting Fold Differences*, Pacific Symposium on Biocomputing, 6:496-507 (2001).

The Tsien et al. reference was submitted with the reply dated January 13, 2010, and entered into the record on January 14, 2010. This is confirmed in the Advisory action dated January 26, 2010.

EXHIBIT A

This material may be protected by Copyright law (Title 17 U.S. Code)

MOLECULAR CLONING, FUNCTIONAL EXPRESSION AND mRNA ANALYSIS OF
HUMAN BETA-ADRENERGIC RECEPTOR KINASE 2

Giustino Parruti, Grazia Ambrosini, Michele Sallesè, and Antonio De Biasi¹

Consorzio Mario Negri Sud,
Istituto di Ricerche Farmacologiche "Mario Negri",
Santa Maria Imbaro, Italy

Received December 1, 1992

In the present study the cDNA of human BARK2 was cloned using both PCR and cDNA library screening, subcloned into an expression vector and transiently expressed in COS7 cells. The expressed kinase activity was ~40% as efficient as human BARK1 in phosphorylating bovine rod outer segments *in vitro*. Northern blot analysis of human and bovine mRNA revealed a species-specific pattern of multiple hybridization bands, with two major transcripts in human rather than one in bovine. High levels of mRNA expression were found in peripheral blood leukocytes. © 1993

Academic Press, Inc.

For a number of receptors a rapid loss of responsiveness has been shown to occur upon exposure to agonists (1). This phenomenon is known as homologous desensitization, and has been best characterized on the model of the β_2 -adrenergic receptor (BAR) (1). Receptor phosphorylation is an early step in the process of desensitization of these receptors. A selective kinase (called β -adrenergic receptor kinase, BARK) has been identified, which phosphorylates the agonist-occupied form of the receptor, as demonstrated *in vitro* for BAR (2). Other G-coupled receptors, including the α_2 -adrenergic receptor (3), muscarinic cholinergic receptors (4) and rhodopsin (5), can be phosphorylated *in vitro* by BARK in an agonist-dependent manner. BAR agonist isoproterenol induces translocation of BARK from cytosol to membranes upon stimulation of BAR (1,6). This represents the

¹To whom correspondence should be addressed at the Consorzio Mario Negri Sud, via Nazionale, 66030 S. Maria Imbaro, Italy. Fax: 39.872.578.240.

Abbreviations: BARK, beta-adrenergic receptor kinase; BAR, beta-adrenergic receptors; PAF, platelet activating factor; F, forward and R, reverse primers; PCR, polymerase chain reaction; PBL, peripheral blood leukocytes (granulocytes+lymphocytes+monocytes); MNL, mononuclear leukocytes (lymphocytes+monocytes); ROS, rod outer segments.

first step of BARK activation. A role for $\beta\gamma$ subunits of G-proteins has been recently demonstrated in the process of BARK translocation and activation (7). Two subtypes of BARK have been identified by molecular cloning in the bovine, called BARK1 and BARK2 (8). The highest levels of specific mRNA were found in the central nervous system and in highly innervated tissues, suggesting that the BARK-mediated mechanism of receptor desensitization may be primarily active on synaptic receptors (1,2,8). We have recently cloned the cDNA for human BARK1 and shown that peripheral blood leukocytes (PBL) represent a major site of expression (6). β -adrenergic agonist isoproterenol and platelet activating factor (PAF), which in these cells act as potent immunomodulators, were able to induce BARK translocation (6). We suggested a role of BARK in the regulation of receptor-mediated immune functions (6).

We present here the molecular cloning and functional expression of human BARK2. mRNA tissue distribution of human BARK2 was also investigated. High levels of specific mRNA are present in PBL, further supporting a possible role for these kinases in immunological settings.

MATERIALS AND METHODS

Tissue and cell sources - Cultured cells (American Tissue Culture Collection), growing under standard conditions, were harvested directly in guanidine isothiocyanate (BRL). Four different human cell lines were studied: two hepatomas (Hep G2 and SK-HEP-1), one lung carcinoma (A549), one neuroblastoma (IMR-32). Human umbilical vein endothelial cells (HEC) were isolated from umbilical cord vein and analyzed at the 4th - 6th passage. Human and bovine PBL and mononuclear leukocytes (MNL) were fractionated as previously described (6). Bovine tissues were frozen in liquid nitrogen after collection in the local slaughterhouse and total RNA prepared as described (6).

PCR cloning - The general PCR cloning strategy was as described in detail in ref.6. Forward (F) and reverse (R) primers indicated below are positioned on sequences numbered starting at the beginning of the coding region, i.e. base 1 is the A of ATG. When this study was planned, the cloning of bovine BARK2 had not been yet reported. Based on the sequence of bovine BARK1 (2) we designed oligonucleotides F3 (bp 586-608 of the coding region as in ref.2) and R3 (bp 1092-1069, ref.2) to amplify human BARK subtypes. We obtained a PCR product which turned out to correspond to bp 586-1069 of human BARK2 cDNA. To clone the entire coding region, we used primers F1, R1 and R2 (bp 1-19, 2064-2048 and 1566-1546 respectively of the coding sequence of bovine BARK2, ref.8), and primers F2 (bp 291-310), F4 (bp 913-932), F5 (bp 1300-1320), F6 (bp 1407-1428), R4 (bp 543-524) and R5 (bp 252-232) designed on the human sequence obtained from previously sequenced PCR products or library clones. The cDNA fragments cloned are: F1-R5, F2-R4, F3-R3, F4-R2 and F5-R1 and F6-R1. To obtain the first cDNA strand, 1 μ g total RNA from human adipose tissue or MNL was reverse-transcribed using random hexamers (Pharmacia LKB) and M-MLV reverse transcriptase (BRL). Amplifications were carried out as previously described (6). PCR products were subcloned blunt-end in PTZ18R or Bluescript and sequenced in both directions with T7 DNA polymerase (Pharmacia LKB).

cDNA library screening - A human pituitary cDNA library in lambda bluemicid (cloning site Eco RI and Hind III; Clontech, Palo Alto, CA), containing

1.5X10⁶ recombinants, was screened. The 609-1068 cDNA fragment of human BARK2, labelled by random priming (Amersham International kit), was used as a probe. The screening was done under high stringency conditions.

Expression of BARK2 in COS7 cells and phosphorylation assays -

The 2.1 kb full length cDNA of BARK2 was subcloned into the eukaryotic expression vector pBJI-neo (a kind gift of Dr. S. Alberti, Ist. Mario Negri), using restriction endonucleases from BRL. COS7 cells, grown to ~70% confluence in 80 mm plates, were transfected by the DEAE dextran procedure, using 10 µg of plasmid DNA for each plate. Cells were harvested 72 hours after transfection and cytosolic proteins prepared as previously described (9). Bovine rod outer segments (ROS) were prepared from bovine retina by stepwise sucrose gradient sedimentation. Retinal rhodopsin kinase was degraded by treatment with 5M urea. Phosphorylation reactions were carried out as described (9), using 3-5 µg of cytosolic proteins prepared from transfected cells, 300 pmol urea-treated ROS and 65 µM [γ -³²P]ATP (0.5-5 cpm/fmol) in a final volume of 40 µl. Following electrophoresis in polyacrylamide gels, for quantitative measurement of BARK activity rhodopsin bands (mw ~35Kd), identified by Coomassie Blue staining, were cut and counted for ³²P radioactivity.

Northern blot analysis - Total RNA was isolated by the guanidine isothiocyanate/cesium chloride method as described (6). Total RNA (20 µg) was fractionated on a 1% agarose-formaldehyde gel and transferred to a Gene Screen Plus membrane (New England Nuclear, Boston, MA). The RNA blot was hybridized with a random primed radioactive cDNA fragment (bp 609-1068) of human BARK2 in 50% formamide, 10% dextran sulphate, 1% SDS, 5.8% NaCl, and denatured salmon sperm DNA (100 µg/ml) for 24h at 42°C. Blots were washed in 2X SSC-1% SDS at 60°C (low stringency) or in 0.2X SSC-0.1% SDS at 65°C (high stringency) and subjected to autoradiography for 1-5 days at -80°C. All the results were confirmed on RNA from at least two different preparations.

RESULTS AND DISCUSSION

The cDNA of human BARK2 was cloned by PCR and cDNA library screening. The first PCR clone obtained (bp 609-1068) was amplified with non-degenerate primers designed on sequences in the catalytic domain of bovine BARK1 (2). This cDNA fragment was used to screen a human pituitary cDNA library. Two partial and partly overlapping clones provided the sequence from bp 149 to 1115 of the coding region. The cloning was then completed by PCR. cDNA² and amino acid sequences of human BARK2 are 72% and 84% identical to the corresponding sequences of human BARK1, in keeping with what reported for bovine subtypes (8). In addition, the amino acid sequence of human BARK2 is 95% identical to that of bovine BARK2, a very high level of interspecies conservation. Amino acid sequences of human and bovine BARK1 and BARK2 are aligned in Fig.1. In most cases of interspecies amino acid variation for both BARK1 and BARK2, one amino acid is the same as that conserved in the other subtype, consistent with the idea that all four genes are derived from a common ancestor. The highest levels of conservation are found in the catalytic domain of the kinases (aa 198-436), and in

²The nucleotide sequence of human BARK2 cDNA has been submitted to the GenBank/EMBL Data Bank with accession number X69117.

```

[REDACTED] MADLEAVLAD VSYLMAMEKS KATPAARASK RIVLPEPSIR SVMQKYLAER NEITFDKIFN QKIGFLLFKD 70
b BARK2 MADLEAVLAD VSYLMAMEKS KATPAARASK RIVLPEPSIR SVMQKYLEER HEITFDKIFN QRIGFLLFKD
[REDACTED] MADLEAVLAD VSYLMAMEKS KATPAARASK KILLPEPSIR SVMQKYLEDR GEVTFEKIFS QKLGYLFLFRD
b BARK1 MADLEAVLAD VSYLMAMEKS KATPAARASK KILLPEPSIR SVMQKYLEDR GEVTFEKIFS QKLGYLFLFRD
*****

FCLNEINEAV PQVKFYEEIK EYEKLDNEED RLCRSRQIYD AYIMKELLSC SHPFSKQAVE HVQSHLSKKQ 140
FCLNEINEAV PQVKFYEEIK EYEKLDNEED RLCRSRQIYD AYIMKELLSC SHPFSKQAVE HVQSHLSKKQ
FCLNHLEEAR PLVEFYEEIK KYEKLETEEE RVARSRIFD SYIMKELLAC SHPFSKSAIE HVQSHLSKKQ
FCLKHLEEAR PLVEFYEEIK KYEKLETEEE RLVCSREIFD TYIMKELLAC SHPFSKSAIE HVQSHLSKKQ
*****

VTSTLFQPYI EEICESLRGD IFQKFMESDK FTRFCQWKNV ELNIHLTMNE FSVHRIIGRG GFGEVYGCRC 210
VTSTLFQPYI EEICESLRGS IFQKFMESDK FTRFCQWKNV ELNIHLTMND FSVHRIIGRG GFGEVYGCRC
VPPDLFQPYI EEICQNLRGD VFQKFIESDK FTRFCQWKNV ELNIHLTMND FSVHRIIGRG GFGEVYGCRC
VPPDLFQPYI EEICQNLRGD VFQKFIESDK FTRFCQWKNV ELNIHLTMND FSVHRIIGRG GFGEVYGCRC
*****

ADTGKMYAMK CLDKKRIKMK QGETLALNER IMLSLVSTGD CPFIVCMTYA FHTPDKLCFI LDLMNGGDLH 280
ADTGKMYAMK CLDKKRIKMK QGETLALNER IMLSLVSTGD CPFIVCMTYA FHTPDKLCFI LDLMNGGDLH
ADTGKMYAMK CLDKKRIKMK QGETLALNER IMLSLVSTGD CPFIVCMTYA FHTPDKLSFI LDLMNGGDLH
ADTGKMYAMK CLDKKRIKMK QGETLALNER IMLSLVSTGD CPFIVCMTYA FHTPDKLSFI LDLMNGGDLH
*****

YHLSQHGVS EKEMRFYATE IILGLEHVN RVVYRDLKP ANILLDEHGH ARISDLGLAC DFSKKKPHAS 350
YHLSQHGVS EKEMRFYATE IILGLEHVN RVVYRDLKP ANILLDEHGH ARISDLGLAC DFSKKKPHAS
YHLSQHGVS EADMRFYAAE IILGLEHVN RVVYRDLKP ANILLDEHGH ARISDLGLAC DFSKKKPHAS
YHLSQHGVS EADMRFYAAE IILGLEHVN RVVYRDLKP ANILLDEHGH ARISDLGLAC DFSKKKPHAS
*****

VGTHGYMAPE VLQKGTAYDS SADWFSLGCM LFKLLRGHSP FRQHKTKDKH EIDRMTLTVN VELPDTSFSE 420
VGTHGYMAPE VLQKGTAYDS SADWFSLGCM LFKLLRGHSP FRQHKTKDKH EIDRMTLTVN VELPDTSFSE
VGTHGYMAPE VLQKGTAYDS SADWFSLGCM LFKLLRGHSP FRQHKTKDKH EIDRMTLTMA VELPDTSFSE
VGTHGYMAPE VLQKGTAYDS SADWFSLGCM LFKLLRGHSP FRQHKTKDKH EIDRMTLTMA VELPDTSFSE
*****

LKSLEGLLQ RDVSKRLGCH GGSQAEVKES SFFKGVQWQH VYLQKYPPL IPPRGEVNAA DAFDIGSFDE 490
LKSLEGLLQ RDVSKRLGCH GGSQAEVKES SFFKGVQWQH VYLQKYPPL IPPRGEVNAA DAFDIGSFDE
LKSLEGLLQ RDVSKRLGCH GGSQAEVKES SFFKGVQWQH VYLQKYPPL IPPRGEVNAA DAFDIGSFDE
LKSLEGLLQ RDVSKRLGCH GGSQAEVKES SFFKGVQWQH VYLQKYPPL IPPRGEVNAA DAFDIGSFDE
*****

EDTRGIKLLD CDQELYKNFP LVISERWQOE VAETVYEAVN ADTKIEARK RAKNKQLGHE EDYALGKDCI 560
EDTRGIKLLD CDQELYKNFP LVISERWQOE VAETVYEAVN ADTKIEARK RAKNKQLGHE EDYALGKDCI
EDTRGIKLLD SDQELYRNFP LTISERWQOE VAETVFDITN AETDRLEARK RAKNKQLGHE EDYALGKDCI
EDTRGIKLLD SDQELYRNFP LTISERWQOE VAETVFDITN AETDRLEARK RAKNKQLGHE EDYALGKDCI
*****

MHGYMLKLG N PFLTQWRRY FYLFPPNLEW RGESESQNL LTMEQISVE ETQIKDKKCI LFRIRGGKQF 630
MHGYMLKLG N PFLTQWRRY FYLFPPNLEW RGESESQNL LTMEQISVE ETQIKDKKCI LFRIRGGKQF
MHGYMLKLG N PFLTQWRRY FYLFPPNLEW RGESESQNL LTMEQISVE ETQIKDKKCI LFRIRGGKQF
MHGYMLKLG N PFLTQWRRY FYLFPPNLEW RGESESQNL LTMEQISVE ETQIKDKKCI LFRIRGGKQF
*****

VLQCESDPEF VQKKELNET FKEAQRLLR APKFLNKPRS GTVELPKPSL CHRNS-NGL 688
VLQCESDPEF VQKKELNET FKEAQRLLR APKFLNKPRS GTVELPKPSL CHRNS-NGL
VLQCESDPEF VQKKELNET FKEAQRLLR APKFLNKPRS GTVELPKPSL CHRNS-NGL
VLQCESDPEF VQKKELNET FKEAQRLLR APKFLNKPRS GTVELPKPSL CHRNS-NGL
*****

```

Figure 1. Alignment of the amino acid sequences of human BARK2, bovine BARK2, human BARK1 and bovine BARK2. Human BARK1 is from ref.6, bovine BARK1 from ref.2, bovine BARK2 from ref.8. Asterisks indicate amino acids that are conserved among all four genes.

the first 47 aminoacids, that are identical in the 4 sequences except for two conservative substitutions. Our sequence data support the view that aminoacid substitutions are clustered (8), as most of them fall in three regions, i.e. the central portion of the amino-terminal domain and the initial and final portions of the carboxyl-terminal domain. As no data are presently available as to which regions determine substrate specificity in these kinases, it is likely that aminoacid stretches where differences are clustered be involved in substrate recognition and binding. The carboxy-terminal region of these proteins is known to be involved in binding of $\beta\gamma$ subunits of G proteins (7). This region appears as the most variable, suggesting that different subtypes of BARK may specifically interact with different subtypes of $\beta\gamma$ subunits.

The full-length cDNA of human BARK2 was subcloned into the expression vector pBJI-neo (called pBJI-BARK2). Parallel transfections were done with the expression vector alone (pBJI-neo) and with the full-length cDNA for human BARK1, inserted in the same expression vector (pBJI-BARK1) (9). BARK activity was assayed *in vitro* by ROS phosphorylation assays. When compared with COS7 cells transfected with pBJI-neo, a 10 to 15 fold increase in BARK activity was obtained in COS7 cells transfected with pBJI-BARK2, whereas a 25 to 40 fold increase in BARK activity was revealed in cells transfected with pBJI-BARK1 (Fig.2). As expected, kinase activity was inhibited by heparin (Fig.2). Human BARK2 phosphorylated bovine ROS less efficiently than human BARK1 expressed in parallel experiments, that is with ~40% efficiency of human BARK1. This was in reasonable agreement with a previous report on bovine BARK2, which phosphorylated bovine ROS ~20% as efficiently as bovine BARK1 (8). Our expression system provides a simple and powerful tool for the screening of inhibitors or modulators of both human kinases, making use of the same assay, based on phosphorylation of ROS.

Northern blot analysis of human BARK2 revealed two major hybridization species present in all human cells tested, appearing as a doublet at ~8 and ~7 kb respectively, whereas a single major hybridization band was detected on bovine RNAs at ~7 kb (Fig.3 and ref.8). The finding of two major mRNA species in human instead of one in bovine is unexpected and peculiar, as this difference in mRNA expression distinguishes two otherwise highly conserved genes. The relative abundance of the two human hybridization species varied significantly, with a prevalence of the longer transcript in IMR32, a cell line from human neuroblastoma, and nearly equal intensities for the two transcripts in monocytes and granulocytes (Fig.3, left). In many cases, additional hybridization bands were revealed both in human and bovine. These bands, sized ~3.5 and 2 kb in human and ~3 kb in bovine, were detected even after high stringency washings. Multiple transcripts from a single gene and analogous interspecies differences in the hybridization pattern have already been reported for two subtypes of protein kinase C (10). A likely explanation for both phenomena may be alternative mRNA processing of the lengthy non-coding sequences present in these mRNAs.

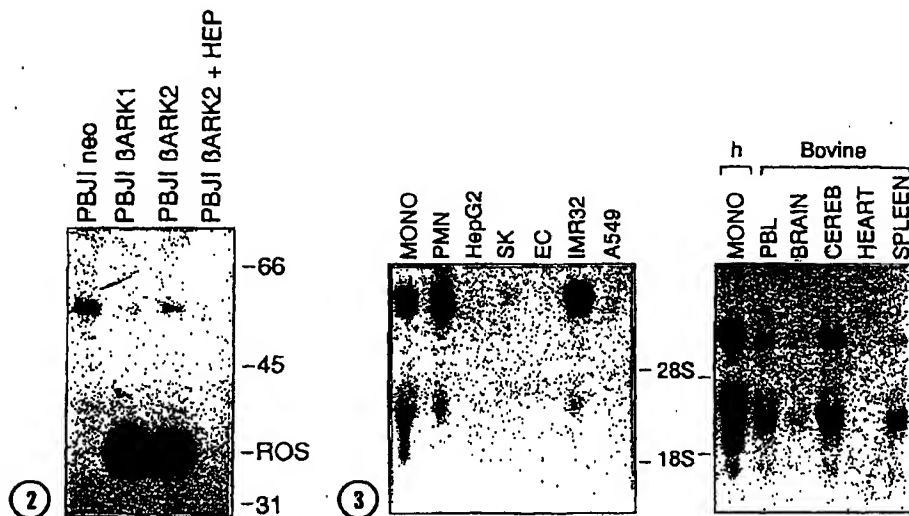


Figure 2. *In vitro* rhodopsin phosphorylation by transiently expressed BARK2. BARK activity was assayed in COS7 cells transfected with pBJI-neo, with pBJI-BARK1 and with pBJI-BARK2. Inhibition of BARK2 activity by heparin (10 μ g/ml, Sigma H-3125) is also shown (PBJI-BARK2 + Hep). The dried gel was exposed for 18 hours at -80°C . The position of molecular mass standards expressed in kilodaltons and that of rhodopsin bands (ROS) are indicated.

Figure 3. Northern blot analysis of human and bovine mRNA from various tissues and cell types. Two separate blots are shown. *left*, total RNA (20 μ g) from human monocytes (MONO), granulocytes (PMN), HepG2, SK-HEP-1 (SK), endothelial cells (EC), IMR32 and A549 cell lines was probed with a random primed BARK2 cDNA fragment (bp 609-1068). Washed filters were exposed at -80°C for 36-72h. *right*, total RNA (20 μ g) from human monocytes (h MONO) and bovine leukocytes (PBL), brain, cerebellum (CEREB), heart and spleen was probed as above. Washed filters were exposed at -80°C for 36-96h.

High levels of BARK2 mRNA were detected in human leukocytes compared to various human cell types (Fig.3). A detectable signal was found in most cell lines studied, IMR32 being the most expressive one (Fig.3, left). Analysis of BARK2 mRNA in human tissues revealed moderate expression in lung, heart and adipose tissue (not shown). Comparison of mRNA expression in leukocytes and brain was performed on bovine material. Bovine leukocytes were slightly less expressive than bovine cerebellum, but more expressive than bovine brain (Fig.3, right).

The finding of high levels of BARK2 mRNA in leukocytes is in line with other data obtained in our laboratory, showing that PBL represent a major site of expression for BARK (6). We found high levels of BARK1 mRNA as well as high levels of BARK activity in leukocytes (6). A functional role for BARK in immune cells was suggested by our finding of BARK translocation in MNL exposed to β -adrenergic receptor agonist isoproterenol and PAF, which act as potent immunomodulators on these cells. Another cytosolic protein, β -arrestin, acts as a cofactor of BARK to induce maximal desensitization of phosphorylated receptors (11). Indeed, we also found high levels of expression of both known β -arrestin subtypes in human MNL (G. Parruti and A. De Blasi, unpublished observation). Altogether

these data strongly support a functional role of the BARK/ β -arrestin mechanism of receptor desensitization in immune cells. Receptors for many immunomodulators present on PBL, such as PAF receptors, belong to the superfamily of G-coupled receptors and share relevant homology in terms of sequence and structure with G-coupled receptors that are known to be regulated by the BARK/ β -arrestin system. It is conceivable that these receptors also share the same molecular mechanisms of homologous desensitization. However, the possibility that any of the BARK subtypes, highly expressed in PBL, is actually involved in the regulation of any of these candidate receptors mediating immune functions remains to be investigated.

In conclusion, with the cloning of the cDNA for human BARK2, sequence information is now available for both known subtypes of BARK in human. This will help testing the possible involvement of these kinases in the regulation of candidate G-coupled receptors as well as in the pathogenesis of diseases for which an anomalous regulation of receptors has been reported.

Acknowledgments: We are grateful to G. D'Alessandro for oligonucleotide synthesis and R. Bertazzi and S. Menna for expert assistance in the preparation of figures. This work was supported in part by a grant from "P.F.Ingegneria Genetica, CNR" and by the "Agenzia per la Promozione dello Sviluppo del Mezzogiorno" (del. N.6166, PR 1). G.P. is the recipient of a fellowship from the "Centro di Formazione e Studi per il Mezzogiorno (FORMEZ), progetto speciale Ricerca Scientifica e Applicata nel Mezzogiorno".

REFERENCES

1. Hausdorff, W. P., Caron, M. G., and Lefkowitz, R. J. (1990) *FASEB J.* 4, 2881-2889.
2. Benovic, J. L., De Biasi, A., Stone, W. C., Caron, M. G., and Lefkowitz, R. J. (1989) *Science* 246, 235-240.
3. Benovic, J. L., Regan, J. W., Matsui, H., Mayor, F., Jr., Cotecchia, S., Leeb-Lundberg, L. M. F., Caron, M. G., and Lefkowitz, R. J. (1987) *J. Biol. Chem.* 262, 17251-17253.
4. Kwatra, M. M., Benovic, J. L., Caron, M. G., Lefkowitz, R. J., and Hosey, M. M. (1989) *Biochemistry* 28, 4543-4547.
5. Benovic, J. L., Mayor, F., Jr., Somers, R. L., Caron, M. G., and Lefkowitz, R. J. (1986) *Nature* 321, 869-872.
6. Chuang, T. T., Sallese, M., Ambrosini, G., Parruti, G., and De Biasi A. (1992) *J. Biol. Chem.* 267, 6886-6892.
7. Pitcher, J. A., Inglese, J., Higgins, J. B., Arriza, J. L., Casey, P. J., Kim, C., Benovic, J. L., Kwatra, M. M., Caron, M. G., Lefkowitz, R. J. (1992) *Science* 257, 1264-1267.
8. Benovic, J. L., Onorato, J. J., Arriza, J. L., Stone, W. C., Lohse, M., Jenkins, N. A., Gilbert, D. J., Copeland, N. G., Caron, M. G., and Lefkowitz, R. J. (1991) *J. Biol. Chem.* 266, 14939-14946.
9. Parruti, G., Lombardi, M. S., Chuang, T. T., and De Biasi, A. (1993) *J. Rec. Res.*, In press.
10. Coussens, L., Parker, P. J., Rhee, L., Yang-Feng, T. L., Chen, E., Waterfield, M. D., Francke, U., Ullrich, A. (1986) *Science* 233, 859-866.
11. Lohse, M. J., Andexinger, S., Pitcher, J., Trukawinski, S., Codina, J., Faure, J.-P., Caron, M. G., and Lefkowitz, R. J. (1992) *J. Biol. Chem.* 267, 8558-8564.

EXHIBIT B

An evaluation of the performance of cDNA microarrays for detecting changes in global mRNA expression

Huabin Yue, P. Scott Eastman*, Bruce B. Wang, James Minor, Michael H. Doctolero, Rachel L. Nuttall, Robert Stack, John W. Becker, Julie R. Montgomery, Marina Vainer and Rick Johnston

Advanced Research Group, Incyte Genomics, 6519 Dumbarton Circle, Fremont, CA 94555, USA

Received as resubmission February 13, 2001; Accepted February 18, 2001

ABSTRACT

The cDNA microarray is one technological approach that has the potential to accurately measure changes in global mRNA expression levels. We report an assessment of an optimized cDNA microarray platform to generate accurate, precise and reliable data consistent with the objective of using microarrays as an acquisition platform to populate gene expression databases. The study design consisted of two independent evaluations with 70 arrays from two different manufactured lots and used three human tissue sources as samples: placenta, brain and heart. Overall signal response was linear over three orders of magnitude and the sensitivity for any element was estimated to be 2 pg mRNA. The calculated coefficient of variation for differential expression for all non-differentiated elements was 12–14% across the entire signal range and did not vary with array batch or tissue source. The minimum detectable fold change for differential expression was 1.4. Accuracy, in terms of bias (observed minus expected differential expression ratio), was less than 1 part in 10 000 for all non-differentiated elements. The results presented in this report demonstrate the reproducible performance of the cDNA microarray technology platform and the methods provide a useful framework for evaluating other technologies that monitor changes in global mRNA expression.

INTRODUCTION

The construction of gene expression databases is a high priority of today's research community. Such databases, closely integrated with other types of genomic information, promise not only to facilitate our understanding of many fundamental biological processes, but also to accelerate drug discovery and lead to customized diagnosis and treatment of disease (1–6).

These databases will require the development of one or more underlying supporting technologies that can accurately and reproducibly measure changes in global mRNA expression

levels. The ideal technology should be able to process large numbers of samples, require minimal amounts of biological source material and be applicable across a wide range of cell or tissue types. Several different technologies are currently being investigated for their ability to meet these stringent requirements (7–12). While many of these technologies show significant promise in preliminary studies, it is critically important that each technology be comprehensively evaluated as a complete system for producing accurate, precise and reliable expression data (13,14).

The Incyte cDNA microarray technology platform simultaneously analyzes the relative expression levels of up to 10 000 genes, each of which is present as a unique cDNA element (7). The platform is potentially scalable to include all of the elements in the human genome. PCR-derived elements averaging 1000 nt in length are physically arrayed in a two-dimensional grid on a chemically modified glass slide. Aliquots from two purified mRNA samples are separately reverse transcribed using primer sets labeled with two different fluorophores and the resulting dye-labeled cDNA populations are used to probe the target elements in a competitive hybridization reaction. After hybridization the glass slide is analyzed in a two-channel fluorescence scanner and the ratio between the two fluorophores detected for any given element defines the relative amount of the mRNA corresponding to that element present in the original two samples.

There are many process variables that will impact on the quality of the data generated by any microarray technology platform. In this report we describe parameters for the manufacture of effective cDNA microarrays with highly reproducible performance characteristics, the quality and quantity of sample mRNAs used to create the dye-labeled cDNA probe and the effects of these optimized procedures on the overall performance, accuracy, precision and reliability of expression data generated from the two-channel ratiometric approach.

MATERIALS AND METHODS

Synthesis of PCR products

PCR was used to generate large quantities of defined target DNA for microarray production. Plasmids containing cloned genes were grown in *Escherichia coli* and were amplified using vector primers SK536 (5'-GCGAAGGGGGATGT-GCTG-3') and SK865 (5'-GCTCGTATGTTGTGTGGAA-3')

*To whom correspondence should be addressed. Tel: +1 510 739 2172; Fax: +1 510 739 2250; Email: seastman@incyte.com

(Operon Technologies, Alameda, CA). Briefly, 1 μ l of bacterial cell culture was added to 75 μ l of reaction buffer, containing 10 mM Tris-HCl pH 8.3, 1.5 mM MgCl₂, 50 mM KCl, 0.2 mM each dNTP, 0.5 μ M each primer and 2 U *Taq* polymerase. The mixture was incubated for 3 min at 95°C and 30 cycles of PCR were performed at 94°C for 30 s, 56°C for 30 s and 72°C for 90 s. A final incubation for 5 min at 72°C was followed by reduction of the temperature to 4°C in order to terminate the reaction. PCR products were then purified by centrifugal chromatography with Sephadex S400 resin (Amersham-Pharmacia Biotech, Uppsala, Sweden) in a 96-well format. Briefly, 400 μ l of S400 resin pre-equilibrated in 0.2 \times standard saline citrate buffer (SSC) was added to each well of a 96-well microtiter plate. A unique PCR product prepared as described above was loaded into each well and the plate was centrifuged in an Eppendorf 5810 centrifuge at 885 r.c.f. (relative centrifugal force). Purified PCR products were concentrated to dryness and resuspended in 10 μ l of H₂O. DNA was resolubilized by thermal cycling (five cycles of 85°C for 30 s and 20°C for 30 s).

Qualification and quantification of PCR products

PCR products were routinely analyzed for quality by agarose gel electrophoresis and samples that failed to amplify or had multiple bands were annotated in the GEMTools database management software (Incyte Genomics, Fremont, CA). PCR products were quantified using PicoGreen dye (Molecular Probes, Eugene, OR) in a fluorescent assay specific for measuring double-stranded DNA concentration according to the manufacturer's instructions.

Arraying and post-processing

Ten thousand PCR products were arrayed by high speed robotics (7) on amino-modified glass slides (M.Reynolds, unpublished results). Each element occupied a spot of ~150 μ m in diameter and spot centers were 170 μ m apart. DNA adhesion to the glass was achieved by irradiation in a Stratilinker Model 2400 UV illuminator (Stratagene, San Diego, CA) with light at 254 nm and an energy output of 120 000 μ J/cm². To minimize any potential non-specific probe interactions with the glass the microarrays were washed for 2 min in 0.2% SDS (Life Technologies, Rockville, MD), followed by three rinses in H₂O for 1 min each. The microarrays were treated with 0.2% (w/v) I-block (Tropix, Bedford, MA) in phosphate-buffered saline (PBS) for 30 min at 60°C. They were washed again for 2 min in 0.2% SDS, rinsed three times in H₂O for 1 min each and finally dried by a brief centrifugation. Dried microarrays were routinely stored in opaque plastic slide boxes at room temperature.

Array qualification: SYTO 61 dye

As SYTO 61 nucleic acid staining has generally been applied to cells, the standard procedure was modified to allow its use for measurement of DNA bound to microarrays. A 5 μ M stock solution of SYTO 61 dye (Molecular Probes) in DMSO was diluted 1:100 in 10 mM Tris-HCl pH 7, 0.1 mM EDTA (TE). Several microarrays from each manufactured batch were immersed in this solution for 5 min at room temperature, rinsed with TE, rinsed with H₂O and finally with absolute ethanol. After drying the microarrays were scanned on a GenePix 4000A scanner (Axon Instruments, Foster City, CA) at 535 nm.

mRNA preparation and probe synthesis

Briefly, mRNA was isolated by a single round of poly(A) selection using Oligotex resin (Qiagen, Valencia, CA) from commercially available human placenta, brain and heart total RNA (Biochain, San Leandro, CA). The purified mRNA was quantified using RiboGreen dye (Molecular Probes) in a fluorescent assay. RiboGreen dye was diluted 1:200 (v/v final) and mixed with known RNA concentrations (determined by absorbance at 260 nm) ranging from 1 to 5000 ng/ml. A Millennium RNA size ladder (Ambion, Austin, TX) was used to generate standard curves and unknown samples were diluted as necessary. Fluorescence was measured in 96-well plates with a FLUOstar fluorometer (BMG Lab Technologies, Germany) fitted with 485 nm (excitation) and 520 nm (emission) filters.

Between 25 and 100 ng mRNA were separated on an Agilent 2100 Bioanalyzer, a high resolution electrophoresis system (Agilent Technologies, Palo Alto, CA), to examine the mRNA size distribution. 200 ng of purified mRNA were converted to either a Cy3- or Cy5-labeled cDNA probe using a custom labeling kit (Incyte Genomics). Each reaction contained 50 mM Tris-HCl pH 8.3, 75 mM KCl, 15 mM MgCl₂, 4 mM DTT, 2 mM dNTPs (0.5 mM each), 2 μ g Cy3 or Cy5 random 9mer (Trilink, San Diego, CA), 20 U RNase inhibitor (Ambion), 200 U MMLV RNase H-free reverse transcriptase (Promega, Madison, WI) and mRNA. Correspondingly labeled Cy3 and Cy5 cDNA products were combined and purified on a size exclusion column, concentrated by ethanol precipitation and resuspended in hybridization buffer.

Array qualification: complex and vector-specific hybridizations

Hybridization of labeled cDNA probes was performed in 20 μ l of 5 \times SSC, 0.1% SDS, 1 mM DTT at 60°C for 6 h. Hybridization with a Cy3-labeled vector-specific oligonucleotide (5'-TTCCG-AGCTTGGCGTAATCATGGTCATAGCTGTTTCCTGTGTGAAATTGTTATCCGCTCA-3') (Operon Technologies) was performed at 10 ng/ μ l in 5 \times SSC, 0.1% SDS, 1 mM DTT at 60°C for 1 h. The microarrays were washed after hybridization in 1 \times SSC, 0.1% SDS, 1 mM DTT at 45°C for 10 min and then in 0.1 \times SSC, 0.2% SDS, 1 mM DTT at room temperature for 3 min. After drying by centrifugation, microarrays were scanned with an Axon GenePix 4000A fluorescence reader and GenePix image acquisition software (Axon) at 535 nm for Cy3 and 625 nm for Cy5. An image analysis algorithm in GEMTools software (Incyte Genomics) was used to quantify signal and background intensity for each target element. The ratio of the two corrected signal intensities was calculated and used as the differential expression ratio (DE) for this specific gene in the two mRNA samples.

The Axon scanner was calibrated using a primary standard and a secondary standard to account for the differences in scanner performance [laser and photomultiplier tube (PMT)] between the Cy3 and Cy5 channels. For the primary standard hundreds of probe samples were prepared that were fluorescently balanced in the Cy3 and Cy5 channels as determined by a Fluorolog3 fluorescence spectrophotometer (Instruments SA, Edison, NJ). These probes were hybridized to microarrays and the scanner PMTs were adjusted to give balanced fluorescence and the greatest dynamic range. Using these PMT values

a fluorescent plastic slide was scanned to obtain corresponding fluorescent values. This secondary standard was used to calibrate scanners on a daily basis.

Data acquisition and analysis

Two low frequency data correction algorithms were applied to compensate for systematic variations in data quality. The first procedure, a gradient correction algorithm, modeled the signal response surfaces of each channel. On a 10 000 element microarray the signal responses of Cy3 and Cy5 should be random due to the random physical location of the target elements. The signal response surfaces were first examined for non-random patterns. If non-random patterns were detected, a second order response model was applied to model the gene signal responses according to their positions on the surface. The non-randomness was then corrected using the fitted model. The second procedure, a signal correction algorithm, corrected for differential rates of incorporation of the Cy3 and Cy5 dyes. In an idealized homotypic hybridization, a scatter plot of log Cy3 signal versus log Cy5 signal should show a signal distribution along a line with a slope of 1. If the center line of the signals does not have a slope of 1 there may be different rates of incorporation of the Cy3 and Cy5 dyes. The signal correction algorithm tested whether the slope of the regression line for log Cy3 signal versus log Cy5 signal was 1 and applied a regression model to rotate the regression line to a slope of 1 if necessary.

RESULTS AND DISCUSSION

Impact of arrayed DNA concentration on DEs

Because of the competitive nature of two channel fluorescent hybridizations it has been assumed that the amount of target DNA deposited on the glass slide would have little or no impact on any observed DEs (15). We tested this assumption directly by hybridizing a series of samples at predetermined input ratios to microarrays containing varying amounts of target DNA. For these experiments the target DNAs were yeast fragments, a set of PCR products derived from the non-coding regions of *Saccharomyces cerevisiae*. The amount of PCR product was quantified using a fluorescent dye (PicoGreen) specific for double-stranded DNA. The targets were spotted in three sets containing quadruplicate points from a 2-fold dilution series of DNA concentrations ranging from 2.0 to 0.062 $\mu\text{g}/\text{well}$ (10 $\mu\text{l}/\text{well}$).

Probes for hybridization to the yeast fragments were made from T7 RNA transcripts of PCR products. Templates for *in vitro* transcription were made by incorporating a T7 promoter in the upstream PCR primer and poly(A) sequences in the downstream PCR primer. *In vitro* transcripts of the yeast fragments were purified, quantified and included in every labeling reaction at predetermined Cy3:Cy5 input levels (fragment 22, 123:4 pg; fragment 6, 123:123 pg; fragment 25, 4:123 pg). All probe labeling reactions were done in the presence of 200 ng poly(A) mRNA, from either human brain or heart (Biochain, Hayward, CA). Hybridization of these probes was performed on three different days, across 20 microarrays representing two different batches and by multiple operators. A comparison of the expected differential expression and the experimentally observed differential expression is shown in Figure 1. These results indicate that target DNA arrayed at input concentrations

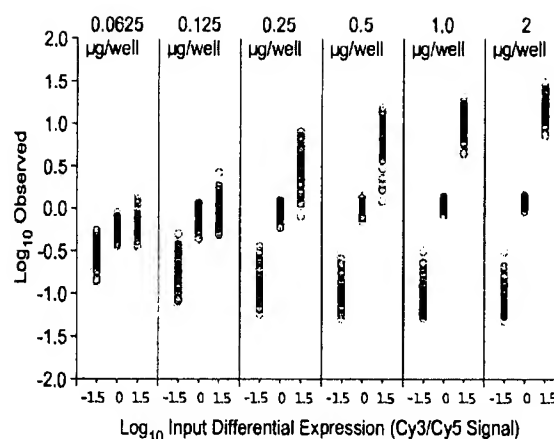


Figure 1. Impact of input DNA concentration on differential gene expression. A dilution series of PCR product for three yeast control fragments was arrayed in triplicate in each of four quadrants. The amount of PCR product in the well prior to arraying is indicated above each panel. Input RNA ratios for labeling with Cy3 versus Cy5 for the three fragments were 30:1, 1:1 and 1:30. The \log_{10} of observed differential expression is plotted as a function of \log_{10} of input RNA ratios.

<1.0 $\mu\text{g}/10 \mu\text{l}$ results in an underestimate or compression of the observed differential expression, with more compression occurring at lower DNA concentrations.

Quantification of DNA amplimers on the array by a hybridization-independent method

The DNA concentration of the input printing solutions may not be directly predictive of the amount of DNA actually retained on the glass. Variations in the transfer efficiency of individual DNA sequences to the glass and variations in its subsequent retention through the post-arraying and processing procedures may have an impact on the amount of DNA retained. Therefore, a second DNA staining assay was developed using SYTO 61 fluorescent dye, which directly measured the amount of DNA actually retained on the glass, independent of hybridization.

Qualification of 10 000 element cDNA microarrays

Based on the preliminary experiments we applied the PicoGreen and SYTO 61 assays to evaluate two independent 10 000 element microarrays (Fig. 2). Each of the 104 96-well plates used to print the arrays was qualified by PicoGreen analysis and all plate sets had high levels of PCR amplimer (>1.0 $\mu\text{g}/\text{well}$) (Fig. 2A). The plate sets used to prepare the HGG1 arrays, however, had a greater overall average DNA concentration than those used to prepare the UGV1 arrays: median 3.6 versus 1.85 $\mu\text{g}/\text{well}$, respectively.

An array from each batch was hybridized with a complex cDNA probe derived from placenta RNA in both the Cy3 and Cy5 channels. SYTO 61 staining was performed on an additional array from each batch and a comparison of the signal outputs for SYTO 61 and hybridization probes for both array batches is shown in Figure 2B and C. Observed hybridization signals were generally higher for the HGG1 array (Fig. 2C) as

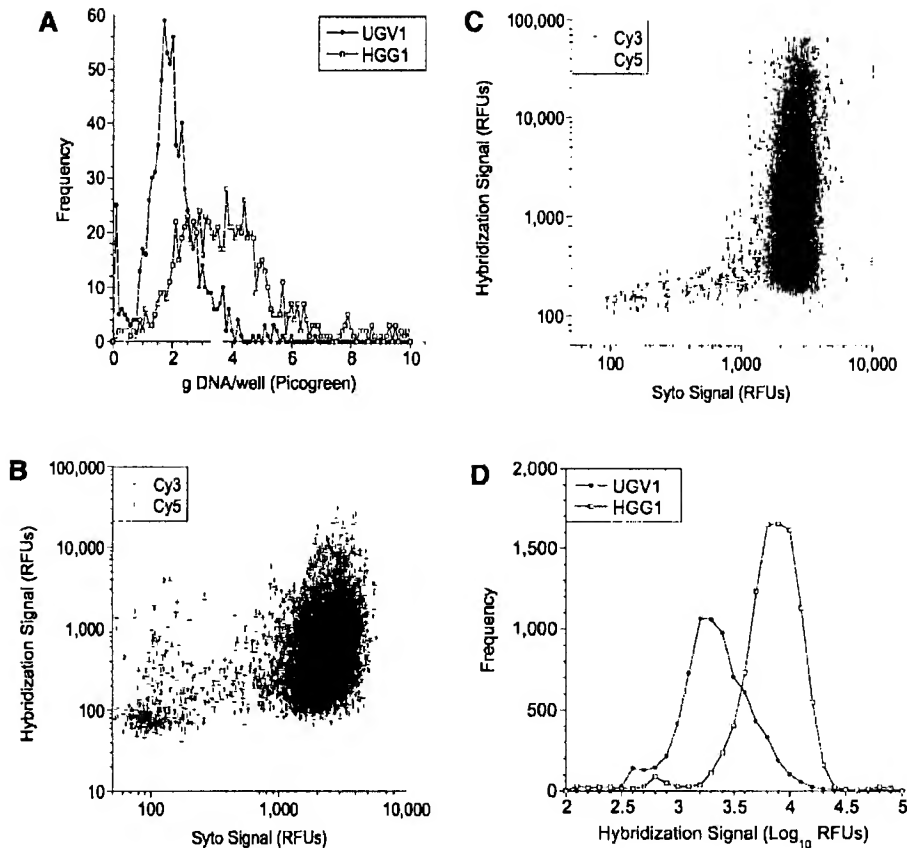


Figure 2. Quality control analysis of microarray batches. A set of eight wells randomly selected from each of 104 96-well plates from microarray types UGV1 and HGG1 was analyzed with PicoGreen. The distribution of DNA concentrations is shown in (A). The amount of hybridization signal with a complex probe (Cy3 Brain/Cy5 Heart) is shown as a function of the amount of DNA retained on the glass for microarray types UGV1 (B) and HGG1 (C). Signal distributions from hybridizations with a vector-specific oligonucleotide probe for each array type are shown in (D).

compared to the UGV1 array (Fig. 2B): median Cy3 1049 versus 310 relative fluorescence units (r.f.u.), median Cy5 1137 versus 302 r.f.u., respectively. This was consistent with the higher amount of DNA on the glass for the HGG1 array: median 2532 versus 1905 r.f.u. Higher hybridization signals (>10 000 r.f.u.) were routinely observed when the amount of target DNA bound to the glass approached 2000 r.f.u. by SYTO 61 staining (data not shown). In the examples shown, 35% of the elements on the UGV1 microarray have SYTO 61 stain values <2000 r.f.u., as compared to only 9% of the elements on the HGG1 array. There was an apparent discrepancy in the UGV1 microarray, 65% of all elements on the UGV1 array having higher levels of bound DNA but few yielding hybridization signals >10 000 r.f.u..

To address this issue a third assay was developed. An array from each batch was hybridized with a Cy3-labeled oligonucleotide probe specific for the common vector sequence found in all the PCR products. The signal distribution for these vector hybridizations is presented in Figure 2D. The majority of elements on the UGV1 microarray had significantly lower

hybridization signals than the HGG1 array: median 1901 versus 6507 r.f.u. These results correlated better with complex probe hybridization than SYTO 61 staining (Fig. 2B and C).

The manufacture of high quality, reproducible arrays with 10 000 or more unique PCR products is an expensive and time-consuming effort. It requires considerable attention to the details of each step in the process and defined procedures to ensure quality and reproducibility. The data presented in this report show that low concentrations of DNA in the input printing solutions result in reduced amounts of arrayed DNA and this, in turn, reduces the dynamic signal range and produces an apparent compression or underestimation of differential expression. The assay procedures reported here have been implemented in the large-scale production of microarrays for use in generating expression databases.

mRNA input

The impact of varying the amount of input mRNA on net cDNA probe synthesis and hybridization was evaluated. Placental mRNAs of varying amounts (25–400 ng) were

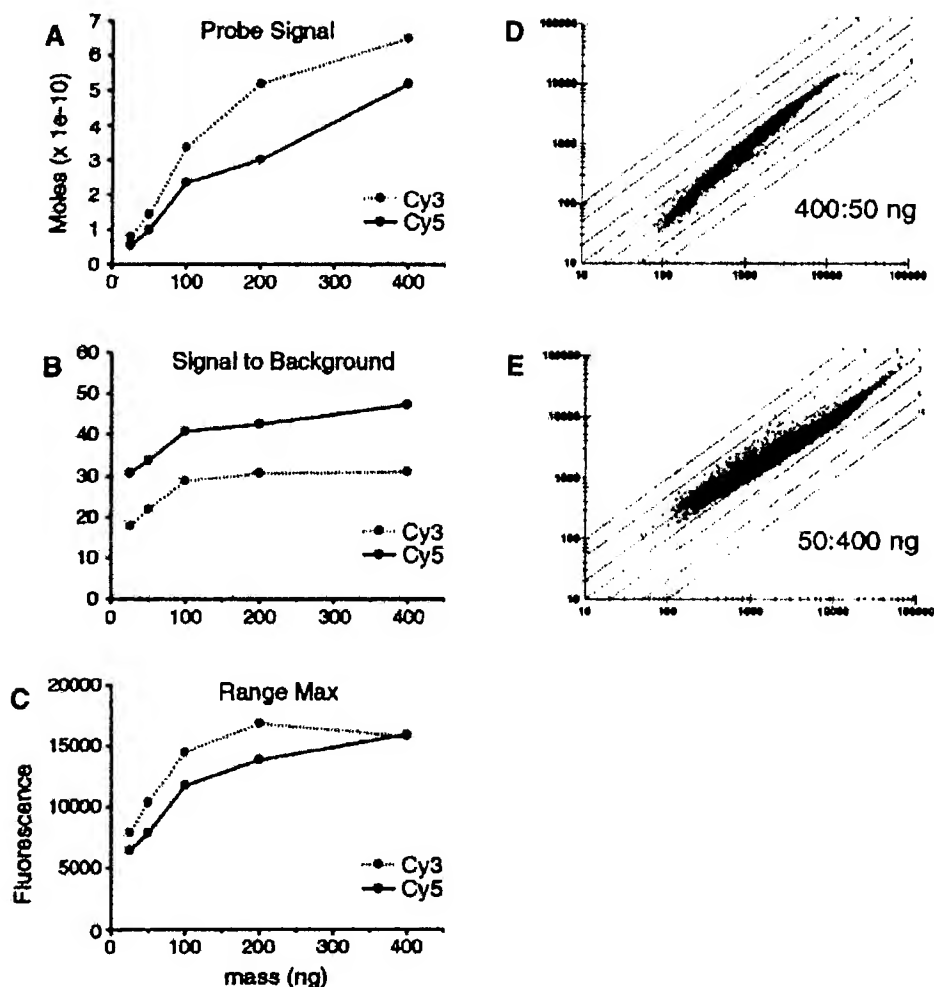


Figure 3. mRNA titration and balance. (A–C) Probe fluorescent signals, signal-to-background and dynamic range as a function of input mRNA mass. Duplicate labeling reactions containing equal amounts of placenta mRNA in both the Cy3 and Cy5 channels were labeled and hybridized to UniGEM V2 arrays. Each data point is an average from the two hybridizations. Probe fluorescence signal was converted to moles product using a standard curve. Range minimum values remained between 100 and 200 U for all hybridizations. (D and E) An aliquot of 50 or 400 ng placenta mRNA was labeled with Cy3 and hybridized to either 400 or 50 ng mRNA labeled with Cy5, respectively, in duplicate. Only one of the two hybridizations is shown. The axes are in arbitrary fluorescent units.

labeled with Cy3 and hybridized to an equal aliquot labeled with Cy5. Increasing the placental mRNA input yielded increasing amounts of total cDNA product (Fig. 3A). Hybridization signal-to-background and dynamic range also increased as the mRNA input increased, although a clear point of ‘diminishing returns’ occurs above 200 ng mRNA input (Fig. 3B and C). Based on this mRNA titration series, we believe that using 200 ng mRNA as the standard input for labeling reactions is the optimal amount. A representative example of a competitive hybridization with balanced RNA inputs (200:200 ng) is presented in Figure 4A.

We tested the effect of unbalanced competitive hybridization by hybridizing product prepared from different input levels of placental mRNA in the labeling process (Fig. 3D and E). We observed significant loss in precision and a distortion of the

population from the theoretical DE of 1, especially in the lower signal range. This distortion reflects both the impact of differential labeling and hybridization of transcripts with different amounts of mRNA input. Reversing the ratio of input mRNA for probe synthesis resulted in the opposite curvature (Fig. 3E). We conclude that accurate quantification and use of an equivalent mRNA mass for labeling in both channels is essential for optimum results.

Homotypic response

An estimate of the accuracy and precision of array-generated expression data was first made by performing a series of replicate experiments using various homotypic hybridizations. A competitive hybridization of fluorescently labeled Cy3 and Cy5 cDNA, both prepared from the same placental mRNA,

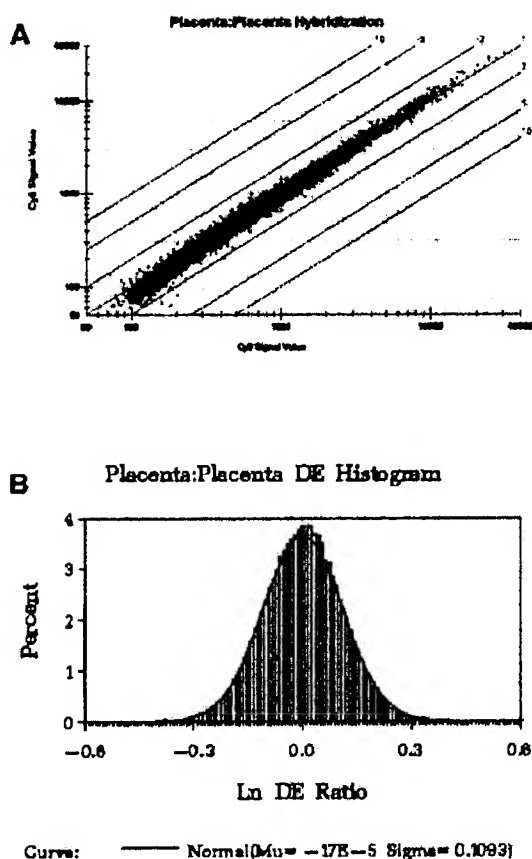


Figure 4. (A) Scatter plot of the calibrated Cy3 versus Cy5 fluorescence response from a typical placenta:placenta hybridization. The diagonal line through the origin corresponds to the expected DE of 1. The other diagonal lines define DE values as indicated next to the line. (B) Histogram showing the distribution of elements by \log_{10} of their experimentally derived DEs for 10 homotypic placental hybridizations.

should theoretically give a DE (or Cy3 fluorescence divided by Cy5 fluorescence) of 1 for all 10 000 elements arrayed on the slide. With replicate hybridizations we can evaluate the overall precision of the data using various statistical parameters and obtain an estimate of accuracy from any deviation(s) observed from the theoretical value.

A scatter plot of the Cy3- versus Cy5-calibrated fluorescent response from a single placenta:placenta hybridization is shown in Figure 4A. Virtually all gene elements lie close to the diagonal line corresponding to the expected DE of 1. Overall system response was observed to be linear over about three orders of magnitude.

Approximately 100 000 data points from 10 homotypic placenta hybridizations were used to construct a histogram showing the frequency or distribution of gene elements (as a percentage of the total) around \log_{10} of the expected DE ($\ln 1.0 = 0$). Effectively, the histogram (Fig. 4B) is a graphical measure of the range of the signal response for each selected element. The coefficient

of variation (CV), or relative standard deviation, provides a quantitative estimate of the precision of differential expression. The calculated CV for differential expression for all elements was 12% across the entire signal range. The same 12% variance was observed across two independently manufactured batches of cDNA microarrays (data not shown).

Ten similar homotypic hybridization experiments were conducted with both human brain and heart samples and the data were compared to the placenta results described above. Results for both sets of hybridizations were identical (data not shown). The same 12% CV for differential expression was observed independent of tissue type over the entire signal range.

Accuracy, in terms of bias, was estimated by calculating an average experimental DE directly from observed fluorescence output and comparing it to the expected value of 1.00. For each of the three tissue types above (placenta, brain and heart) the average ($n = 10$) experimental DE values were 0.999983, 0.99977 and 0.9998, respectively. The overall average was 0.9999, or less than 1 part in 10 000. These values are in good agreement not only within the group, but also with the expected theoretical value of 1.00.

The observed variation in individual element responses (from the expected DE = 0) for 180 randomly selected genes across the full range of observed signal response (as a function of Cy5 signal) is shown in Figure 5A–C for placenta, brain and heart tissue. For each of the 180 elements selected all 10 replicate data points are plotted for each gene from each tissue type. Regardless of tissue type we observed few data points with a differential expression greater than 2, even at low overall signal levels.

From the above data we can calculate the change in DE required before the value has statistical significance. Mathematically this can be written in terms of the two-sided statistical tolerance interval for the differential expression of non-differentiated elements (16). A statistical tolerance interval is one that contains a specified portion, p , of the entire sampled population with a specified degree of confidence, $100(1 - q)\%$. Table 1 shows the 99.5% tolerance intervals for 99% of the elements from each tissue type: all observed differential expression values fall between ± 1.4 .

Analysis of variance (ANOVA) was used to estimate the contribution of specific potential sources of variance to the overall variance measured. Analyses were performed using the method of restricted maximum likelihood under SAS for Windows v.6.12 procedure PROC MIXED (17). All of the homotypic placenta, brain and heart data sets were used for this analysis.

There are four general sources of variation in the DE ratios: microarray batch, array-to-array hybridization variance (including sample preparation), biological source tissue and gene sequence variance. Table 2 lists the estimated contribution of these potential sources of variation to the overall variance measured. The two sources contributing most significantly to the overall variation were hybridization variance and sequence variance. Hybridization variance represents a source of variation from hybridization to hybridization. Sequence variance indicates that different elements demonstrate different levels of variation. Microarray batches and source tissues were not significant sources of variance.

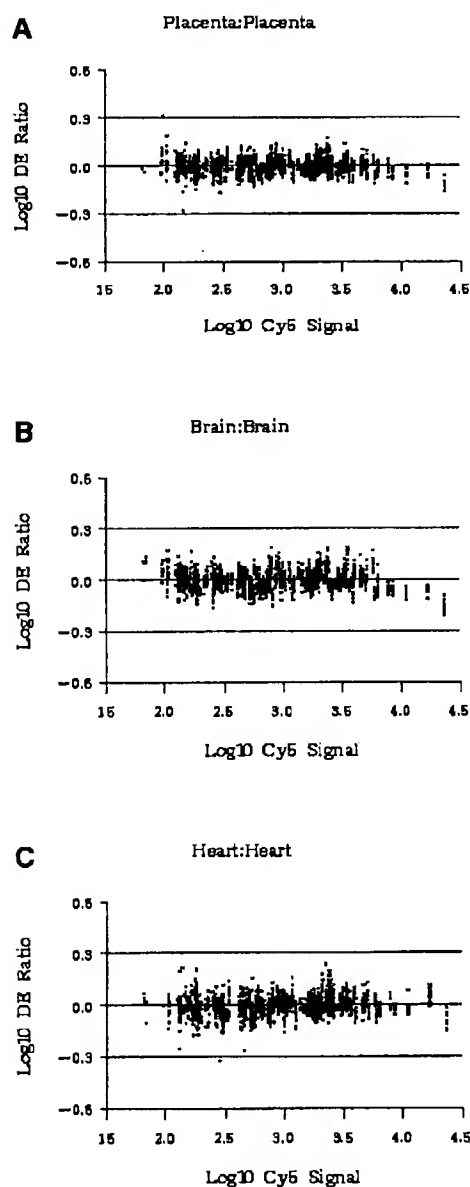


Figure 5. Variation in individual element responses for 180 randomly selected genes over the full range of observed signal response (expressed as log Cy5 signal). All 10 replicate data points for each selected element are plotted along the vertical axis. Horizontal lines define the tolerance interval outside of which DE was deemed significant (see text). (A) Homotypic placental hybridizations. (B) Homotypic brain hybridizations. (C) Homotypic heart hybridizations.

Differential expression

Using placental mRNA as a common reference, four sets of experimental conditions to measure differential expression were evaluated. Each set contained 10 replicate hybridizations: brain:placenta, placenta:brain, heart:placenta and placenta:heart. Estimates of system precision and detection limits were made as described above for the homotypic hybridizations.

Table 1. Tolerance intervals for homotypic hybridizations

Source	Tolerance interval
Placenta:placenta	(-1.332, 1.332)
Brain:brain	(-1.397, 1.397)
Heart:heart	(-1.384, 1.384)
All combined	(-1.370, 1.370)

The 99.5% tolerance intervals contain at least 99% of the elements on each microarray.

Table 2. Variance component estimation for homotypic hybridizations

Variation source	Estimated CV contribution
Microarray batch	0.0%
Source tissue	0.0%
Hybridization	7.8%
Gene sequence	9.4%
Total	12.0%

ANOVA was performed on placenta, brain and heart homotypic hybridizations.

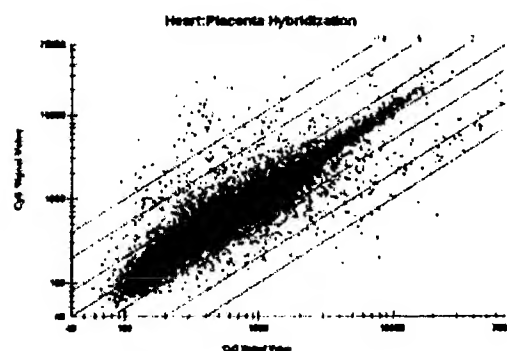


Figure 6. Scatter plot of Cy3-labeled cDNA from heart (x-axis) hybridized to the array with Cy5-labeled cDNA from placenta (y-axis) (single experiment). Compare with Figure 4A.

Figure 6 shows the fluorescence response plot of a single representative experiment conducted with Cy3-labeled cDNA from heart competitively hybridized to the array with Cy5-labeled cDNA prepared from placenta. Most of the elements (>90%) fell on or close to the 45° line representing no differential expression (or DE = 1.00). However, in contrast to the homotypic hybridizations (Fig. 4A), 10% of the elements were also observed to fall outside the tolerance interval, which may indicate significant differential expression (Table 1).

From 10 such replicate experiments in this set we calculated a CV for each of the 10 000 elements and plotted the values against the overall dynamic signal range (as a function of log Cy5 fluorescence signal) as shown in Figure 7A. The average CV was observed to be 10–12% across the entire signal range, although there was slightly greater variation at low signal

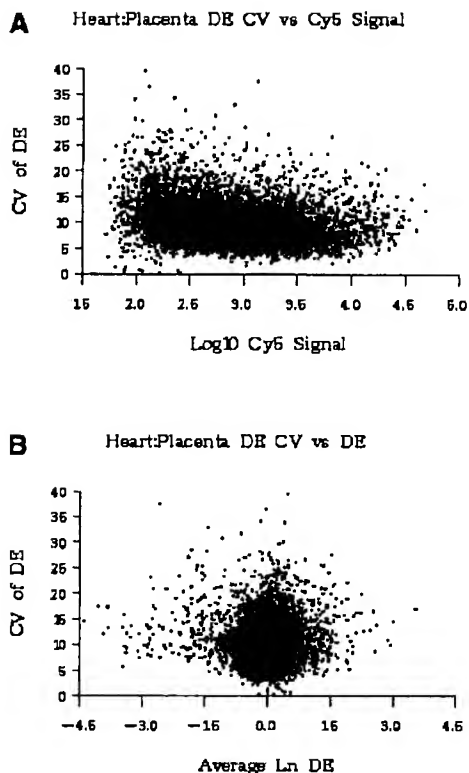


Figure 7. (A) CV for each of 10 000 elements derived from 10 replicate heart:placenta hybridizations plotted as a function of the average observed signal (as Cy5 signal). (B) CV for the same 10 000 elements plotted as a function of \log_{10} of the average observed DE (ln DE).

levels. Figure 7B shows the CV for the same 10 000 elements above plotted as a function of average DE. Most elements are observed to cluster near the value 0, indicating no differential expression. However, the CV of 12% observed for non-differentiated elements, on average, was slightly smaller than the CV for differentiated elements in either direction. The observed average CV ranged from 12% for non-differentiated elements to a maximum value of 25% for elements differentially expressed by a factor of 100. Since the DE is a ratio of the signals from the two channels, variations in the denominator at lower signal levels have a larger impact. Despite these minor differences, overall system precision remains excellent.

The same 180 random elements in Figure 5 were evaluated in 'reciprocal dye labeling' experiments. Theoretically, the Cy3- and Cy5-labeled primers should function equivalently for cDNA synthesis. However, any differences in incorporation of label would, if significant, identify differential expression where none exists. It could also account for some of the variation we observe in the different parameters evaluated in this study. Therefore, we performed a series of additional experiments specifically designed to address this issue.

The data from 10 replicates of the brain:placenta hybridizations were compared to the data from 10 replicates of the reciprocally labeled placenta:brain hybridizations. Figure 5A shows a plot

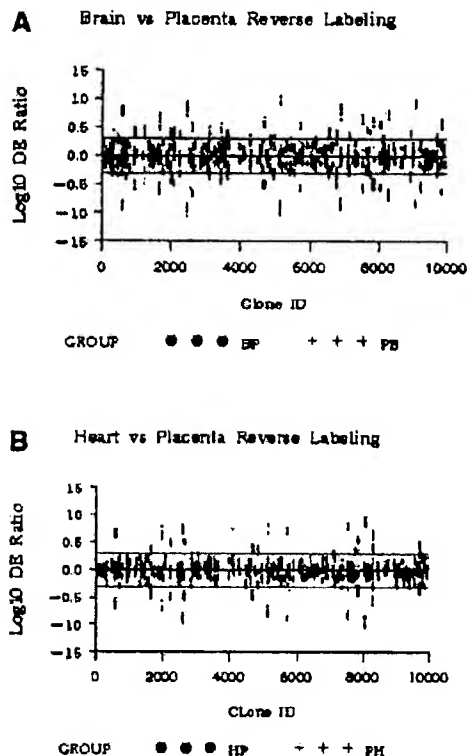


Figure 8. Reciprocal labeling experiments showing the data plotted from 180 random elements from (A) 10 replicate brain:placenta (black symbols) and 10 replicate placenta:brain (blue symbols) hybridizations versus log DE, and (B) 10 replicate heart:placenta (black) and 10 replicate placenta:heart (blue) hybridizations.

of the DE for 180 random elements from both sets of data. The DE for any given element in the first set of hybridizations should simply be the reciprocal of the DE for the same element in the second set (when the labeling is reversed). As Figure 8A shows, the cluster of 10 data points for each element from set 1 lies the same distance above the horizontal line through $\log_{10} 1.0 = 0$ as the corresponding cluster from set 2 lies below it. Figure 8B shows a similar plot generated from 20 microarrays, where 10 heart:placenta hybridizations were compared to the reciprocally labeled placenta:heart hybridizations, with essentially equivalent results.

For each element we can define the axial symmetry of reflection (ASR) as the inflection point between the DEs from the reciprocal labeling experiments, calculated by averaging the two DE ratios. Calculated average ASR values of 0.998 and 0.999 were obtained from the placenta:brain and placenta:heart data sets, respectively, in good agreement with the theoretical value of 1.00. Thus any systematic bias introduced into the DE by reciprocal labeling must be less than 1–2 parts in 1000. These results independently verify the precision in measuring differential expression, as well as in identifying those genes that are not differentially expressed. Histograms showing the distribution of all elements (as a percentage of the total) as a function of ln ASR (Fig. 9A and B) were similar to the histogram

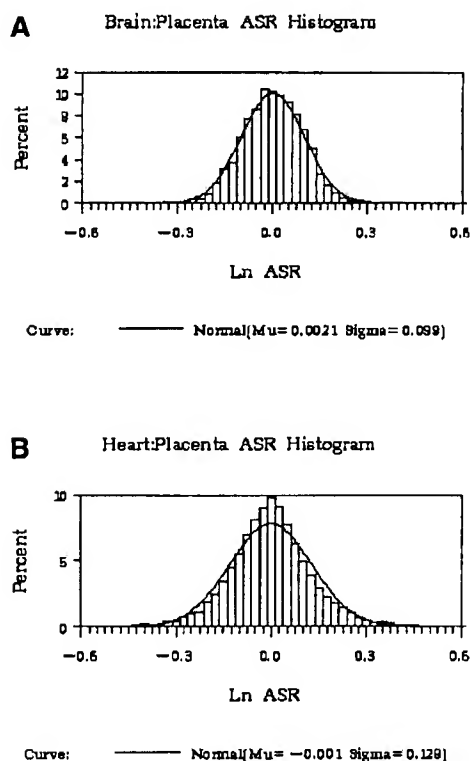


Figure 9. Histograms showing the distribution of all elements as a function of \ln ASR from reciprocal labeling experiments. (A) Data for brain:placenta and placenta:brain hybridizations. (B) Data for heart:placenta and placenta:heart hybridizations.

observed for non-differentiated elements (Fig. 4B). They also had the same standard deviation. Therefore, any variation observed in DE was likely a result of real variations in experimental mRNA levels, rather than an artifact of the labeling system.

A series of independent yeast standards was also included on each microarray to assist in evaluating overall system performance. These controls demonstrated linearity in overall signal response over three orders of magnitude, a CV of 12% and a limit of detection of 2 pg mRNA at a signal-to-background ratio of 2.5 (data not shown).

CONCLUSION

In this report we have described measures important in the manufacture of cDNA microarrays and in the preparation and labeling of mRNAs for use in a two-channel hybridization system. Furthermore, the results presented in this report demonstrate in a quantitative fashion the performance of the cDNA microarray technology platform. The usefulness of any expression database is ultimately dependent on the quality of the underlying data used to construct it. We report that the cDNA microarray platform does provide the high quality data needed to establish reliable gene expression databases.

The analytical methods used to evaluate the performance of the cDNA microarray platform described in this report provide a practical framework for evaluating the performance of other technologies that purport to measure global mRNA expression. Only by disclosing the performance characteristics in a rigorous manner can researchers gauge the utility of any data produced by other platforms.

ACKNOWLEDGEMENTS

We thank the Incyte Microarray Production Facility (Fremont, CA) for manufacturing the microarrays, preparing the probes and performing the hybridizations used in this report. We also thank Drew Watson for providing resources and his encouragement to complete these experiments and Jeanne Loring for useful discussions.

REFERENCES

1. Zweiger, G. (1999) Knowledge discovery in gene-expression-microarray data: mining the information output of the genome. *Trends Biotechnol.*, **17**, 429–436.
2. Strachan, T., Abitbol, M., Davidson, D. and Beckmann, J.S. (1997) A new dimension for the human genome project: towards comprehensive expression maps. *Nat. Genet.*, **16**, 126–132.
3. Khan, J., Bittner, M.L., Chen, Y., Meltzer, P.S. and Trent, J.M. (1999) DNA microarray technology: the anticipated impact on the study of human disease. *Biochim. Biophys. Acta*, **1423**, M17–M28.
4. Marra, M., Hillier, L., Kucaba, T., Allen, M., Burstead, R., Beck, C., Blistain, A., Bonaldo, M., Bowers, Y., Bowles, L. et al. (1999) An encyclopedia of mouse genes. *Nat. Genet.*, **21**, 191–194.
5. Aach, J., Rindone, W. and Church, G.M. (2000) Systematic management and analysis of yeast gene expression data. *Genome Res.*, **10**, 431–445.
6. The FlyBase Consortium (1999) FlyBase. The FlyBase database of the Drosophila Genome Projects and community literature. *Nucleic Acids Res.*, **27**, 85–88.
7. Schena, M., Shalon, D., Davis, R.W. and Brown, P.O. (1995) Quantitative monitoring of gene expression patterns with a complementary DNA microarray. *Science*, **270**, 467–470.
8. Lockhart, D.J., Dong, H., Byrne, M.C., Follettie, M.T., Gallo, M.V., Chee, M.S., Mittmann, M., Wang, C., Kobayashi, M., Horton, H. and Brown, E.L. (1996) Expression monitoring by hybridization to high-density oligonucleotide arrays. *Nat. Biotechnol.*, **14**, 1675–1680.
9. Velculescu, V.E., Zhang, L., Vogelstein, B. and Kinzler, K.W. (1995) Serial analysis of gene expression. *Science*, **270**, 484–487.
10. Adams, M.D., Kelley, J.M., Gocayne, J.D., Dubnick, M., Polymeropoulos, M.H., Xiao, H., Merril, C.R., Wu, A., Old, B., Moreno, R.F. et al. (1991) Complementary DNA sequencing: expressed sequence tags and human genome project. *Science*, **252**, 1651–1656.
11. Brenner, S., Johnson, M., Bridgman, J., Golda, G., Lloyd, D.H., Johnson, D., Luo, S., McCurdy, S., Foy, M., Ewan, M. et al. (2000) Gene expression analysis by massively parallel signature sequencing (MPSS) on microbead arrays. *Nat. Biotechnol.*, **18**, 630–634.
12. Sutcliffe, J.G., Foy, P.E., Erlander, M.G., Hilbush, B.S., Bodzin, L.J., Durham, J.T. and Hasel, K.W. (2000) TOGA: an automated parsing technology for analyzing expression of nearly all genes. *Proc. Natl. Acad. Sci. USA*, **97**, 1976–1981.
13. Bartosiewicz, M., Trounstein, M., Barker, D., Johnston, R. and Buckpitt, A. (2000) Development of a toxicological gene array and quantitative assessment of this technology. *Arch. Biochem. Biophys.*, **376**, 66–73.
14. Evertsz, E., Starink, P., Gupta, R. and Watson, D. (2000) Technology and applications of gene expression microarrays. In Schena, M. (ed.), *Microarray Biochip Technology*. Eaton Publishing, Natick, MA, pp. 149–166.
15. Winzler, E.A., Schena, M. and Davis, R.W. (1999) Fluorescence-based expression monitoring using microarrays. *Methods Enzymol.*, **306**, 3–18.
16. Hahn, G.J. and Meeker, W.Q. (1991) *Statistical Intervals: A Guide for Practitioners*. John Wiley & Sons, New York.
17. Littell, R.C., Milliken, G.A., Stroup, W.W. and Wolfinger, R.D. (1996) *SAS System for Mixed Models*. SAS Institute, Cary, NC.

EXHIBIT C

REPORTS

- reached. This approach was used to estimate relative maximum leaf size during the period of study (Fig. 3).
29. The threshold for thermal damage of nonsucculent leaves (45° to 52°C) is a highly conserved characteristic across a wide range of extant taxa [W. Larcher, in *Ecophysiology of Photosynthesis*, E. D. Schulze and M. M. Caldwell, Eds. (Springer-Verlag, Berlin, 1994), pp. 261–277; Y. Gauslaa, *Holarct. Ecol.* 7, 1 (1984)], implying little evolutionary change through time.
 30. T. A. Mansfield, A. M. Hetherington, C. J. Atkinson, *Annu. Rev. Plant Physiol. Plant Mol. Biol.* 41, 55 (1990).
 31. A review of fossil Ginkgoalean leaves revealed that species with the most dissected leaves, characterized by multidichotomies 0.5 to 2 mm wide, are restricted to Late Triassic to early Middle Jurassic facies [T. Kimura, G. Naito, T. Ohana, *Bull. Natl. Sci. Mus. Tokyo* 9, 91 (1983)].
 32. The cause of T-J floral turnover has traditionally been attributed to a sedimentary hiatus (3). However, this hypothesis is unsupported by sedimentological evidence [G. Dam and F. Surlyk, *Geology* 20, 749 (1992); *Spec. Publ. Int. Assoc. Sedimentol.* 18, 4189 (1993)], which identifies no major facies changes or unconformities between the T-J strata in Greenland. Furthermore, the absence of the upper Rhaetian *Riccia-parites*-*Polypodsporites* acme zone [W. M. L. Schuurman, *Rev. Palaeobot. Palynol.* 23, 159 (1977)] in Greenland (10) and Sweden (11), which has also been tentatively interpreted as evidence of a hiatus at both localities, is questionable, as acme zones are generally considered of only local use, owing to the effects of ecological, environmental, and postdepositional processes on relative pollen abundances.
 33. The value of $\delta^{13}\text{C}$ is

$$\delta^{13}\text{C} = \left(\frac{({}^{13}\text{C}_{\text{unk}}/{}^{12}\text{C}_{\text{unk}})}{({}^{13}\text{C}_{\text{std}}/{}^{12}\text{C}_{\text{std}})} - 1 \right) \times 1000$$

where unk the ratio of unknown to sample and std is the ratio of the pee dee belemnite standard.

34. F. M. Grandstein et al., *J. Geophys. Res.* 99, 24051 (1994).
35. We thank E. M. Frills (Swedish Museum of Natural History) and S. Funder (Danish Geological Museum) for loans and provision of fossil leaves; P. E. Olsen, F. Surlyk, W. G. Chaloner, D. J. Read, R. A. Spicer, C. K. Kelly, and P. Wignall for comments on earlier versions; and the isotope Laboratory at Royal Holloway College, University of London, for making measurements of $\delta^{13}\text{C}$. We gratefully acknowledge funding from the Natural Environment Research Council, UK (GR9/02930), and through Royal Society Research Fellow and Equipment grants to D.J.B.

21 April 1999; accepted 26 July 1999

Gene Expression Profile of Aging and Its Retardation by Caloric Restriction

Cheol-Koo Lee,^{1,3} Roger G. Klopp,²
Richard Weindruch,^{4*} Tomas A. Prolla^{3*}

The gene expression profile of the aging process was analyzed in skeletal muscle of mice. Use of high-density oligonucleotide arrays representing 6347 genes revealed that aging resulted in a differential gene expression pattern indicative of a marked stress response and lower expression of metabolic and biosynthetic genes. Most alterations were either completely or partially prevented by caloric restriction, the only intervention known to retard aging in mammals. Transcriptional patterns of calorie-restricted animals suggest that caloric restriction retards the aging process by causing a metabolic shift toward increased protein turnover and decreased macromolecular damage.

Most multicellular organisms exhibit a progressive and irreversible physiological decline that characterizes senescence, the molecular basis of which remains unknown. Postulated mechanisms include cumulative damage to DNA leading to genomic instability, epigenetic alterations that lead to altered gene expression patterns, telomere shortening in replicative cells, oxidative damage to critical macromolecules by reactive oxygen species (ROS), and nonenzymatic glycation of long-lived proteins (1, 2).

Genetic manipulation of the aging process in multicellular organisms has been achieved in *Drosophila* through the overexpression of

catalase and Cu/Zn superoxide dismutase (3), in the nematode *Caenorhabditis elegans* through alterations in the insulin receptor signaling pathway (4), and through the selection of stress-resistant mutants in either organism (5). In mammals, mutations in the Werner Syndrome locus (WRN) accelerate the onset of a subset of aging-related pathology in humans (6), but the only intervention that appears to slow the intrinsic rate of aging is caloric restriction (CR) (7). Most studies have involved laboratory rodents which, when subjected to a long-term, 25 to 50% reduction in calorie intake without essential nutrient deficiency, display delayed onset of age-associated pathological and physiological changes and extension of maximum lifespan. Postulated mechanisms of action include increased DNA repair capacity, altered gene expression, depressed metabolic rate, and reduced oxidative stress (7).

To examine the molecular events associated with aging in mammals, we used oligonucleotide-based arrays to define the transcriptional response to the aging process in mouse gastrocnemius muscle. Our choice of tissue was guided by the fact that skeletal muscle is primarily composed of long-lived, high oxygen-consuming postmitotic cells, a

feature shared with other critical aging targets such as heart and brain. Loss of muscle mass (sarcopenia) and associated motor dysfunction is a leading cause of frailty and disability in the elderly (8). At the histological level, aging of gastrocnemius muscle in mice is characterized by muscle cell atrophy, variations in size of muscle fibers, presence of lipofuscin deposits, collagen deposition, and mitochondrial abnormalities (9).

A comparison of gastrocnemius muscle from 5-month (adult) and 30-month (old) mice (10–12) revealed that aging is associated with alterations in mRNA levels, which may reflect changes in gene expression, mRNA stability, or both. Of the 6347 genes surveyed in the oligonucleotide microarray, only 58 (0.9%) displayed a greater than twofold increase in expression levels as a function of age, whereas 55 (0.9%) displayed a greater than twofold decrease in expression. These findings are in agreement with a differential display analysis of gene expression in tissues of aging mice (13). Thus, the aging process is unlikely to be due to large, widespread alterations in gene expression.

Functional classes were assigned to genes displaying the largest alterations in expression (Table 1). Of the 58 genes that increased in expression with age, 16% were mediators of stress responses, including the heat shock factors Hsp71 and Hsp27, protease Do, and the DNA damage-inducible gene GADD45 (14). The largest differential expression between adult and aged animals (a 3.8-fold induction) was observed for the gene encoding the mitochondrial sarcomeric creatine kinase, a critical target for ROS-induced inactivation (15).

A consequence of skeletal muscle aging is loss of motor neurons followed by reinnervation of muscle fibers by the remaining intact neuronal units (16). Genes involved in neuronal growth accounted for 9% of genes highly induced in 30-month-old animals, including neurotrophin-3 (17), a growth factor induced during reinnervation, and synaptic vesicle protein-2, implicated in neurite extension (18). PEA3, a transcriptional factor induced in the response to

¹Environmental Toxicology Center, ²Institute on Aging, ³Departments of Genetics and Medical Genetics, University of Wisconsin, Madison, WI 53706, USA.

⁴Department of Medicine and Wisconsin Regional Primate Research Center, University of Wisconsin, Madison, WI and Veterans Administration Hospital, Geriatric Research, Education and Clinical Center, Madison, WI 53705, USA.

*To whom correspondence should be addressed at Department of Medicine, VA Hospital (GRECC 4D), 2500 Overlook Terrace, Madison, WI 53705, USA. E-mail: rweindr@facstaff.wisc.edu (R.W.); Departments of Genetics and Medical Genetics, 445 Henry Mall, University of Wisconsin, Madison, WI 53706, USA. E-mail: taprolla@facstaff.wisc.edu (T.A.P.)

REPORTS

muscle injury and previously shown to be highly expressed in muscle from old rats (19), was also induced in aged muscle. We also observed parallels between our results and data from fibroblasts undergoing in vitro replicative senescence. For example, HIC-5, a transcriptional factor induced by oxidative damage, and insulin-like growth factor binding protein, both associated with in vitro senescence (20), are induced in aged skeletal muscle.

Fifty-five (0.9%) genes displayed a greater than twofold age-related decrease in expression. Genes involved in energy metabolism accounted for 13% of these alterations (Table 1). These include alterations in genes associated with mitochondrial function and turnover, such as the adenosine 5'-triphosphate (ATP) synthase A chain and nicotinamide adenine dinucleotide phosphate (NADP) transhydrogenase genes (both involved in mitochondrial bioenergetics), the LON protease implicated in mito-

chondrial biogenesis, and the ERV1 gene involved in mitochondrial DNA (mtDNA) maintenance (21). Additionally, a decrease in metabolic activity is suggested through a decline in the expression of genes involved in glycolysis, glycogen metabolism, and the glycerophosphate shunt (Table 1).

Aging was also characterized by large reductions (twofold or more) in the expression of biosynthetic enzymes such as squalene synthase (fatty acid and cholesterol synthesis), stearoyl-coenzyme A (CoA) desaturase (polyunsaturated fatty acid synthesis), and EF-1-gamma (protein synthesis). This suppression was accompanied by a concerted decrease in the expression of genes involved in protein turnover, such as the 20S proteasome subunit, the 26S proteasome component TBP1, ubiquitin-thioesterase, and the Unp ubiquitin-specific protease, all of which are involved in the ubiquitin-proteasome pathway of protein turn-

over (22). The directions of changes in other functional categories, such as signal transduction, and transcriptional and growth factors, did not present a consistent age-related trend.

In order to study the effects of CR on the gene expression profile of aging, we reduced caloric intake of C57BL/6 mice to 76% of that fed to control animals in early adulthood (2 months of age), and this dietary regimen was maintained until animals were killed at 30 months. A comparison of 30-month-old control and CR mice revealed that aging-related changes in gene expression profiles were remarkably attenuated by CR. Of the largest age-associated alterations (twofold or higher), 29% were completely prevented by CR and 34% were partially suppressed (Table 1). Of the four major gene classes that displayed consistent age-associated alterations, 84% were either completely or partially suppressed by CR. Thus, at the molecular level,

Table 1 (left). Aging-related changes in gene expression in gastrocnemius muscle. The extent to which caloric restriction prevented age-associated alterations in gene expression is denoted as either C (complete, >90%), N (none), or partial (20 to 90%, percentage effect indicated). The fold increase shown represents the average of all nine possible pairwise comparisons among individual mice determined by means of a specific algorithm (12). GenBank accession numbers are listed under ORF. A more comprehensive list that includes genes

that did not fit into the six classes can be found at www1.genetics.wisc.edu/prolla/Prola_Tables.html. **Table 2 (right).** Caloric restriction-induced alterations in gene expression. The data represent a comparison between 30-month-old CR-fed and control-fed mice. The gene expression alterations listed in this Table are diet related and do not include those representing prevention of age-associated changes (see Table 1). Additional CR-induced changes are posted at the aforementioned Web site.

ORF	Δ Age (fold)	Gene	Function	CR Prevention	ORF	Δ CR (fold)	Gene	Function
W08057	↑ 3.5	Heat Shock 27 kDa Protein	Chaperone	C	U05809	↑ 4.5	Transketolase	Pentose phosphate pathway
M17790	↑ 3.5	Serum Amyloid A Isoform 4	Unknown	N	W53351	↑ 4.1	Fructose-bisphosphate Aldolase	Glycolysis/Gluconeogenesis
AA114578	↑ 3.4	Heat Shock 71 kDa Protein	Chaperone	C	AA071778	↑ 3.5	Glucose-6-Phosphate isomerase	Glycolysis/Gluconeogenesis
L28177	↑ 2.8	GADD45	DNA damage response	77%	U34295	↑ 2.3	Glucose Dependent Insulinotropic Polypeptide	Insulin sensitizer
M74570	↑ 2.4	Aldehyde Dehydrogenase II	Aldehyde detoxification	29%	U01841	↑ 2.3	Peroxisome Proliferator Receptor Gamma	Insulin sensitizer
AA059852	↑ 2.2	Protease Do Precursor	Protease	C	L28118	↑ 2.0	PPAR Delta	Peroxisome induction
L22482	↑ 2.2	HIC-5	Senescence and differentiation	C	O42063	↑ 1.9	Fructose 1,8-bisphosphatase	Gluconeogenesis
X99963	↑ 2.2	rhoB	Unknown	87%	AA041828	↑ 1.9	Protein Phosphatase Inhibitor 2 (IPP-2)	Inhibition of glycogen synthesis
X65627	↑ 2.1	TN2	RNA metabolism	64%	U37091	↑ 1.8	Carbonic Anhydrase IV	CO ₂ disposal
X67277	↑ 1.8	Rac1	JNK activator	C	M13366	↑ 1.8	Glycerophosphate Dehydrogenase	Electron transport to mitochondria
AA071777	↑ 3.8	Synaptic Vesicle Protein 2	Neurite extension	51%	AA119888	↑ 1.7	Pyruvate Kinase	Glycolysis
X53257	↑ 2.5	Neurotrophin-3	Reinnervation of muscle	60%	AA145829	↑ 2.3	26S Proteasome Subunit TBP-1	Protein turnover
X78197	↑ 2.2	AP-2 Beta	Neurogenesis	N	AA107752	↑ 2.2	Elongation Factor 1-gamma	Protein synthesis
X89749	↑ 2.1	mTGF	Differentiation	C	C W53731	↑ 2.1	Signal Recognition Receptor Alpha Subunit	Protein synthesis
AA014024	↑ 2.1	Dynactin	Transport	55%	U60328	↑ 2.1	Proteasome Activator PA28 Alpha Subunit	Protein turnover
X63190	↑ 2.1	PEA3	Response to muscle injury	C	X59990	↑ 2.0	mCyp-S1 (Cytochrome P450)	Protein folding
AA106112	↑ 3.8	Mitochondrial Sarcomeric Creatine Kinase	ATP generation	C	W08293	↑ 1.9	Translocin-Associated Protein Delta	Protein translocation
AA061888	↑ 2.0	Dihydropyridine-sensitive L-type Calcium Channel	Calcium channel	67%	W57495	↑ 1.8	60S Ribosomal Protein L23	Protein synthesis
AA061310	↓ 4.1	Mitochondrial LON Protease	Mitochondrial biogenesis	C	X13135	↑ 4.7	Fatty Acid Synthase	Fatty acid synthesis
W55037	↓ 2.9	Alpha Enolase	Glycolysis	68%	X16314	↑ 2.5	Glutamine Synthetase	Glutamine synthesis
V00719	↓ 2.6	Alpha-Amylase-1	Carbohydrate metabolism	N	AA137859	↑ 2.4	Cytochrome P450-11C12	Steroid biosynthesis
M81475	↓ 2.6	Phosphoprotein Phosphatase	Glycogen metabolism	C	L32973	↑ 2.0	Thymidylate Kinase	dTTP synthesis
AA034642	↓ 2.1	ERV1	mtDNA maintenance	46%	X56548	↑ 2.0	Purine Nucleoside Phosphorylase	Purine turnover
AA106408	↓ 2.0	ATP Synthase A Chain	ATP synthesis	N	AA022083	↑ 2.0	Huntingtin	Unknown
AA041828	↓ 2.0	IPP-2	Glycogen metabolism	C	D78440	↑ 1.9	Necdin	Growth suppressor
L27842	↓ 2.0	PMP35	Peroxisome assembly	80%	AA062328	↓ 3.4	DnaJ Homolog 2	Chaperone
Z49204	↓ 2.0	NADP Transhydrogenase	Glycerophosphate shunt	N	X63023	↓ 1.9	Cytochrome P-450-IIIa	Detoxification
AA071776	↓ 1.9	Glucose-6-Phosphate isomerase	Glycolysis	C	U03283	↓ 1.8	Cyp1b1 Cytochrome P450	Detoxification
M13366	↓ 1.9	Glycerophosphate Dehydrogenase	Glycerophosphate shunt	C	U14390	↓ 1.8	Aldehyde Dehydrogenase-3	Detoxification
AA107752	↓ 2.9	EF-1-Gamma	Protein synthesis	83%	X78850	↓ 1.8	MAPKAP2	Unknown
U22031	↓ 2.6	20S Proteasome Subunit	Protein turnover	44%	D26123	↓ 1.7	Carbonyl Reductase	Detoxification
AA061604	↓ 2.2	Ubiquitin Thioesterase	Protein turnover	C	L4406	↓ 1.7	Hsp106-beta	Chaperone
AA145829	↓ 2.1	26S Proteasome Component TBP1	Protein turnover	C	U40930	↓ 1.5	Oxidative Stress-Induced Protein	Unknown
L00681	↓ 2.1	Unp Ubiquitin Specific Protease	Protein turnover	N	U68887	↓ 1.8	RAD50	Double strand break repair
U35741	↓ 2.0	Rhodanese	Mitochondrial protein folding	C	AA059718	↓ 1.7	DNA Polymerase Beta	Base excision repair
D63585	↓ 1.7	Proteasome Z Subunit	Protein turnover	C	W42234	↓ 1.8	XPE	Nucleotide excision repair
D76440	↓ 2.9	Necdin	Neuronal growth suppressor	47%	D43884	↓ 1.8	Math-1	Differentiation
X75014	↓ 2.7	Phox2 Homeodomain Protein	Throphic factor	65%	D18464	↓ 1.7	HES-1	Differentiation
M32240	↓ 2.1	GAS3	Myelin protein	55%	W13191	↓ 1.6	Thyroid Hormone Receptor Alpha-2	Thyroid hormone receptor
M18465	↓ 3.4	Calpastin I Light Chain	Calcium effector	C				
L34611	↓ 2.3	PTHR	Calcium homeostasis	N				
AA103355	↓ 2.2	Calmodulin	Calcium effector	N				
D29018	↓ 8.4	Squalene Synthase	Cholesterol/fatty acid synthesis	52%				
M21285	↓ 2.1	Stearyl-CoA Desaturase	PUFA synthesis	C				
U73744	↓ 2.1	HSP70	Chaperone	N				

■ Energy Metabolism ■ Protein Metabolism ■ Biosynthesis
 ■ Neuronal Factors ■ Stress Response ■ Calcium Metabolism

REPORTS

CR mice appear to be biologically younger than animals receiving the control diet.

Caloric restriction induced a metabolic reprogramming characterized by a transcriptional shift toward energy metabolism, increased biosynthesis, and protein turnover (Table 2). CR resulted in the induction of 51 genes (1.8-fold or higher) as compared with age-matched animals consuming the control diet. Nineteen percent of genes in this class are related to energy metabolism. Modulation of energy metabolism was evident through the induction of glucose-6-phosphate isomerase (glycolysis), fructose 1,6-bisphosphatase (gluconeogenesis), IPP-2 (an inhibitor of glycogen synthesis), and transketolase. Fructose 1,6-bisphosphatase switches the direction of a key regulatory step in glycolysis toward a biosynthetic precursor, glucose-6-phosphate. Remarkably, this same adaptation has been observed as part of the transcriptional reprogramming of *Saccharomyces cerevisiae* accompanying the diauxic switch from anaerobic growth to aerobic respiration upon depletion of glucose (23). Transketolase, which controls the nonoxidative branch of the pentose phosphate pathway, provides NADPH for biosynthesis and reducing power for several antioxidant systems. CR also induced transcripts associated with fatty acid metabolism, such as fatty acid synthase and PPAR- δ , a mediator of peroxisome proliferation. Interestingly, CR may act to increase insulin sensitivity through the induction of glucose-dependent insulinotropic peptide and PPAR- γ , a potent insulin sensitizer (24).

Biosynthetic ability also appears to be induced in CR mice. CR up-regulated the expression of glutamine synthase, purine nucleoside phosphorylase (purine turnover), and thymidylate kinase (dTTP synthesis). Remarkably, 16% of transcripts highly induced by CR encode proteins involved in protein synthesis and turnover, including elongation factor 1- γ , proteasome activator PA28,

translocon-associated protein delta, 60S ribosomal protein L23, and the 26S proteasome subunit TBP-1.

CR was associated with a 1.6-fold or greater reduction in expression of 57 genes. Of these, 12% were associated with stress responses or DNA repair pathways, or both (Table 2). Among the 6347 genes examined, the most substantial suppression of gene expression by CR was for a murine DnJ homolog (3.4-fold), a pivotal and inducible heat shock factor that senses and transduces the presence of misfolded or damaged proteins in bacteria (25). CR also lowered the expression of cytochrome P450 isoforms IIIA and Cyp1b1 (involved in detoxification), Hsp105 (a heat shock factor), aldehyde dehydrogenase (an inducible enzyme involved in detoxification of metabolic by-products), and an oxidative stress-induced protein of unknown function. CR reduced the expression of several DNA repair genes including XPE (a factor that recognizes multiple DNA adducts), RAD50 (involved in double-strand break repair), and DNA polymerase- β (a DNA damage-inducible polymerase). We also find molecular evidence to support a state of lower basal metabolic rate in CR mice through lowered expression of the thyroid-hormone receptor alpha gene (26).

The data presented here provide the first global assessment of the aging process in mammals at the molecular level and underscore the utility of large-scale, parallel gene expression analysis in the study of complex biological phenomena. We estimate that the 6347 genes analyzed in this study represent 5 to 10% of the mouse genome. Additional classes of aging-related genes in skeletal muscle may be discovered with the development of higher density mammalian DNA microarrays. The observed collection of gene expression alterations in aging skeletal muscle is complex, reflecting the presence of myocyte, neuronal, and vascular components. Although some of the age-associated alterations in gene

expression could represent maturational changes, this possibility is unlikely given the fact that the 5-month-old (adult) mice used in this study were fully mature animals. Importantly, changes in mRNA levels may not always result in a parallel alteration in protein levels. However, the complete or partial prevention of most age-related alterations by CR suggests that gene expression profiles can be used to assess the biological age of mammalian tissues, providing a tool for evaluating experimental interventions.

Taken as a whole, our results provide evidence that during aging there is an induction of a stress response as a result of damaged proteins and other macromolecules. This response ensues as the systems required for the turnover of such molecules decline, perhaps as a result of an energetic deficit in the cell. In particular, the observed alterations in transcripts associated with energy metabolism and mitochondrial function may reflect either decreased mitochondrial biogenesis or turnover secondary to cumulative ROS-inflicted mitochondrial damage (2), lending support to the concept that mitochondrial dysfunction plays a central role in aging of postmitotic tissues. The gene expression profile also suggests that secondary responses to the aging process in skeletal muscle involve the activation of neuronal and myogenic responses to injury.

A summary of global changes induced by aging, and the contrasting effects of CR, are shown in Table 3. The transcriptional activation of stress response genes that process damaged or misfolded proteins during aging, and the prevention of this induction by CR, suggest a central role for protein modifications in aging. Indeed, aging is characterized by an exponential increase of oxidatively damaged proteins (27). Previous analyses of metabolic rates in CR animals have led to the suggestion that this life-extending regimen acts through a reduction in metabolic rate, resulting in a lower production of toxic by-products of metabolism (28). The CR-mediated reduction of mRNAs encoding inducible genes involved in metabolic detoxification, DNA repair, and the response to oxidative stress supports this view, because it implies lower substrate availability for these systems. Additionally, our analysis indicates that CR may cause a metabolic shift toward increased biosynthesis and macromolecular turnover. A hormonal trigger for this shift may be an alteration in the insulin signaling pathway through increased expression of genes that mediate insulin sensitivity, a finding that links our observations to those obtained through the genetic analysis of aging in the nematode *C. elegans* (4).

References and Notes

1. S. M. Jazwinski, *Science* 273, 54 (1996); G. M. Martin, S. N. Austad, T. E. Johnson, *Nature Genet.* 13, 25 (1996); F. B. Johnson, D. A. Sinclair, L. Guarente, *Cell* 96, 291 (1996).

Table 3. Global view of transcriptional changes induced by aging and caloric restriction.

Aging	Caloric restriction
<p>↑ Stress response Induction of: Heat shock response DNA damage-inducible genes Oxidative stress-inducible genes</p>	<p>↑ Protein metabolism Increased synthesis Increased turnover</p>
<p>↓ Energy metabolism Reduced glycolysis Mitochondrial dysfunction</p>	<p>↑ Energy metabolism Up-regulation of gluconeogenesis, and the pentose phosphate shunt</p>
<p>↑ Neuronal injury Reinnervation Neurite extension and sprouting</p>	<p>↑ Biosynthesis Fatty acid synthesis Nucleotide precursors</p>
	<p>↓ Macromolecular damage Suppression of: Inducible heat shock factors Inducible detoxification systems Inducible DNA repair systems</p>

2. K. B. Beckman and B. N. Ames, *Physiol. Rev.* **78**, S47 (1998).
3. W. C. Orr and R. S. Sohal, *Science* **263**, 1128 (1994); T. L. Parkes et al., *Nature Genet.* **19**, 171 (1998).
4. S. Ogg et al., *Nature* **389**, 994 (1997); K. Lin, J. B. Dorman, A. Rodan, C. Kenyon, *Science* **278**, 1319 (1997); S. Paradis and G. Ruvkun, *Genes Dev.* **12**, 2488 (1998); H. A. Tissenbaum and G. Ruvkun, *Genetics* **148**, 703 (1998).
5. T. E. Johnson, *Science* **249**, 908 (1990); S. Murakami and T. E. Johnson, *Genetics* **143**, 1207 (1996); Y.-J. Lin, L. Seroude, S. Benzer, *Science* **282**, 943 (1998).
6. C. E. Yu et al., *Science* **272**, 258 (1996); L. Ye et al., *Am. J. Med. Genet.* **68**, 494 (1997).
7. R. Weindruch and R. L. Walford, *The Retardation of Aging and Disease by Dietary Restriction* (Thomas, Springfield, IL, 1988).
8. C. Dutta, E. C. Hadley, J. Lexell, *Muscle Nerve* **5**, S5 (1997).
9. R. Ludatscher, M. Silberman, D. Gershon, A. Reznick, *Exp. Gerontol.* **18**, 113 (1983).
10. Methods used to house and feed male C57BL/6 mice, a commonly used model in aging research with an average life-span of ~30 months, were recently described [T. D. Pugh, T. D. Oberley, R. Weindruch, *Cancer Res.* **59**, 642 (1999)].
11. Total RNA was extracted from frozen tissue by using TRIzol reagent (Life Technologies). Polyadenylate [poly(A)⁺] RNA was purified from the total RNA with oligo-dT-linked Oligotex resin (Qiagen). One microgram of poly(A)⁺ RNA was converted into double-stranded cDNA (ds-cDNA) by using Superscript Choice System (Life Technologies) with an oligo-dT primer containing a T7 RNA polymerase promoter (Genset). After second-strand synthesis, the reaction mixture was extracted with phenol-chloroform-isoamyl alcohol, and ds-cDNA was recovered by ethanol precipitation. In vitro transcription was performed by using a T7 Megascript Kit (Ambion) with 1.5 µl of ds-cDNA template in the presence of a mixture of unlabeled ATP, CTP, GTP, and UTP and biotin-labeled CTP and UTP [bio-11-CTP and bio-16-UTP (Enzo)]. Biotin-labeled cRNA was purified by using an RNeasy affinity column (Qiagen), and fragmented randomly to sizes ranging from 35 to 200 bases by incubating at 94°C for 35 min. The hybridization solutions contained 100 mM MES, 1 M Na⁺, 20 mM EDTA, and 0.01% Tween 20. The final concentration of fragmented cRNA was 0.05 µg/µl in the hybridization solutions. After hybridization, the hybridization solutions were removed and the gene chips were washed and stained with streptavidin-phycoerythrin. DNA chips were read at a resolution of 6 µm with a Hewlett-Packard GeneArray Scanner.
12. Detailed protocols for data analysis of Affymetrix microarrays and extensive documentation of the sensitivity and quantitative aspects of the method have been described [D. J. Lockhart, *Nature Biotechnol.* **14**, 1675 (1996)]. Briefly, each gene is represented by the use of ~20 perfectly matched (PM) and mismatched (MM) control probes. The MM probes act as specificity controls that allow the direct subtraction of both background and cross-hybridization signals. The number of instances in which the PM hybridization signal is larger than the MM signal is computed along with the average of the logarithm of the PM/MM ratio (after background subtraction) for each probe set. These values are used to make a matrix-based decision concerning the presence or absence of an RNA molecule. Positive average signal intensities after background subtraction were observed for over 4000 genes for all samples. To determine the quantitative RNA abundance, the average of the differences representing PM minus MM for each gene-specific probe family is calculated, after discarding the maximum, the minimum, and any outliers beyond 3 SDs. Averages of pairwise comparisons were made between animals with Affymetrix software. To determine the effect of age, each 5-month-old mouse (*n* = 3) was compared to each 30-month-old (*n* = 3) mouse, generating a total of nine pairwise comparisons. To determine the effect of diet, 30-month-old CR-fed (*n* = 3) and 30-month-old control-fed (*n* = 3) animals were similarly compared. Pearson correlation coefficients were calculated between individual animals in the same

age/diet groups. No correlation coefficient between two animals in the same age/diet group was less than 0.98.

13. M. H. Goyns et al., *Mech. Ageing Dev.* **101**, 73 (1998).
14. J. Jackman, I. Alamo Jr., A. J. Fornace Jr., *Cancer Res.* **54**, 5656 (1994).
15. O. Stachowiak, M. Dolder, T. Wallimann, C. Richter, *J. Biol. Chem.* **273**, 16694 (1998).
16. L. Larsson, *J. Gerontol. Biol. Sci.* **50A**, 96 (1995); J. Lexell, *J. Nutr.* **127**, 1011S (1997).
17. J. C. Copray and N. Brouwer, *Neurosci. Lett.* **236**, 41 (1997).
18. G. Marazzi and K. M. Buckley, *Dev. Dyn.* **197**, 115 (1993).
19. C. A. Peterson and J. D. Houle, *J. Nutr.* **127**, 1007S (1997).
20. M. Shibanuma, J. Mashimo, T. Kuroki, K. Nose, *J. Biol. Chem.* **269**, 26767 (1994); S. Wang, E. J. Moerman, R. A. Jones, R. Thweatt, S. Goldstein, *Mech. Ageing Dev.* **92**, 121 (1996).
21. ATP synthase: W. Junge, H. Lill, S. Engelbrecht, *Trends Biochem. Sci.* **22**, 420 (1997); NADP transhydroge-

nase: J. B. Hoek and J. Rydstrom, *Biochem. J.* **254**, 1 (1988); LON protease: K. Luciakova, B. Sokolikova, M. Chloupekova, B. D. Nelson, *FEBS Lett.* **444**, 186 (1999); ERV1: T. Lisowsky, *Curr. Genet.* **26**, 15 (1994).
- 22. A. L. Schwartz and A. Ciechanover, *Annu. Rev. Med.* **50**, 57 (1999).
- 23. J. L. DeRisi, V. R. Iyer, P. O. Brown, *Science* **278**, 680 (1997).
- 24. J. R. Zierath et al., *Endocrinology* **139**, 5034 (1998).
- 25. T. Tomoyasu, T. Ogura, T. Tatsu, B. Bukau, *Mol. Microbiol.* **30**, 567 (1998); T. Yura, H. Nagai, H. Mori, *Annu. Rev. Microbiol.* **47**, 321 (1993).
- 26. L. Wikstrom et al., *EMBO J.* **17**, 455 (1998).
- 27. E. R. Stadtman, *Science* **257**, 1220 (1992).
- 28. R. S. Sohal and R. Weindruch, *ibid.* **273**, 59 (1996).
- 29. Supported by NIH grants PO1 AG11915 (R.W.) and RO1 CA78723 (T.A.P.). T.A.P. is a recipient of the Shaw Scientist (Milwaukee Foundation) and Burroughs Wellcome Young Investigator awards.

19 May 1999; accepted 22 July 1999

Dual Function of the Selenoprotein PHGPx During Sperm Maturation

Fulvio Ursini,¹ Sabina Heim,² Michael Kless,² Matilde Maiorino,¹ Antonella Roveri,¹ Josef Wissing,² Leopold Flohé^{3*}

The selenoprotein phospholipid hydroperoxide glutathione peroxidase (PHGPx) changes its physical characteristics and biological functions during sperm maturation. PHGPx exists as a soluble peroxidase in spermatids but persists in mature spermatozoa as an enzymatically inactive, oxidatively cross-linked, insoluble protein. In the midpiece of mature spermatozoa, PHGPx protein represents at least 50 percent of the capsule material that embeds the helix of mitochondria. The role of PHGPx as a structural protein may explain the mechanical instability of the mitochondrial midpiece that is observed in selenium deficiency.

Selenium is essential for male fertility in rodents and has also been implicated in the fertilization capacity of spermatozoa of livestock and humans (1). Selenium deficiency is associated with impaired sperm motility, structural alterations of the midpiece, and loss of flagellum (1). However, three decades after the discovery of selenium as an integral constituent of redox enzymes (2), the molecular basis of the relationship of the essential trace element and male fertility remains obscure. The selenoprotein PHGPx (Enzyme Commission number 1.11.1.12) is abundantly expressed in spermatids and displays high activity in postpubertal testis (3). In mature spermatozoa, however, selenium is largely restricted to the mitochondrial capsule, a keratin-like matrix that embeds the

helix of mitochondria in the sperm midpiece (4). A "sperm mitochondria-associated cysteine-rich protein (SMCP)" (5) had been considered to be the selenoprotein accounting for the selenium content of the mitochondrial capsule (4–6). The rat SMCP gene, however, does not contain an in-frame TGA codon (7) that would enable a selenocysteine incorporation (8). In mice, the three in-frame TGA codons of the SMCP gene are upstream of the translation start (5). SMCP can therefore no longer be considered as a selenoprotein. Instead, the "mitochondrial capsule selenoprotein (MCS)," as SMCP was originally referred to (4–7), is here identified as PHGPx.

Routine preparations of rat sperm mitochondrial capsules (9) yielded a fraction that was insoluble in 1% SDS containing 0.2 mM dithiothreitol (DTT) and displayed a vesicular appearance in electron microscopy (Fig. 1A). The vesicles readily disintegrated upon exposure to 0.1 M mercaptoethanol (Fig. 1B) and became fully soluble in 6 M guanidine-HCl. When the solubilized capsule material was subjected to polyacrylamide gel electrophoresis (PAGE), four bands in the 20-kD

¹Dipartimento di Chimica Biologica, Università di Padova, Viale G. Colombo 3, I-35121 Padova, Italy. ²National Research Centre for Biotechnology (GBF), Mascheroder Weg 1, D-38124 Braunschweig, Germany. ³Department of Biochemistry, Technical University of Braunschweig, Mascheroder Weg 1, D-38124 Braunschweig, Germany.

*To whom correspondence should be addressed. E-mail: lfi@gbf.de

EXHIBIT D

Research

Open Access

Gene expression profiling by DNA microarray analysis in mouse embryonic fibroblasts transformed by ras^{V12} mutated protein and the E1A oncogene

Sophie Vasseur¹, Cédric Malicet¹, Ezequiel L Calvo², Claude Labrie², Patrice Berthezene¹, Jean Charles Dagorn¹ and Juan Lucio Iovanna*¹

Address: ¹Centre de Recherche INSERM EMI 0116, 163 Avenue de Luminy, BP172, 13009 Marseille, France and ²Molecular Endocrinology and Oncology Research Center, Laval University Medical Center 2705 Laurier Boulevard, Quebec, G1V 4G2, Canada

Email: Sophie Vasseur - vasseur@marseille.inserm.fr; Cédric Malicet - malicet@marseille.inserm.fr; Ezequiel L Calvo - ecalvo@crchul.ulaval.ca; Claude Labrie - claudelabrie@crchul.ulaval.ca; Patrice Berthezene - berthezene@marseille.inserm.fr; Jean Charles Dagorn - dagorn@marseille.inserm.fr; Juan Lucio Iovanna* - iovanna@marseille.inserm.fr

* Corresponding author

Published: 19 March 2003

Received: 24 January 2003

Molecular Cancer 2003, 2:19

Accepted: 19 March 2003

This article is available from: <http://www.molecular-cancer.com/content/2/1/19>

© 2003 Vasseur et al; licensee BioMed Central Ltd. This is an Open Access article: verbatim copying and redistribution of this article are permitted in all media for any purpose, provided this notice is preserved along with the article's original URL.

Abstract

Background: Ras is an area of intensive biochemical and genetic studies and characterizing downstream components that relay ras-induced signals is clearly important. We used a systematic approach, based on DNA microarray technology to establish a first catalog of genes whose expression is altered by ras and, as such, potentially involved in the regulation of cell growth and transformation.

Results: We used DNA microarrays to analyze gene expression profiles of ras^{V12}/E1A-transformed mouse embryonic fibroblasts. Among the ~12,000 genes and ESTs analyzed, 815 showed altered expression in ras^{V12}/E1A-transformed fibroblasts, compared to control fibroblasts, of which 203 corresponded to ESTs. Among known genes, 202 were up-regulated and 410 were down-regulated. About one half of genes encoding transcription factors, signaling proteins, membrane proteins, channels or apoptosis-related proteins was up-regulated whereas the other half was down-regulated. Interestingly, most of the genes encoding structural proteins, secretory proteins, receptors, extracellular matrix components, and cytosolic proteins were down-regulated whereas genes encoding DNA-associated proteins (involved in DNA replication and reparation) and cell growth-related proteins were up-regulated. These data may explain, at least in part, the behavior of transformed cells in that down-regulation of structural proteins, extracellular matrix components, secretory proteins and receptors is consistent with reversion of the phenotype of transformed cells towards a less differentiated phenotype, and up-regulation of cell growth-related proteins and DNA-associated proteins is consistent with their accelerated growth. Yet, we also found very unexpected results. For example, proteases and inhibitors of proteases as well as all 8 angiogenic factors present on the array were down-regulated in transformed fibroblasts although they are generally up-regulated in cancers. This observation suggests that, in human cancers, proteases, protease inhibitors and angiogenic factors could be regulated through a mechanism disconnected from ras activation.

Conclusions: This study established a first catalog of genes whose expression is altered upon fibroblast transformation by ras^{V12}/E1A. This catalog is representative of the genome but not exhaustive, because only one third of expressed genes was examined. In addition, contribution to ras signaling of post-transcriptional and post-translational modifications was not addressed. Yet, the information gathered should be quite useful to future investigations on the molecular mechanisms of oncogenic transformation.

Background

Cancer is a disease caused by multiple genetic alterations that lead to uncontrolled cell proliferation. This process often involves activation of cellular proto-oncogenes and inactivation of tumour-suppressor genes. One of the earliest and most potent oncogenes identified in human cancer is the mutant *ras* [1,2]. *Ras* family of proto-oncogenes encodes small GTP-binding proteins that transduce mitogenic signals from tyrosine-kinase receptors [reviewed in [3]]. *In vitro*, oncogenic *ras* efficiently transforms most immortalized rodent cell lines but fails to transform mouse primary cells [4]. However, *ras* can transform primary mouse cells by cooperating with other oncogenic alterations such as overexpression of c-Myc, dominant negative p53, D-type cyclins, Cdc25A and Cdc25B, or loss of *p53*, *p16* or *IRF-1* [5–7]. Several viral onco-proteins can also cooperate with *ras*, for example SV40 T-antigen, adenovirus E1A, human papillomavirus E7 and HTLV-1 Tax [reviewed in [6,7]]. When expressed alone in primary cells, most of these alterations facilitate their immortalization [7]. Oncogenic transformation of primary cells by co-expression of *ras* and immortalizing mutations constitutes a model of multistep tumorigenesis that has been reproduced in animal systems [reviewed in [8,9]].

Ras has been an area of intensive biochemical and genetic studies [10]. These studies helped to characterize downstream signaling events and components that relay *ras*-induced mitogenic signals to the ultimate transcription factors which regulate expression of genes involved in cell growth and transformation. Downstream signaling elicited by the oncogenic form of *Ras* protein impairs regulation of gene expression with eventual disruption of normal cellular functions. Downstream transcription factors were found essential for *ras*-mediated cell transformation [11–13]. However, compared with our knowledge on *ras* signaling events, little is known on target genes involved in the phenotypic changes resulting from *ras* activation, such as cell transformation. Thus, identification of genes whose expression is altered during *ras*-mediated cell transformation would provide important information on the underlying molecular mechanism. In the present work, we used DNA microarray technology to analyze gene expression profiles of *ras*^{V12}/E1A-transformed primary mouse embryonic fibroblasts (MEFs), in order to identify genes whose expression is transformation-dependent.

Results

Analysis of gene expression changes after *ras*^{V12}/E1A-transformation

We used microarray analysis to compare expression profiles of ~12,000 genes in normal vs. *ras*^{V12}/E1A-transformed fibroblasts. Figure 1 shows the phenotypic changes of the *ras*^{V12}/E1A-transformed MEFs. With Af-

fymetrix microarray technology, differential expression values greater than 1.7 are likely to be significant, based on internal quality control data. We present data which use a more stringent ratio, restricting our analysis to genes that are overexpressed or under-expressed at least 2.0 fold in *ras*^{V12}/E1A-transformed fibroblasts relative to the empty retrovirus-transduced MEFs. We summarize the highlights below and present the full profile in Figure 2.

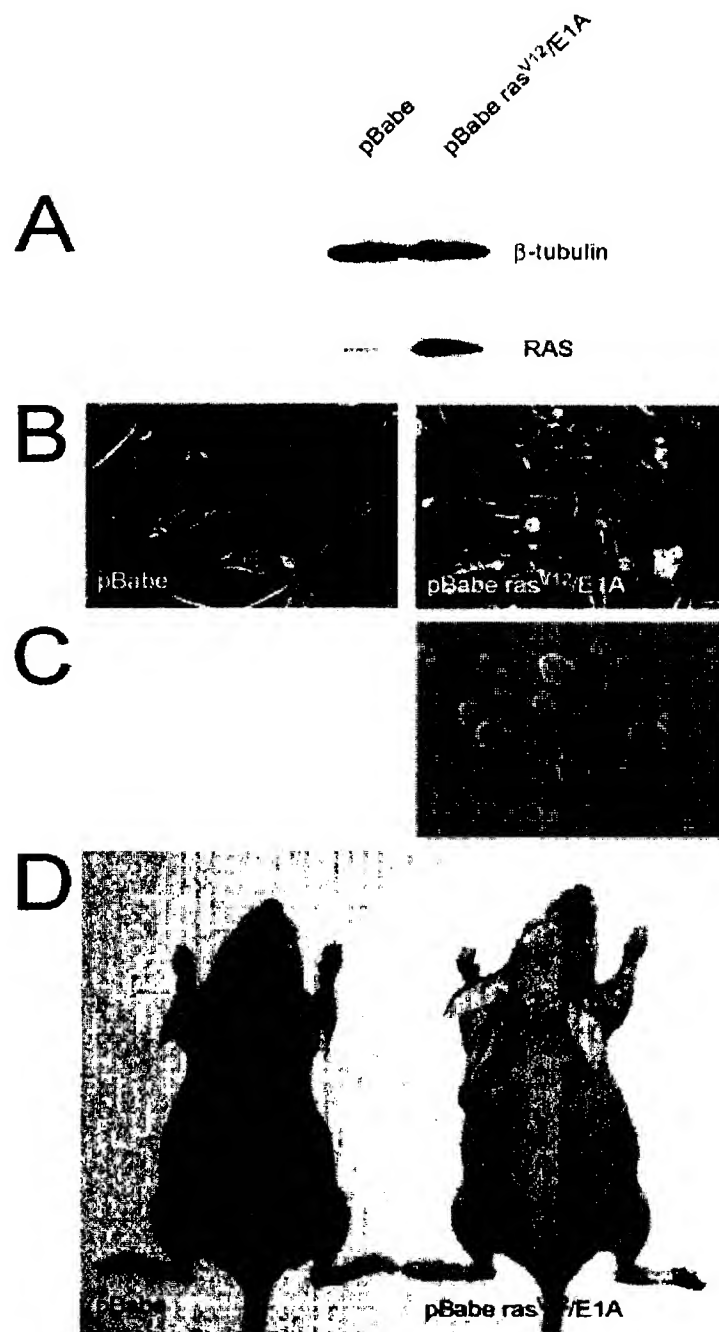
Among the ~12,000 genes and ESTs analyzed, expression of 815 showed to be altered by at least 2.0 fold in the *ras*^{V12}/E1A-transformed fibroblasts, of which 203 corresponded to ESTs. Among known genes, 202 were up-regulated (Table 1)(see Additional file 1) whereas 410 were down-regulated (Table 2)(see Additional file 2) by *ras*^{V12}/E1A-transformation. It is interesting to note that about one half of genes encoding transcription factors, signaling proteins, membrane proteins, channels, or apoptosis-related proteins was up-regulated whereas the other half was down-regulated (Figure 2). However, after *ras*^{V12}/E1A-transformation most of genes encoding structural proteins, secretory proteins, receptors, proteases, protease inhibitors, extracellular matrix components, proteins involved in angiogenesis and cytosolic proteins, were down-regulated whereas genes encoding DNA-associated proteins (involved in DNA replication and reparation) and cell growth-related proteins were up-regulated (Figure 2). These data may explain, at least in part, the behavior of transformed cells. For example, down-regulation of structural proteins, extracellular matrix components, secretory proteins and receptors is consistent with reversion of the phenotype of transformed cells towards a less differentiated phenotype and up-regulation of cell growth-related proteins and DNA-associated proteins is consistent with their accelerated growth.

Transcription factors

57 genes encoding transcription factors were up-regulated and 45 down-regulated by *ras*^{V12}/E1A-transformation. The most strongly activated genes corresponded to the homeobox protein SPX1 (39 fold), myb proto-oncogene (25 fold) and the paired-like homeodomain transcription factor (19 fold), whereas the most repressed were the osteoblast specific factor 2 (123 fold), the p8 protein (51 fold), the H19 mRNA (21 fold) and the early B-cell factor (20 fold).

Structural proteins

Expressions of 10 genes encoding structural proteins were up-regulated in MEFs-transformed cells, 44 being down-regulated. The most important up-regulation was observed for cytokeratin (26 fold) and desmoplakin I (17 fold), the strongest down-regulations for smooth muscle calponin (115 fold), transgelin (49 fold), debrin (41

**Figure 1**

A. Expression of RAS was verified by immunoblot analysis in MEFs transduced with pBabe (control) or pBabe-ras^{V12}/E1A (transformed) retroviruses. B. Morphological aspect of the pBabe and pBabe-ras^{V12}/E1A transduced mouse embryonic fibroblasts. C. Anchorage-independent growth of the ras^{V12}/E1A transformed MEF. Fifty thousand cells were plated on 0.6% agar in DMEM-10% FCS and overlaid on 0.6% agar in the same medium. Photomicrographs were taken 10 days after plating. D. ras^{V12}/E1A transformed MEF induce tumor formation. One million of pBabe and pBabe-ras^{V12}/E1A transduced mouse embryonic fibroblast were injected in 200 μ l PBS as xenografts in nude mice. Representative mice at day 18.

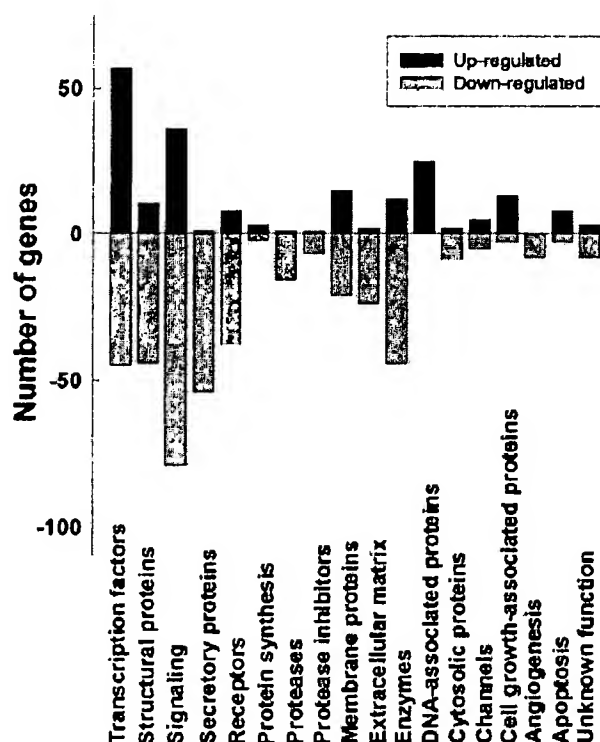


Figure 2

Gene expression changes after ras^{V12}/E1A-transformation. Number of genes up-regulated or down-regulated were grouped by function (Transcription factors, structural proteins, signaling, secretory proteins, receptors, protein synthesis, proteases, protease inhibitors, membrane proteins, extracellular matrix, enzymes, DNA-associated proteins, cytosolic proteins, channels, cell growth-associated proteins, angiogenesis, apoptosis and unknown function). Bars represent the number of genes in each group.

fold), p50b (35 fold) and vascular smooth muscle alpha-actin (34 fold).

Signaling factors

36 genes encoding proteins involved in numerous signaling pathways were up-regulated and 79 down-regulated in ras^{V12}/E1A-transformed MEFs. The EGP314 precursor (also known as the calcium signal transducer 1) was found 25 fold up-regulated, whereas the cysteine rich intestinal protein (41 fold) and ASM-like phosphodiesterase 3a (31 fold) were the most strongly down-regulated genes.

Secretory proteins

Only one gene, encoding the transforming growth factor alpha, was detected as up-regulated (3 fold) in transformed cells. By contrast, expressions of 54 secretory pro-

teins were repressed after ras^{V12}/E1A-transformation. The most affected genes were those encoding cholecystokinin (112 fold), serum amyloid A3 (85 fold), PRDC (58 fold), insulin-like growth factor binding protein 5 (41 fold), gremlin (36 fold), follistatin (33 fold), the small inducible cytokine subfamily B (27 fold), cytokine SDF-1-beta (23 fold) and the small inducible cytokine A7 (22 fold).

Receptors

8 receptors were up-regulated and 38 down-regulated in transformed fibroblasts. Overexpression was observed for acetylcholine receptor beta (8 fold), tyrosine kinase receptor (3 fold), growth hormone releasing hormone receptor (3 fold), semaphorin M-sema G (3 fold) and amphiregulin (2 fold). Strongest down-regulations were found for integrin alpha 5 (43 fold), transient receptor protein 2 (19 fold), retinoic acid receptor alpha (14 fold), retinoic orphan receptor 1 (11 fold) and platelet derived growth factor receptor (12 fold).

Protein synthesis

3 genes involved in protein synthesis (BRIX, nucleolin, ribosomal protein L44 and SIK similar protein) were over-expressed and 2 (ribosomal protein S4X and ribosomal protein L39) were down-regulated, suggesting that protein synthesis is not strongly affected by transformation.

Proteases and protease inhibitors

Only the kallikrein B protease and the elafin-like protein II protease inhibitor were up-regulated (3 and 2 fold respectively) after ras^{V12}/E1A-transformation. By contrast, 16 proteases and 7 protease inhibitors were found repressed in transformed MEFs. The tollid-like (41 fold) and meltrin beta (33 fold) were proteases most down-regulated and the tissue factor pathway inhibitor 2 (44 fold) and the plasminogen activator inhibitor (31 fold) were the most affected protease inhibitors.

Membrane proteins

15 genes encoding membrane proteins were up-regulated and 21 were down-regulated. Histocompatibility 2, D region locus, (16 fold) and melanoma differentiation associated protein (9 fold) were the most overexpressed genes, whereas Thy-1.2 glycoprotein (36 fold), cadherin 11 (14 fold) and vascular cell adhesion molecule 1 (13 fold) were the most repressed.

Extracellular matrix

Laminin gamma 1 (20 folds) and entactin-2 (6 folds) were the two extracellular matrix encoding genes found up-regulated during transformation, whereas 24 genes were down-regulated. Among them, procollagen type VI, alpha 1 (121 folds), procollagen type III, alpha 1 (56 folds), procollagen type I, alpha 1 (44 folds), procollagen type I, alpha 2 (37 folds), collagen type VI, alpha 3

subunit (21 folds) and decorin (19 folds) were the most affected.

Enzymes

Twelve enzymes involved in cellular metabolism were found overexpressed after *ras*^{V12}/E1A-transformation and 44 were found down-regulated. The most activated genes were serine hydroxymethyl transferase 1 (6 fold), acetyl coenzyme A dehydrogenase (5 fold) and the acetyltransferase (GNAT) family containing protein (4 fold), whereas the most repressed genes were lysozyme P (88 fold), lysyl oxydase (61 fold) and lysozyme M (55 fold). Interestingly, maximal overexpressions were 6, 5 and 4 fold, whereas down-regulations were 88, 61 and 55 fold indicating that in addition to the fact that more genes were down-regulated (44 vs. 12), change in expression was also more important for down-regulated genes.

DNA-associated proteins

25 genes encoding DNA-associated proteins were up-regulated, whereas no gene of this family was found down-regulated. The most strongly activated genes were nucleoside diphosphate kinase (9 fold), the topoisomerase-inhibitor suppressed (7 fold), the helicase lymphoid specific (6 fold) and the DNA2-like homolog (6 fold).

Cytosolic proteins

Expression of 2 genes encoding cytosolic proteins was activated after *ras*^{V12}/E1A-transformation, whereas expression of 6 genes was repressed. Genes coding for acyl-CoA-binding protein (3 fold) and tubulin-specific chaperone (2 fold) were overexpressed, whereas the most strongly repressed gene was that coding cytochrome P450 (61 fold).

Channels

5 genes encoding channels were up-regulated and also 5 were down-regulated. Chloride channel protein 3 was the most up-regulated gene (11 fold) and the channel beta-1 subunit (15 fold) was the most down-regulated gene.

Cell growth-associated proteins

As expected for transformed cells which grow more rapidly, 13 genes encoding proteins involved in cell growth were found overexpressed, whereas only 3 were found down-regulated in *ras*^{V12}/E1A-transformed MEFs. The most activated genes were those coding for cyclin-dependent kinase-like 2 (6 fold) and cell division cycle 7-like 1 (5 fold) whereas the most repressed gene was cyclin D2 (4 fold).

Angiogenesis

Angiogenesis is a key process in carcinogenesis. Contrary to the expected for a tumoral cell, we were unable to find angiogenesis-associated genes up-regulated by *ras*^{V12}/E1A-transformation. To our surprise, all 8 genes as-

sociated with angiogenesis showing differential expression were down-regulated. These included genes coding for thrombospondins 1 (15 fold), 2 (32 fold) and 3 (6 fold), pigment epithelium-derived factor (26 fold), pleiotrophin (24 fold), GRO1 oncogene (16 fold), angiogenin-related protein (4 fold) and tumor necrosis factor induced protein 2 (3 fold).

Apoptosis

8 apoptosis-related genes were up-regulated in transformed MEFs and 3 down-regulated. The p53 apoptosis effector related to Pmp22 was the most activated gene (19 fold) and death-associated protein 1 gene was the most under-expressed (4 fold) after transformation.

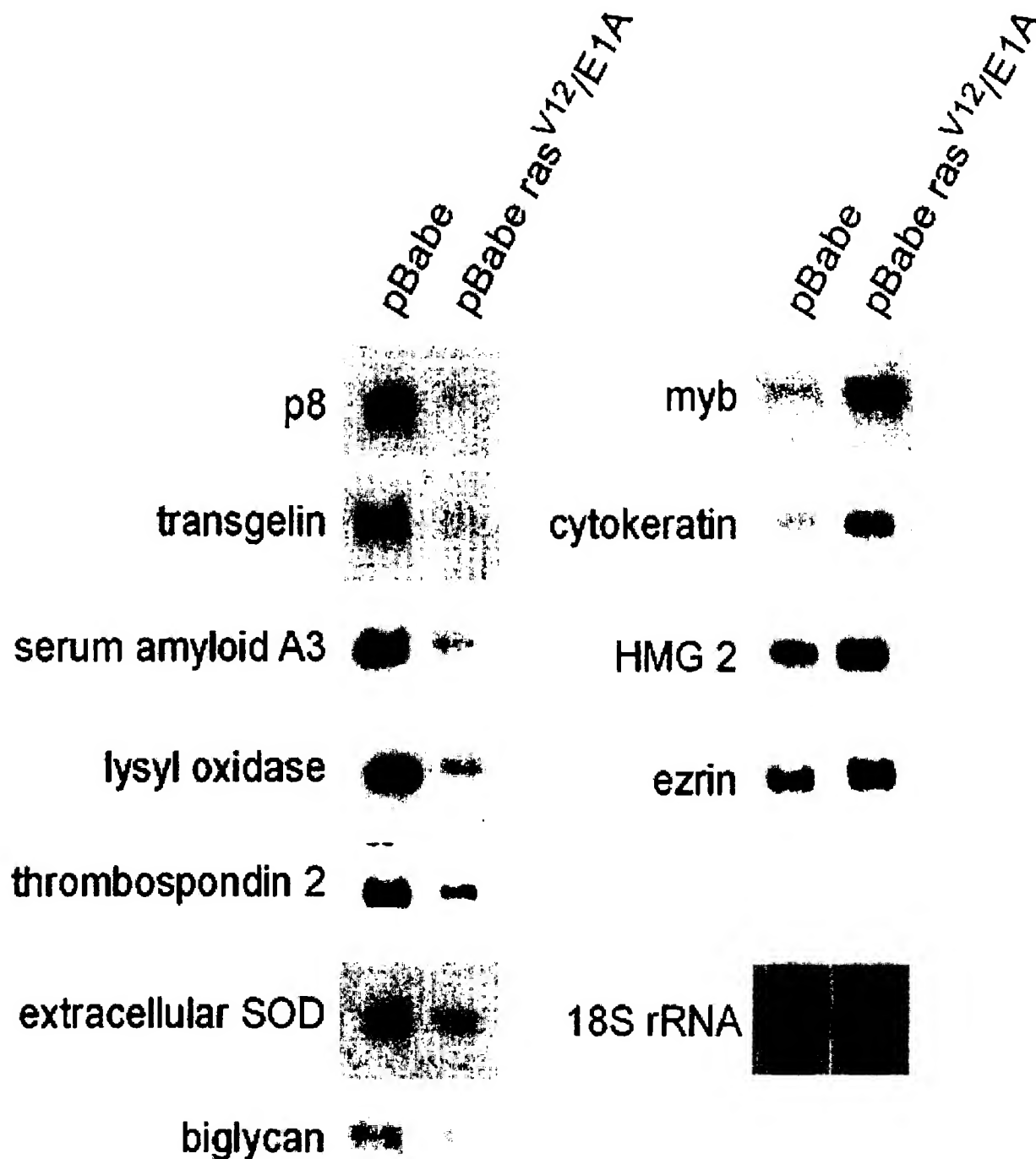
Unknown function

3 genes encoding proteins without well defined function were found up-regulated in mutated *ras*-E1A expressing fibroblasts, whereas 8 were found to be down-regulated.

As a proof-of-principle, we verified the relative expression levels of 11 of these 815 genes by Northern blot analysis. The following 11 genes were tested : p8, transgelin, serum amyloid A3, lysyl oxidase, thrombospondin 2, extracellular superoxide dismutase, biglycan, myb, cytokeratin, HMG2 and ezrin. In all of them Northern blot data confirmed microarray data. The first 7 were down-regulated in transformed MEFs, the 4 others being overexpressed (Figure 3).

Discussion

A number of *ras*-regulated genes have been identified by studies on immortalized cells or cancer cells expressing the oncogenic *ras* [14–21]. However, although these results are quite interesting, it is important to note that established cell lines are frequently subject to genetic and epigenetic changes that are selected during passaging or immortalization and may affect *ras* target-gene expression. Primary cultures, such as mouse embryonic fibroblasts, do not have that drawback. This is why, to identify *ras* target genes, we decided to analyze global gene expression shortly after retroviral transfer of an ectopic mutated *ras* in MEFs. Yet, because activated *ras* alone induces MEF senescence instead of transformation, we associated to it the adenovirus-derived oncogene E1A. The *ras*^{V12}/E1A transformation of MEFs (and of other non-immortalized cells as well) is specific and controlled. Using the Affymetrix technology on ~12,000 genes, we found that expression of 6.8% of them was significantly modified in MEFs by *ras*^{V12}/E1A-transformation. Because oncogenic transformation of fibroblasts allows tumor development when cells are injected in the immunocompromised mouse (see Figure 1), studying target genes of activated *ras* should improve our understanding of the molecular mechanisms by which *ras* transforms cells and eventually

**Figure 3**

Confirmation of microarray results by Northern blot analysis. 18S rRNA was used as a loading control. Total RNA isolated from pBabe and pBabe-ras^{V12/E1A} transduced MEFs were blotted onto Hybond-N membranes and hybridized with ³²P-labeled probes as described in Material and Methods section.

allows tumor formation. It is interesting to note that only 24% of down-regulated and 40% of up-regulated genes showed strong modification (i.e.: >5 fold change) of its expression after transformation.

Several examples of genes up- or down-regulated upon *ras* transformation have already been reported [22–25]. Present data on systematic analysis of about one third of the expressed genome confirm those reports while extending considerably our knowledge of genes activated or repressed by oncogenic *ras* in association with the E1A adenoviral protein. Our results may explain the behavior of transformed cells. For example and as expected, virtually all of the genes coding for secreted factors or extracellular matrix component, which are associated with a differentiated phenotype, were down-regulated. Also, morphological changes observed after transformation (see Figure 1), may be explained by the fact that 44 genes encoding structural proteins were under-expressed. Another expected result was that cell growth-related proteins (involved in the regulation of the cell cycle or inducing cell proliferation) and DNA-associated proteins (involved in DNA replication and reparation) were up-regulated in transformed MEFs, in agreement with their accelerated growth. Also, it is not a surprise to find an altered expression for 56 enzymes involved in cell metabolism because, compared to normal fibroblasts, transformed cells show accelerated growth, increased migration capacity and strong morphological changes. These enzymes could be involved in some of these changes.

Several genes coding for transcription factors ($n = 102$) and proteins involved in signaling pathways ($n = 115$) were up- or down-regulated suggesting that modification of the amounts of these factors could be responsible for the dramatic changes in gene expression observed in transformed cells. It is interesting to note that approximately as many transcription factors were up-regulated ($n = 57$) as down-regulated ($n = 45$).

Besides data coherent with previous knowledge, we also found very unexpected results. For example, we found that genes coding for proteases and inhibitors of proteases were strongly down-regulated by *ras*^{V12}/E1A transformation. This was surprising since these factors are up-regulated and strongly involved in tumor progression involving mutated *ras*. This observation could suggest that in human cancers, proteases and protease inhibitors are activated through a mechanism disconnected from *ras* activation. We were similarly surprised by the fact that all 8 angiogenic factors present on the array were found down-regulated by *ras*^{V12}/E1A transformation. Like proteases and inhibitors of proteases, angiogenic factors are involved in tumour progression and still repressed during *ras*^{V12}/E1A-mediated transformation. It is therefore high-

ly unlikely that their overexpression reported in several cancers is controlled by a *ras*-dependent pathway. Finally, it was also unexpected that only 5 genes involved in protein synthesis were up- or under-expressed, suggesting that protein synthesis is not strongly altered after *ras*^{V12}/E1A transformation.

Conclusions

In conclusion, this study of a large number of genes has identified those whose expression is altered upon fibroblast transformation by *ras*^{V12}/E1A. It is however not exhaustive because the analyzed genes are only representative of the genome (one third of the expressed genes was examined), and post-transcriptional and post-translational modifications were not addressed. Yet, information gathered should be quite useful to future investigations on the molecular mechanisms of oncogenic transformation.

Methods

Primary mouse embryo fibroblasts (MEFs)

Primary embryo fibroblasts were isolated from 14.5 day-old SV129 mouse embryos following standard protocols [26]. Cells were grown in Dulbecco's modified Eagle's medium (DMEM) supplemented with 10% foetal calf serum, 2 mM L-glutamine, 100 IU/ml penicillin G and 100 µg/ml streptomycin.

Retroviral infection

Oncogenic *ras* transforms most immortal rodent cells to a tumorigenic state, whereas transformation of mouse primary cells requires either a cooperating oncogene or the inactivation of a tumour suppressor gene. The adenovirus E1A oncogene cooperates with *ras* to transform primary mouse fibroblasts [7] and abrogates *ras*-induced senescence [27]. Therefore, we transduced MEFs with the pBabe-*ras*^{V12}/E1A retroviral vector which expresses both the *ras*^{V12} mutated protein and the E1A oncogene to obtain transformed fibroblasts. pBabe-*ras*^{V12}/E1A [described in ref. [27]] and pBabe (as control) plasmids were obtained from S. Lowe. Bosc 23 ecotropic packaging (10^6) cells were plated in a 6-well plate, incubated for 24 hr, and then transfected with PEI with 5 µg of retroviral plasmid. After 48 hr, the medium containing the virus was filtered (0.45 µm filter, Millipore) to obtain the first supernatant. MEFs were plated at 2×10^5 cells per 35 mm dish and incubated overnight. For infections, the culture medium was replaced by an appropriate mix of the first supernatant and culture medium (V/V), supplemented with 4 µg/ml polybrene (Sigma), and cells were incubated at 37°C. As a control, we evaluated the ability of the retroviral vector to transduce MEFs by using a retroviral vector expressing the EGFP under control of the retroviral promoter located in the long terminal repeat. About 30% of MEFs expressed high levels of EGFP fluorescence 48 h after

transduction (data not shown), indicating that retroviral vectors are well adapted to our experimental set-up. Retrovirus-infected cells were selected with puromycin (0.7 µg/ml). Transformation of MEFs by the pBabe-ras^{V12}/E1A retroviral vector was evaluated by examining changes in their morphological aspect, by quantifying expression of the RAS protein by western blot, by monitoring cell proliferation, colony formation in soft-agar and tumors in nude mice. In soft-agar assays, pBabe-ras^{V12}/E1A transformed cells formed colonies at high frequency (Figure 1). Similarly, transformed cells produced tumors in all (3/3) athymic nude mice when injected subcutaneously, whereas control MEFs did not (0/3) (Figure 1).

Western blot analysis

One hundred µg of total protein extracted from cells was separated with standard procedures on 12.5% SDS-PAGE using the Mini Protean System (Bio-Rad) and transferred to a nitrocellulose membrane (Sigma). The intracellular level of RAS was estimated by Western blot using the H-ras (C-20) polyclonal antibody (1:200) purchased from Santa Cruz Biotechnology, Inc.

Microarray

Total RNA was isolated by Trizol (Gibco-BRL by Invitrogen). Twenty µg of total RNA was converted to cDNA with SuperScript reverse transcriptase (Gibco-BRL by Invitrogen), using T7-oligo-d(T)₂₄ as a primer. Second-strand synthesis was performed using T4 DNA polymerase and E. Coli DNA ligase followed by blunt ending by T4 polynucleotide kinase. cDNA was isolated by phenol-chloroform extraction using phase lock gels (Brinkmann). cDNA was *in vitro* transcribed using the T7 BioArray High Yield RNA Transcript Labeling Kit (Enzo Biochem, New York, N.Y.) to produce biotinylated cRNA. Labelled cRNA was isolated using an RNeasy Mini Kit column (Qiagen). Purified cRNA was fragmented to 200–300 mer cRNA using a fragmentation buffer (100 mM potassium acetate-30 mM magnesium acetate-40 mM Tris-acetate, pH 8.1), for 35 min at 94°C. The quality of total RNA, cDNA synthesis, cRNA amplification and cRNA fragmentation was monitored by micro-capillary electrophoresis (Bioanalyzer 2100 by Bioanalyser 2100, Agilent Technologies). The cRNA probes were hybridized to an MGu74Av2 Genechip (Affymetrix, Santa Clara, CA). The MGu74Av2 Genechip represents ~6,000 sequences of mouse Unigene that have been functionally characterized and ~6,000 sequences ESTs clusters. Each sequence in the chip is represented by 32 probes: 16 "perfect match" (PM) probes that are complementary to the mRNA sequence and 16 "mismatch" (MM) probes that only differ by a single nucleotide at the central base (more detailed information about the MGu74Av2 Genechip can be obtained in the web site <http://www.affymetrix.com>). Fifteen micrograms of fragmented cRNA was hybridized for 16 h at 45°C with

constant rotation (60 rpm). Microarrays were processed in an Affymetrix GeneChip Fluidic Station 400. Staining was made with streptavidin-conjugated phycoerythrin (SAPE) followed by amplification with a biotinylated anti-streptavidin antibody and a second round of SAPE, and then scanned using an Agilent GeneArray Scanner (Agilent Technologies). Expression value (signal) is calculated using Affymetrix Genechip software MAS 5.0 (for fully description of the statistical algorithms see http://affymetrix.com/support/technical/whitepapers/sadd_whitepaper.pdf). Briefly, signal is calculated as follow: First, probe cell intensities are processed for global background. Then, MM value is calculated and subtracted to adjust the PM intensity in order to incorporate some measure of non-specific cross-hybridization to mismatch probes. Then, this value is log-transformed to stabilize the variance. Signal is output as the antilog of the resulting value. The 20 probe pairs representing each gene are consolidated into a single expression level. Finally, software scales the average intensity of all genes on each array within a data set. Final value of signal is considered representative of the amount of transcript in solution.

Housekeeping controls β-actin and GAPDH genes serve as endogenous controls and are useful for monitoring the quality of the target. Their respective probe sets are designed to be specific to the 5', middle, or 3' portion of the transcript. The 3'/5' signal ratio from these probe sets is informative about the reverse transcription and *in vitro* transcription steps in the sample preparation. Then, an ideal target in which all transcripts was full-length transcribed would have an identical amount of signal 3' and 5' and the ratio would be equal to 1. Differences greater than three fold between signal at 3' and 5' for these housekeeping genes indicate that RNA was incompletely transcribed or target may be degraded. Ratio of fluorescent intensities for the 5' and 3' ends of these housekeeping genes was <2.

Hybridization experiments were repeated twice using independent cRNA probes synthesized with RNA from two independent sets of MEF-infected cells. Genes were considered as differentially expressed when both hybridizations showed >2 folds change. Data presented in this work represent the average of both hybridizations. The list of unchanged genes should be obtained from authors upon request.

Validation of gene expression profiles by Northern blot hybridization

Synthesis of probes: One microgram of total RNA from MEF cells was subjected to PCR with reverse transcription using the One Step RT-PCR kit (Gibco-BRL) according to the manufacturer's protocol to synthesize specific cDNA probes. PCR were carried out for 32 cycles, each cycle consisting in a denaturing step for 1 min at 94°C, an

annealing step for 2 min at 56°C, and a polymerization step for 2 min at 72°C. Selected RNA species were amplified using the following primers: p8, sense, 5'-ggagagagcagctaggcata-3' and antisense, 5'-gttgctgccaccaaggcat-3'; transgelin, sense, 5'-ccagccagctctgcagatggg-3' and antisense, 5'-gcaggcagatttctgagttc-3'; serum amyloid A3, sense, 5'-ggatgaagccttcattgcc-3' and antisense, 5'-gaagagctacacgcgcactc-3'; lysyl oxidase, sense, 5'-taaaacgactgtcccaacc-3' and antisense, 5'-tcacggccgtgttagtga-3'; thrombospondin 2, sense, 5'-aagccagctgggcttacgg-3' and antisense, 5'-tgctggagctggagccctgc-3'; extracellular superoxide dismutase, sense, 5'-ccttagttaaccagaaatc-3' and antisense 5'-gtacctcaaagtgctcactgg-3'; biglycan, sense, 5'-ggctgctttctgtctcacagg-3' and antisense 5'-gcaactgaccatcacctccta-3'; myb proto-oncogene, sense, 5'-ctaaaccattcatgaggag-3' and antisense, 5'-aacaatgcaaaattcaccc-3'; cytokeratin, sense, 5'-ctggctcagcagattgagg-3' and antisense, 5'-ggtagtggaatctctgcc-3'; high mobility group protein 2, sense, 5'-cgtctgcttctgctgttttg-3' and antisense 5'-gcccttgacacggtatgcagc-3' and ezrin, sense, 5'-caacgaggagaagcgatca-3' and antisense 5'-gtgtgacacctgctgcagtg-3'. Specificity of the PCR products was confirmed by direct DNA sequencing.

Northern blot hybridization: RNA samples (10 µg) were submitted to electrophoresis on a 1% agarose gel and vacuum blotted onto Hybond-N membranes (Amersham). The filters were hybridized with the ³²P-labeled probes for 16 h at 65°C in 5X SSPE (1X SSPE is 180 mM NaCl, 1 mM EDTA, 10 mM NaH₂PO₄, pH 7.5), 5X Denhardt solution, 0.5% SDS and 100 µg/ml single stranded herring sperm DNA. Filters were then washed four times for 5 min at room temperature in 2X SSC, 0.2% SDS, twice for 15 min at 50°C in 0.2X SSC, 0.2% SDS, and once for 30 min in 0.1X SSC at 50°C before autoradiography exposure on Kodak X-Omat films at -80°C from 8 hr to 4 days.

Authors' contributions

SV prepared cells and retroviruses, CM carried out RNA purification and Northern blot analysis, ELC and CL were in charge of microarray hybridization, PB participated in the analysis of gene expression data, JCD participated in the design of the study, JLI participated in the analysis of data and wrote the manuscript. All authors read and approved the final manuscript.

Additional material

Additional File 1

Mouse embryo fibroblasts genes over-expressed upon ras^{V12}/E1A transformation (Microsoft Word document). Genes found over-expressed by microarray analysis are listed, with their GenBank accession number, the over-expression factors (relative to control) observed in two separate experiments and the average over-expression factor.

Click here for file

[<http://www.biomedcentral.com/content/supplementary/1476-4598-2-19-S1.doc>]

Additional File 2

Mouse embryo fibroblasts genes under-expressed upon ras^{V12}/E1A transformation (Microsoft Word document). Genes found under-expressed by microarray analysis are listed, with their GenBank accession number, the under-expression factors (relative to control) observed in two separate experiments and the average under-expression factor.

Click here for file

[<http://www.biomedcentral.com/content/supplementary/1476-4598-2-19-S2.doc>]

Acknowledgements

We thank Dr. S. Lowe for the kind gift of pBabe-ras^{V12}/E1A and pBabe plasmids and R. Grimaud and F. Roche for technical assistance. We also thanks to Dr M.J. Pébusque for critical reading of the manuscript. This work was supported by a grant from the Ligue Nationale Contre le Cancer (LNCC) and Association pour la Recherche sur le Cancer (ARC).

References

1. Capon DJ, Chen EY, Levinson AD, Seeburg PH and Goeddel DV: **Complete nucleotide sequences of the T24 human bladder carcinoma oncogene and its normal homologue.** *Nature* 1983, **302**:33-37.
2. Shih C and Weinberg RA: **Isolation of a transforming sequence from a human bladder carcinoma cell line.** *Cell* 1982, **29**:161-169.
3. Barbacid M: **ras genes.** *Annu Rev Biochem* 1987, **56**:779-827.
4. Newbold RF and Overell RW: **Fibroblast immortality is a prerequisite for transformation by EJ c-Ha-ras oncogene.** *Nature* 1983, **304**:648-651.
5. H Land, LF Parada and RA Weinberg: **Tumorigenic conversion of primary embryo fibroblasts requires at least two cooperating oncogenes.** *Nature* 1983, **304**:596-602.
6. Weinberg RA: **Oncogenes, antioncogenes, and the molecular bases of multistep carcinogenesis.** *Cancer Res* 1989, **49**:3713-3721.
7. Ruley HE: **Transforming collaborations between ras and nuclear oncogenes.** *Cancer Cells* 1990, **2**:258-268.
8. Hunter T: **Cooperation between oncogenes.** *Cell* 1991, **64**:249-270.
9. Vogelstein B and Kinzler KW: **The multistep nature of cancer.** *Trends Genet* 1993, **9**:138-141.
10. Gibbs JB, Oliff A and Kohl NE: **Farnesyltransferase inhibitors: Ras research yields a potential cancer therapeutic.** *Cell* 1994, **77**:175-178.
11. Langer SJ, Bortner DM, Roussel MF, Sherr CJ and Ostrowski MC: **Mitogenic signaling by colony-stimulating factor 1 and ras is suppressed by the ets-2 DNA-binding domain and restored by myc overexpression.** *Mol Cell Biol* 1992, **12**:5355-5362.
12. Johnson R, Spiegelman B, Hanahan D and Wisdom R: **Cellular transformation and malignancy induced by ras require c-jun.** *Mol Cell Biol* 1996, **16**:4504-4511.
13. Finco TS, Westwick JK, Norris JL, Beg AA, Der CJ and Baldwin AS: **Oncogenic Ha-Ras-induced signaling activates NF-kappaB**

- transcriptional activity, which is required for cellular transformation. *J Biol Chem* 1997, **272**:24113-24116
14. Krzyzosiak WJ, Shindo-Okada N, Teshima H, Nakajima K and Nishimura S Isolation of genes specifically expressed in flat revertant cells derived from activated ras-transformed NIH 3T3 cells by treatment with azatyrosine. *Proc Natl Acad Sci USA* 1992, **89**:4879-4883
 15. Liang P, Averboukh L, Zhu W and Pardee AB Ras activation of genes: *Mob-1* as a model. *Proc Natl Acad Sci USA* 1994, **91**:12515-12519
 16. Jo H, Zhang H, Zhang R and Liang P Cloning oncogenic ras-regulated genes by differential display. *Methods* 1998, **16**:365-372
 17. Jo H, Cho YJ, Zhang H and Liang P Differential display analysis of gene expression altered by ras oncogene. *Methods Enzymol* 2001, **332**:233-244
 18. Shields JM, Der CJ and Powers S Identification of Ras-regulated genes by representational difference analysis. *Methods Enzymol* 2001, **332**:221-232
 19. Habets GG, Knepper M, Sumartin J, Choi YJ, Sasazuki T, Shirasawa S and Bollag G cDNA array analyses of K-ras-induced gene transcription. *Methods Enzymol* 2001, **332**:245-260
 20. Brem R, Certa U, Neeb M, Nair AP and Moroni C Global analysis of differential gene expression after transformation with the v-H-ras oncogene in a murine tumor model. *Oncogene* 2001, **20**:2854-2858
 21. Sers C, Tchernitsa OI, Zuber J, Diatchenko L, Zhumabayeva B, Desai S, Htun S, Hyder K, Wiechen K, AgoulNIK A, Scharff KM, Siebert PD and Schafer R Gene expression profiling in RAS oncogene-transformed cell lines and in solid tumors using subtractive suppression hybridization and cDNA arrays. *Adv Enzyme Regul* 2002, **42**:63-82
 22. Diaz-Guerra M, Haddow S, Bauluz C, Jorcano JL, Cano A, Balmain A and Quintanilla M Expression of simple epithelial cytokeratins in mouse epidermal keratinocytes harboring Harvey ras gene alterations. *Cancer Res* 1992, **52**:680-687
 23. Hiwasa T, Yokoyama S, Ha JM, Noguchi S and Sakiyama S c-Ha-ras gene products are potent inhibitors of cathepsins B and L. *FEBS Lett* 1987, **211**:23-26
 24. Contente S, Kenyon K, Rimoldi D and Friedman RM Expression of gene *rrg* is associated with reversion of NIH 3T3 transformed by LTR-c-H-ras. *Science* 1990, **249**:796-798
 25. Shields JM, Rogers-Graham K and Der CJ Loss of transgelin in breast and colon tumors and in RIE-1 cells by Ras deregulation of gene expression through Raf-independent pathways. *J Biol Chem* 2002, **277**:9790-9799
 26. Harvey M, Sands AT, Weiss RS, Hegl ME, Wiseman RW, Pantazis P, Giovanella BC, Tainsky MA, Bradley A and Donehower LA In vitro growth characteristics of embryo fibroblasts isolated from p53-deficient mice. *Oncogene* 1993, **8**:2457-2467
 27. Serrano M, Lin AWW, McCurrach ME, Beach D and Lowe SW Oncogenic ras provokes premature cell senescence associated with accumulation of p53 and p16INK4a. *Cell* 1997, **88**:593-602

Publish with **BioMed Central** and every scientist can read your work free of charge

"BioMed Central will be the most significant development for disseminating the results of biomedical research in our lifetime."

Sir Paul Nurse, Cancer Research UK

Your research papers will be:

- available free of charge to the entire biomedical community
- peer reviewed and published immediately upon acceptance
- cited in PubMed and archived on PubMed Central
- yours — you keep the copyright

Submit your manuscript here:
http://www.biomedcentral.com/info/publishing_adv.asp



BioMedcentral

EXHIBIT E

ON REPORTING FOLD DIFFERENCES

C.L. TSIENT

*Massachusetts Institute of Technology and Harvard Medical School
545 Technology Square, NE43-420, Cambridge, MA 02139, USA*

T.A. LIBERMANN, X. GU

*New England Baptist Bone and Joint Institute, Beth Israel Deaconess Medical Center, and
Harvard Medical School, 4 Blackfan Circle, Boston, MA 02115, USA*

I.S. KOHANE

*Children's Hospital Informatics Program and Harvard Medical School
300 Longwood Avenue, Boston, MA 02115, USA*

As we enter an age in which genomics and bioinformatics make possible the discovery of new knowledge about the biological characteristics of an organism, it is critical that we attempt to report newly discovered "significant" phenotypes only when they are actually of significance. With the relative youth of genome-scale gene expression technologies, how to make such distinctions has yet to be better defined. We present a "mask technology" by which to filter out those levels of gene expression that fall within the noise of the experimental techniques being employed. Conversely, our technique can lend validation to significant fold differences in expression level even when the fold value may appear quite small (e.g. 1.3). Given array-organized expression level results from a pair of identical experiments, our ID Mask Tool enables the automated creation of a two-dimensional "region of insignificance" that can then be used with subsequent data analyses. Fundamentally, this should enable researchers to report on findings that are more likely to be in nature truly meaningful. Moreover, this can prevent major investments of time, energy, and biological resources into the pursuit of candidate genes that represent false positives.

1 Introduction

As we enter one of the most exciting times in the history of science, in which genomics and bioinformatics are coming together to make possible the discovery of new knowledge about living organisms at their molecular level, it is imperative that we avoid discovery of "truths" that are not so. While the temptation to plunge into tracing out metabolic pathways, cellular interactions, or genetic regulatory circuits—especially now that we have technologies allowing genome-wide study of RNA expression—is very strong, we must pause long enough to consider how best to report our results such that they may be meaningful. Specifically, for microarray-based expression technologies, whether they are glass microarrays, nylon membranes, or other formats, we need to better understand how to distinguish significant fold difference values from those that fall within the noise level of the experiment at hand.

Francis Collins rightfully speculates about the large impact that microarray technology is likely to have, yet reminds us of the “many critically important questions about this new field that are yet unaddressed” [1]. Some have criticized array-based methods for not being model-based, or hypothesis-driven, while others support that the exploratory nature can lead to new hypotheses that then can be tested in the laboratory [2]. Especially because such hypothesis testing of candidate genes, cell-cell interactions, or pathways requires a major investment of time, energy, and biological resources, an important challenge is understanding how to better recognize false-positive results.

We present a “mask technology” by which to filter out those levels of gene expression that fall within the noise of the experimental techniques being employed. Conversely, our technique can lend validation to the significance of fold differences in expression level even when the fold value may appear quite small. Our work is based on the notion that gene expression measurements ought to be repeatable. Fold differences for each corresponding pair of genes in a pair of “identical” experiments should therefore be equal to unity. Identical experiments are ones in which the operating conditions, cell lines, culture media, incubation time, and so forth are controlled to be the same. We first explore whether this is the case by examining several pairs of identical experiments. We then develop the ID Mask Tool, which enables the automated creation of a two-dimensional “region of insignificance” that can be used with subsequent data analyses.

2 Materials and Methods

2.1 Data Collection

The data for this study were collected to evaluate the use of microarray technology for detection of ESE-1 target genes after transient transfection into different cell lines. We hypothesized that a transfection efficiency of greater than 70-80% should be sufficient to detect differences in gene expression between two samples. We first determined the transfection efficiency of various cell lines using a green fluorescent protein (GFP) expression vector. Four of the cell lines tested (HT1080, 293, MCF-7, and MG-63) conformed to the criteria set by us. Total RNA was isolated from MCF-7 human breast cancer cells and MG-63 human osteosarcoma cells transiently transfected with an ESE-1 expression vector 20 and 24 hours after transfection. Experiments were performed in duplicates in order to distinguish, from gene expression, differences due to “biological noise.” Specifically, six pairs of these duplicated experiments served as the source of the data that we subsequently used to develop the identity mask methodology. The ESE-1 expression vector also

expressed GFP, which enabled us to confirm transfection efficiencies for each experiment. ³²P-labeled cDNA probes reverse-transcribed from these RNAs were hybridized to the Atlas Human cDNA Expression Arrays from Clontech (Clontech Laboratories, Inc., Palo Alto, CA) [3]. Each of these Atlas Arrays (Human 1.2 I, Human Cancer) is a nylon membrane on which approximately 1200 human cDNAs have been immobilized. The hybridization results were analyzed with the software provided by Clontech by normalizing to the signals obtained from housekeeping gene controls on the same array as well as by global normalization. The microarray experiments were validated by RT/PCR using the same RNAs.

2.2 Data Analysis and Mask Creation

We developed the ID Mask Tool, a custom-designed computer program written in the C language, to perform mask creation. The ID Mask Tool takes as input two spreadsheet files corresponding to two identical experiments, along with two user customizable parameters to be discussed below. It returns as output an "identity mask," or ID Mask, specifically for those two experiments.

Each spreadsheet contains the names of several hundred genes and their corresponding brightness intensity levels (as assessed by hybridization of the probe of interest). Only genes present in both files are further considered. For each of these genes, we calculate a "fold difference," the ratio of the intensity in file 2 to the intensity in file 1 for a given gene. All fold values are then sorted based on the corresponding intensity values of the set of genes in the first spreadsheet file. Two parameters are used for creation of each identity mask: intensity range (or sliding window) size, plus either scale value or number of standard deviations. These are used to calculate the ID Mask borders and can be experimented with for better results.

Two methods are then explored for creating identity masks. Method 1 relies on segmental calculation of standard deviations. A "data point" refers to an (x , y) pairing in which x is an intensity value from the first spreadsheet file and y is its corresponding fold difference value (calculated as above). Using all data points in a given sliding window of intensity values (e.g., from intensity level 1001 to 2000), the standard deviation of the fold values is calculated. The average of the intensity values within that window is then paired with a fold value equal to the average fold value within that window plus the number of standard deviations specified by the user. This new pair becomes a candidate "upper mask border" point. Similarly, a candidate "lower mask border" point is created by pairing the average intensity value of that window with the average fold value minus the number of standard deviations specified by the user. Each successive group of data points in each

sliding window of intensity values (e.g., all points from 2001 to 3000, then all points from 3001 to 4000, etc.) likewise gives rise to candidate mask border points.

The set of (*intensity value*, *fold value*) pairs comprising the candidate upper mask border points is then fit to a line using least-squares linear regression. This line defines the upper mask border. Similarly, linear regression is used to find the lower mask border from the set of calculated candidate lower mask border points. If one of the derived mask borders fits poorly (based upon relationship to original data points), the “reciprocal reflection” of the other mask border can serve in its place. This simply means that each (x, y) point on the good-fit (linear) border gives rise to a point $(x, 1/y)$ to create the reciprocal reflection border. (See Figures 1 through 6 for examples of mask borders. Figures 2—5 show ID Masks each consisting of one linear regression border and one border derived by taking the reciprocal values of that linear regression border.) The region between these borders represents the “identity” region of insignificant fold differences (i.e., noise).

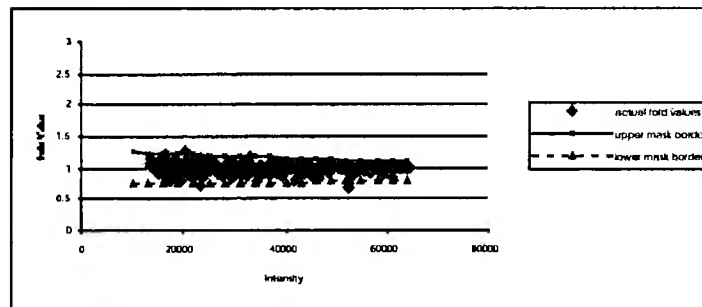


Figure 1: Identity mask for Experiment A. Method 2 with parameters 9000 for intensity sliding window size and 0.975 for scale resulted in the lowest percentage of original data points lying outside of the mask region (0.7%).

Method 2 for creating an identity mask is similar to Method 1 except that candidate mask border points are derived from maximal (and minimal) points in each intensity window rather than from standard deviation calculations. Specifically, amongst all data points in a given window of intensity values, the point with the greatest fold value is chosen. This is repeated for each successive window of intensity values. These fold values can also be scaled before use in linear regression to find the upper mask border. The lower mask border is analogously derived from the smallest fold values.

Once the ID Mask has been derived, all original data points are checked for inclusion or exclusion in the identity mask region. The percentage of data points lying outside of the mask region is reported.

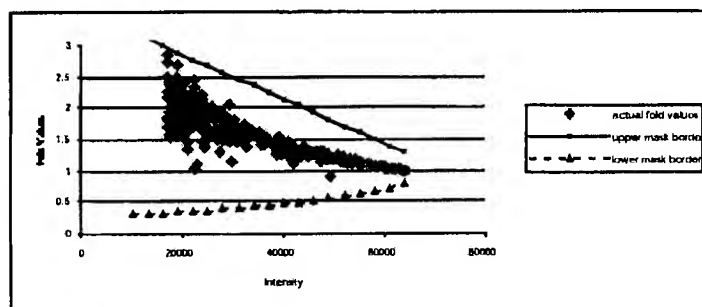


Figure 2: Identity mask for Experiment B. Method 1 with parameters 9000 for intensity window size and standard deviation of 3 resulted in the lowest percentage of original data points lying outside of the mask region (1.7%).

Table 1: Numbers of genes present in each of the experiment pairs, along with the number of genes common to both files in each pair.

	# Genes in 1 st File	# Genes in 2 nd File	# Genes in Both
Expt A	563	559	550
Expt B	292	516	291
Expt C	244	401	244
Expt D	339	518	326
Expt E	365	397	344
Expt F	233	226	180

3 Results

Six pairs of experiments were performed with Clontech nylon membrane filters and tumor cell lines as described in the Methods section, resulting in twelve spreadsheet files of genes and their corresponding expression intensity values. The ID Mask Tool was used to perform all mask creation experiments as well as basic data analysis. Table 1 displays the number of genes present in each of the file pairs, along with the number of genes common to both files in each pair.

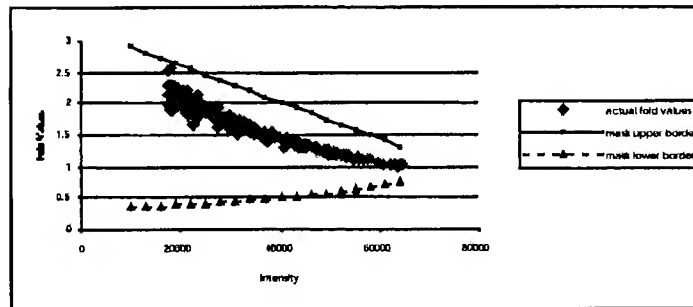


Figure 3: Identity mask for Experiment C. Method 1 with parameters 9000 for intensity window size and standard deviation of 3 resulted in the lowest percentage of original data points lying outside of the mask region (2.0%).

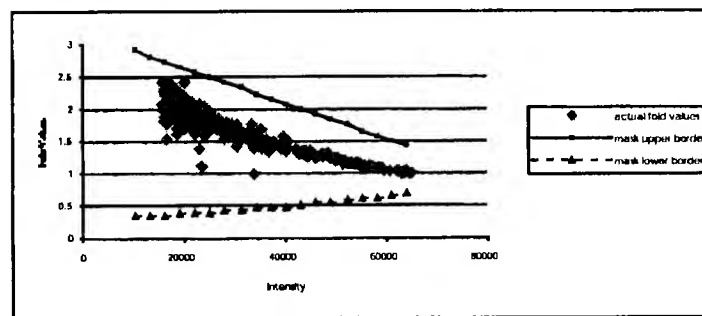


Figure 4: Identity mask for Experiment D. Method 1 with parameters 9000 for intensity window size and standard deviation of 3 resulted in the lowest percentage of original data points lying outside of the mask region (1.5%).

For both Methods 1 and 2 of ID Mask creation, sliding windows of size 1000, 5000, and 9000 on the intensity value axis were chosen for experimentation. Only when calculations were not possible with one of these window sizes (e.g., due to division by zero) was an alternative window size chosen. For Method 1, the number of standard deviations (for calculation of candidate mask border points) was chosen to be 2.5 and 3. For Method 2, the scale factor was chosen to be 0.975 and 1.0.

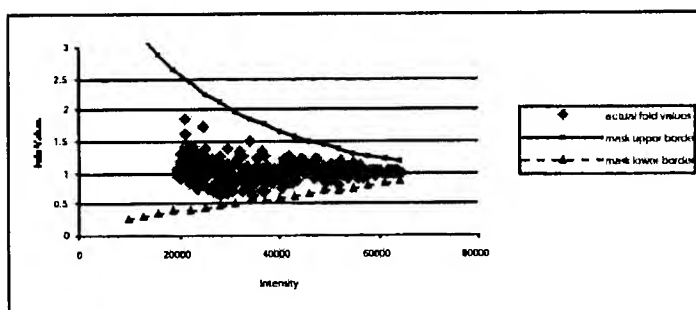


Figure 5: Identity mask for Experiment E. Method 1 with parameters 5000 for intensity window size and standard deviation of 3 resulted in the lowest percentage of original data points lying outside of the mask region (0.9%).

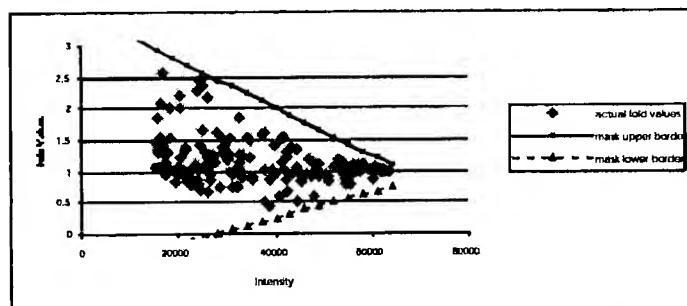


Figure 6: Identity mask for Experiment F. Method 1 with parameters 9000 for intensity window size and standard deviation of 3 resulted in the lowest percentage of original data points lying outside of the mask region (1.7%).

Twelve candidate identity masks were created for each pair of experiments (2 Methods, times 3 intensity window sizes, times 2 scale or standard deviation factors). For each pair of experiments, the ID Mask Tool selected the mask with the lowest percentage of original data points lying outside of the mask region. Figures 1 through 6 show each selected identity mask along with a scatter plot of the original (*intensity value, fold value*) data points for each pair of experiments. Tables 2 and 3 list the percentages of original data points lying outside of the mask region for each of the 12 candidate masks derived for each experiment pair.

Table 2: Each pair of identical experiments gave rise to 12 candidate ID Masks. Six of these twelve were derived by Method 1 (three with standard deviation of 3 and three with standard deviation of 2.5). The other six were derived by Method 2 (three with scale 1.00 and three with scale 0.975). Shown are the percentages of original data points lying outside of the mask region for each of the 12 candidate ID Masks derived for each of Experiments A—C. [σ = standard deviation; intensity range (window) size of 2000 instead of 1000 is used in Experiments B and C for the Method 1 trials.]

	Expt A	A	A	Expt B	B	B	Expt C	C	C
range size	1000	5000	9000	2000; 1000	5000	9000	2000; 1000	5000	9000
$\sigma = 3$	3.1	2.7	2.2	93.2	80.5	1.7	99.6	100.0	2.0
$\sigma = 2.5$	11.1	3.8	3.3	97.3	97.6	2.7	100.0	100.0	2.4
Scale 1.00	19.2	6.2	0.7	100.0	99.0	2.4	100.0	100.0	2.4
Scale 0.975	19.2	6.2	0.7	100.0	99.3	2.4	100.0	100.0	2.9

Table 3: Percentages of original data points lying outside of the mask region for each of the 12 candidate ID Masks derived for Experiments D—F. (See caption in Table 2 for further details.) [σ = standard deviation; intensity range (window) size of 3000 instead of 1000 is used in Experiment D for Method 1 trials, while range (window) size of 2000 instead of 1000 is used in Experiment F for Method 1 trials.]

	Expt D	D	D	Expt E	E	E	Expt F	F	F
range size	3000; 1000	5000	9000	1000	5000	9000	2000; 1000	5000	9000
$\sigma = 3$	17.1	88.4	1.5	0.9	0.9	0.9	5.5	6.1	1.7
$\sigma = 2.5$	24.5	99.4	1.5	2.6	2.0	2.9	7.2	6.6	2.8
Scale 1.00	100.0	99.7	2.4	43.8	18.6	19.7	53.0	9.9	10.5
Scale 0.975	100.0	99.7	3.4	44.3	20.0	20.0	54.7	9.9	11.6

4 Discussion

DNA microarrays clearly are making a large impact on the way we approach problems in molecular biology and genomics. These devices are enabling the genome-wide study of expression in *Escherichia coli* K-12, for example [4]. Others are using DNA microarrays in the study of B-cell lymphomas [5], growth control genes [6], and aging [7]. Some researchers are focusing on developing new [8] or using existing [9] clustering techniques to facilitate the analysis of all the data made available by this relatively new technology. Few, however, have focused specifically on studying the properties of these array data to better understand how to distinguish significant from insignificant "findings."

One way we might be able to better discern meaningful discoveries from the rest is by applying an identity mask technology, such as the one we have presented. Our experiments show that greater amounts of biological noise are present at lower gene expression levels. Thus, there is no magical absolute cut-off for a meaningful fold value. There does appear to exist, however, a "mask of insignificant values," outside of which the fold values are more likely to represent true significance. In Figure 6, for example, a fold difference of 1.5 may be meaningful at an intensity level of 60,000, while a fold difference of 2.5 may be insignificant at an intensity level of 20,000. This result is in stark contrast to a study by Incyte Pharmaceuticals [11], in which they conclude: "any elements with observed ratios greater than or equal to 1.8 should be deemed differentially expressed." A brief glance at the microarray-related literature will quickly confirm that others are also reporting particular fold difference values, such as 1.8, as significant [7]. We argue, however, that the significance of a fold change depends upon the intensity value; genes that are expressed at low levels and hence have weak intensity signals need to show a much greater fold difference than highly expressed genes.

Some have proposed simple statistical tests to determine whether fold differences are significant; t-tests, for example, are included in the GeneSpring software package (Silicon Genetics, San Carlos, CA). Lee *et al.* propose a statistical method using normal distributions and posterior probabilities to determine the likelihood that a gene is truly expressed in a tissue sample [12]. Methods like these are no doubt important; used alone, however, they may under-emphasize the correlation between fold values and intensity values. Future efforts might explore how to best use statistical validation techniques in conjunction with the identity mask method.

While our study used Clontech filters, the general techniques presented for understanding identity masks of insignificance apply to all different types of expression arrays. Both nylon membrane and glass slide array techniques have their

individual advantages. Nylon membrane arrays have sensitive detection using hybridized ^{32}P probes. Glass microarrays have high-resolution fluorescent detection, dual labeling for hybridizing two probes on a single array, and ease in automated handling of slides [3]. Richmond *et al.* compared hybridization of radioactive cDNAs to spot blots on nylon membranes with fluorescence-based hybridization to glass microarrays; they found both methods to be reliable and reproducible [4]. Chen describes a colorimetry detection system for use with nylon membranes [13].

Regardless of the specific array format employed, it seems clear that a custom-derived identity mask is one method that could help improve appropriate reporting of fold difference results. Future work should include an exploration of fitting curves rather than lines for the mask borders. The upper mask border in Figure 2, for example, may benefit from a fitted curve, or at least a piecewise linear model.

An alternative method for mask creation might be to always calculate fold differences greater than 1 by simply swapping the order of individual intensity values whenever the fold value is less than 1. Only the upper mask border would then need to be created. (The lower mask border would be the unity fold difference line.)

It is not clear why there were some large differences between the numbers of genes detected in the experiment pairs of Experiments B, C, and D. These may have been due to experimental error or biological noise. Interestingly, the identity masks for these three also do not fit as nicely as those for Experiments A, E, and F.

While we have selected from amongst the candidate identity masks those with the lowest percentages of points outside the mask region, future work might consider refining the mask fit to purposely exclude approximately 5% of the data points. This could be likened to $p < 0.05$, in which 5% of the time, we may inadvertently report a result as significant even though it is not. A potential benefit is a closer overall mask fit and therefore less likelihood to call a significant finding insignificant.

In only one out of the six pairs of experiments did Method 2 (scaling values) perform better than Method 1 (standard deviations). This is possibly due to the mathematical basis upon which standard deviations are calculated, making them in general more robust and accurate. One way in which scaling actual data points can fail is when there exist outliers. Another is with the choice of too small an intensity window size. This can lead to a sort of "overfitting" problem; our group of candidate "maximum" points from which to derive the upper mask border may then contain several non-maximum values. In Tables 2 and 3, there is a definite trend of worsening mask fit as one decreases the intensity range (window) size from 9000 to 1000. It is likely that in most applications, Method 1 may be more suitable.

Our aim has been to provide a foundation for evaluating fold values. The ultimate goal is to find truly significant fold differences when performing "treatment versus control" comparisons. Analyses of those types of comparisons will likely further our understanding of the masking technique as well. Especially because we recognize the use of DNA microarrays as a method by which to explore the genome in a model-independent fashion [10], it is imperative that we have a basis for judging exploratory findings as being important or simply "in the noise." Candidate genes found through exploration can lead to investment of significant resources; we need to avoid such pursuits of false positive findings.

Acknowledgments

The authors would like to thank Atul Butte, M.D. for assistance with references, and the members of Towia Libermann's laboratory for performing the hybridization experiments.

References

1. F.S. Collins, "Microarrays and macroconsequences" *Nature Genetics* Suppl. **21**, 2 (1999)
2. "The chip challenge" *Nature Genetics* **21**, 61-62 (1999)
3. Clontech web page at <http://www.clontech.com/about/index.html>
4. C.S. Richmond, J.D. Glasner, R. Mau, et al., "Genome-wide expression profiling in *Escherichia coli* K-12" *Nucleic Acids Research* **27**, 3821-3835 (1999)
5. A.A. Alizadeh, M.B. Eisen, R.E. Davis, et al., "Distinct types of diffuse large B-cell lymphoma identified by gene expression profiling" *Nature* **403**, 503-511 (2000)
6. F. Bertucci, S.V. Hulst, K. Bernard, et al., "Expression scanning of an array of growth control genes in human tumor cell lines" *Oncogene* **18**, 3905-3912 (1999)
7. C.-K. Lee, R.G. Klopp, R. Weindruch, et al., "Gene expression profile of aging and its retardation by caloric restriction" *Science* **285**, 1390-1393 (1999)
8. M.B. Eisen, P.T. Spellman, P.O. Brown, et al., "Cluster analysis and display of genome-wide expression patterns" *Proc. Natl. Acad. Sci. USA* **95**, 14863-14868 (1998)
9. A.J. Butte and I.S. Kohane, "Mutual information relevance networks: functional genomic clustering using pairwise entropy measurements" *Proceedings of the Pacific Symposium on Biocomputing* (2000)

10. P.O. Brown and D. Botstein, "Exploring the new world of the genome with DNA microarrays" *Nature Genetics* Suppl. **21**, 33-37 (1999)
11. "GEM microarray reproducibility study" Incyte Technical Survey, Incyte Pharmaceuticals, Inc. (1999)
12. M.T. Lee, F.C. Kuo, G.A. Whitmore, et al., "Importance of replication in microarray gene expression studies: statistical methods and evidence from repetitive cDNA hybridizations" *PNAS* **97**, 9834-9839 (2000)
13. J.J. Chen, R. Wu, P.C. Yang, et al., "Profiling expression patterns and isolating differentially expressed genes by cDNA microarray system with colorimetry detection" *Genomics* **51**, 313-324 (1998)

XI. RELATED PROCEEDINGS APPENDIX

None.